



MASTERTHESIS

Co-activation patterns and modification of spinal sensory-motor transmission during the execution of a volitional standardized motor task

Durchgeführt zum Zwecke der Erlangung
des akademischen Grades des Diplom Ingenieurs.

Ausgeführt unter der Anleitung von
a.o. Univ. Prof. DDDr. Frank Rattay
Institut für Analysis und Scientific Computing
Technische Universität Wien,
Fakultät für Mathematik und Geoinformation

und

Dr. Ursula Hofstötter
Zentrum für Medizinische Physik und Biomedizinische Technik
Medizinische Universität Wien, AKH-4L

von

Martin Schmoll, BSc
e0726627
Fockygasse 51/14
A-1120 Wien

Wien, am 05.11.2012

(Schmoll Martin, BSc)

Declaration

„I confirm that this paper is entirely my own work. All sources and quotations have been fully acknowledged in appropriate places with adequate footnotes and citations. Quotations have been properly acknowledged and marked with appropriate punctuation. The literature consulted is listed in the bibliography. This master thesis has not been submitted to another examination panel in the same or a similar form, and has not been published.“

Vienna, 05.11.2012

Place, Date

Signature

Kurzfassung der Masterarbeit

Koaktivierungsmuster und Modifikationen der sensorischen Reizleitung während der Durchführung einer standardisierten willkürlichen Bewegungsaufgabe.

Motivation und Ziele

Ein wesentlicher Mechanismus, welcher der erfolgreichen neuronalen Steuerung von Bewegungen zugrunde liegt, ist die Fähigkeit des zentralen Nervensystems (ZNS), Gruppen von Motorneuronen selektiv aktivieren bzw. inhibieren zu können, welche den jeweiligen Muskelgruppen zugeordnet sind. Unter gewissen Umständen werden jedoch auch Muskelgruppen ko-aktiviert, welche nicht primär zur Ausführung einer bestimmten Bewegungsaufgabe benötigt werden, z.B. wenn durch eine bestimmte Muskelgruppe eine vordefinierte Kraft konstant gehalten werden soll.

Eines der Ziele der vorliegenden Studie war es, Muster in der Koaktivierung diverser Beinmuskelgruppen während der Ausführung einer isolierten, unilateralen, ein-gelenkigen Bewegungsaufgabe zu untersuchen. Zu diesem Zweck wurde ein Gerät entwickelt, mit dem es möglich war, die erzeugte Kraft einer Dorsiflexion des Sprunggelenks in Echtzeit anzuzeigen und zu messen. Durch die Wiederholung einiger Versuche aus der Literatur (vgl. Dimitrijevic et al., 1992) sollte gezeigt werden, dass die Ausrüstung den funktionellen Erfordernissen entsprach.

Ein weiteres Ziel war die Untersuchung der sensomotorischen Reizleitung auf lumbosakraler Rückenmarksebene während der Ausführung einer definierten, einseitigen Dorsiflexion auf bestimmtem Kraftlevel. Eine Möglichkeit, diese zu beurteilen, stellt die Auslösung spinaler Reflexe und deren Konditionierung durch eine Bewegung dar. Durch die Analyse der modifizierten Reflexantworten erhält man Rückschlüsse auf Veränderungen auf Rückenmarksebene.

Die Arbeitshypothese war, dass sich die Erregung, bei der Erzeugung größerer Kräfte auf andere Muskelgruppen ausbreitet (wodurch ebenso der zentrale Anregungszustand gesteigert wird), und es somit zu verstärkten Reflexmodulationen kommt. Diese Modulationen betreffen sowohl Motorneuronen, die an der Bewegungsaufgabe beteiligt sind, als auch Motorneuronen, die nicht unmittelbar an der Bewegung beteiligt sind.

Methodik

Sechs freiwillige Probanden (4 Männer und 2 Frauen, Durchschnittsalter 25.0 Jahre \pm 3.9 Jahre) ohne Schäden am ZNS nahmen an der Studie teil. Um die Kraft einer Dorsiflexion des Sprunggelenks zu messen, wurde ein spezieller Kraftmessschuh entwickelt. Dieser fixierte den Fuß des Probanden mit einem Riemen, welcher über die metatarsalen Knochen platziert wurde. Mit der Ausrüstung war es möglich, Messungen in Rückenlage, im Stehen und im Sitzen durchzuführen. Elektromyographische Aktivität wurde mittels Ag/AgCl-Oberflächenelektroden, sowohl ipsilateral als auch contralateral, von den Muskelgruppen Quadrizeps (Q), Hamstrings (Ham), Tibialis Anterior (TA) und Trizeps Surae (TS) aufgezeichnet. In dieser Studie wurden drei experimentelle Paradigmen (A, B und C) durchgeführt.

In Paradigma A wurden die Probanden aufgefordert, eine Dorsiflexion mit maximaler willkürlicher Kontraktion (MWK) von TA solange zu halten, bis nur noch 50 % des ursprünglich gemessenen Wertes erreicht werden konnten. Die Versuche fanden im Sitzen statt, wobei das Equipment so eingestellt wurde, dass das Sprunggelenk, Kniegelenk und Hüftgelenk einen Winkel von 90 ° einnehmen konnten. Alle Probanden absolvierten die Messungen beidseitig, jeweils mit und ohne visuelles Feedback (Balkenanzeige der erzeugten Kraft als Prozentsatz von MWK).

In Paradigma B hatten die Probanden die Aufgabe, kurze aufeinanderfolgende Dorsiflexionen für 6 s zu halten, wobei zwischen den Kontraktionen Pausen von 4 s einzuhalten waren. Ein Durchgang begann mit einer Initialkontraktion von 20 % MKW und wurde gefolgt von Kontraktionen mit 40 %, 60 %, 80 % und 100 % MKW. Messungen wurden beidseitig in Rückenlage, im Stehen und im Sitzen durchgeführt, wobei visuelles Feedback bei allen Durchgängen zur Verfügung gestellt wurde.

In Paradigma C kam die transkutane Rückenmarksstimulation zum Einsatz, um sogenannte ‚*Posterior Root Muscle*‘ (PRM) Reflexe (zu deutsch: ‚Hinterwurzel-zu-Muskel‘ Reflexe) auszulösen. In allen Durchgängen wurden zuerst fünf unkonditionierte PRM-Reflexe im entspannten Zustand ausgelöst und aufgezeichnet. Danach wurden weitere fünf konditionierte Reflexe aufgezeichnet, bei denen der Proband eine Dorsiflexion mit vordefiniertem Kraftlevel absolvierte. Messungen wurden beidseitig mit 20 %, 40 %, 60 %, 80 % und 100 % MWK durchgeführt, wobei stets visuelles Feedback zur Verfügung gestellt wurde.

Resultate

Eine willkürliche, unilaterale, anhaltende Kontraktion des Sprunggelenkflexors TA wurde stets von der Koaktivierung einer Vielzahl von Beinmuskeln begleitet. Koaktivität wurde immer zuerst in Muskelgruppen ipsilateral zur Bewegungsaufgabe festgestellt, und breitete sich dann auf die kontralaterale Seite aus. Unter den ipsilateralen Muskelgruppen wurde Q im Allgemeinen immer als Erster koaktiviert. Interessanterweise fand sich auch eine gewisse Koaktivität im Antagonisten TS.

Muskeln auf der kontralateralen Seite wurden generell seltener und später koaktiviert, vergleicht man diese mit ipsilateralen Muskelgruppen. Unter den koaktivierten Muskeln zeigte sich der kontralaterale Q als erste reagierende Muskelgruppe, gefolgt vom kontralateralen Ham. Des Weiteren konnte auch im homologen TA der kontralateralen Seite Koaktivität festgestellt werden.

Die Auswertung der Zeiten, nach denen die jeweiligen Muskelgruppen erstmals koaktiviert wurden, zeigte Veränderungen bei der Bereitstellung von visuellem Feedback. Dies äußerte sich im Allgemeinen in einer Verkürzung der Zeiten bei kontralateralen Muskelgruppen, wohingegen sich eine leichte Erhöhung bei den ipsilateralen Muskelgruppen zeigte.

Die Rekrutierungsreihenfolge der Muskelgruppen blieb durch das visuelle Feedback relativ unbeeinflusst, jedoch konnte festgestellt werden, dass die jeweiligen Muskelgruppen generell öfter koaktiviert wurden.

Die Ausführung unilateraler, kurzer, aufeinanderfolgender Kontraktionen des Sprunggelenkflexors TA, führten ebenfalls zur Koaktivierung diverser Muskelgruppen der unteren Extremitäten. Es zeigte sich, dass das Ausmaß der Koaktivierung – bezogen auf die Anzahl der koaktiven Muskelgruppen und die Stärke der muskulären Aktivität – durch Erhöhung der erzeugten Kraft von TA verstärkt wurde. Wie zuvor schon in den Versuchen mit anhaltender Belastung beobachtet, trat auch hier die erste Koaktivierung ipsilateral zur Bewegungsaufgabe auf.

Unabhängig von der getesteten Körperposition (Rückenlage, Stehen, Sitzen) wurde der synergistisch wirkende ipsilaterale Q immer als Erster koaktiviert. Im Allgemeinen trat die meiste Koaktivität im Stehen auf, wohingegen die Niedrigste im Sitzen beobachtet werden konnte. Bei den Muskeln der kontralateralen Seite trat die meiste Koaktivität ebenfalls im Stehen auf.

Die transkutane Rückenmarkstimulation wurde benutzt, um auf lumbosakraler Rückenmarksebene PRM-Reflexe in einer Vielzahl von Beinmuskeln auszulösen. Die Stimulation erfolgte sowohl in Rückenlage als auch im Stehen. Antworten welche nicht mit Sicherheit als Reflexe identifiziert werden konnten, wurden von der weiteren Analyse ausgeschlossen. Bei solchen Antworten handelte es sich meistens um M-Wellen, welche hauptsächlich in Q gefunden wurden.

Auf Grund der durchgeführten Bewegungsaufgabe konnten Reflexmodulationen in allen untersuchten Muskelgruppen beobachtet werden. Die Effekte in kontralateralen Muskelgruppen waren schwächer ausgeprägt als in den ipsilateralen Muskeln. Generell zeigte sich, dass jegliche Reflexmodifikation (d.h. entweder Verstärkung oder Abschwächung der Reflexantworten) in gesteigertem Ausmaß bei erhöhtem Kraftaufwand auftrat. Des Weiteren konnte beobachtet werden, dass Versuche in Rückenlage im Allgemeinen niedrigere Reflexmodifikationen aufwiesen als im Stehen.

PRM-Reflexe wurden sowohl im aktiven TA als auch im ipsilateralen Q verstärkt, wohingegen gleichzeitig die Antworten im ipsilateralen TS abgeschwächt wurden.

Schlussfolgerungen

Die Ergebnisse der durchgeführten Studie zeigten, dass es mit dem hergestellten Equipment möglich war, die erzeugte Kraft einer unilateralen Dorsiflexion des Sprunggelenks, zu messen. Die korrekte Funktion des Messaufbaus wurde durch die Wiederholung der Versuche von Dimitrijevic et al. (1992) verifiziert. Durch die Messung der erzeugten Kraft konnte die gewünschte Bewegungsaufgabe standardisiert werden, wodurch ein inter-individueller Vergleich der Ergebnisse der einzelnen Probanden möglich wurde.

In der vorliegenden Studie wurden Koaktivierungsmuster der untersuchten Beinmuskeln beschrieben, welche während der Ausführung unilateraler, willkürlicher, lang anhaltender oder kurz andauernder Kontraktionen des Sprunggelenkflexors TA auftraten. In allen sechs Probanden konnten ähnliche Rekrutierungsfolgen der einzelnen Muskelgruppen beobachtet werden, was auf einen zentralen ‚*motor pattern generator*‘ als Quelle der Erregung hindeuten würde.

Die Modulationen der PRM-Reflexe auf Grund der Dorsiflexion des Sprunggelenks reflektierten die funktionellen Rollen der betrachteten (Flexor- und Extensor-) Muskelgruppen. Verstärkte Reflexantworten waren grundsätzlich im aktivierten TA als auch im synergistisch wirkenden ipsilateralen Q zu finden, wohingegen Antworten im antagonistischen TS supprimiert wurden.

Die vorliegende Arbeit stellt eine wertvolle Basis für weitere Studien in größerem Maßstab dar, um die zugrundeliegenden Mechanismen der neuronalen Bewegungskontrolle sowohl in Menschen mit gesunder als auch veränderter Funktion des ZNS besser verstehen zu können.

Summary

Co-activation patterns and modification of spinal sensory-motor transmission during the execution of a volitional standardized motor task

Motivation and objectives

An important mechanism underlying successful neural control of movement is the capacity of the CNS to selectively activate and inhibit, respectively, motoneuron pools associated with antagonistic muscle groups. Yet, there are circumstances when muscle groups extraneous to a particular motor task become co-activated, e.g. during the effort to maintain force in a particular (isolated) muscle group.

One aim of the present thesis was to investigate co-activation patterns of multiple lower limb muscle groups bilaterally, during the execution of a unilateral isolated single-joint movement. To this end, a device to measure and online monitor the force produced during a sustained or intermittent dorsiflexion of the ankle was designed and manufactured. The functional suitability of the equipment was verified by repeating measurements previously described in the literature (Dimitrijevic et al., 1992).

A further goal of the present work was to assess the gain of sensory-motor transmission at several lumbosacral spinal cord levels during the execution of a unilateral ankle dorsiflexion at defined levels of force. This sensory-motor transmission can be assessed by eliciting spinal reflexes and studying their modifications with conditioning-test paradigms. The working hypothesis was that higher levels of produced force – associated with a spread of activity to several muscle groups bilaterally (and thus, with an increased central state of excitability) – will lead to more profound reflex modulations affecting various motoneuron pools pertinent as well as extraneous to the intended task.

Methods

Six volunteers (4 male and 2 female, mean age 25.0 years \pm 3.9 years) with intact nervous system participated to the study. The force produced during a unilateral sustained or intermittent dorsiflexion of the ankle was measured using a specially designed force measurement shoe, which fixated the exercised lower limb with a strap located over the metatarsal bones. The equipment allowed performing measurements in supine, standing and sitting position. Electromyographic activity was recorded from the ipsilateral and contralateral quadriceps (Q), hamstrings (Ham), tibialis anterior (TA) and triceps surae (TS) using Ag/AgCl-surface electrodes. Three experimental paradigms were carried out, named A, B and C.

In Paradigm A, the subjects were instructed to maintain a maximum voluntary contraction (MVC) of the ankle dorsiflexor until the force decreased to 50 % of its initial value. This procedure was executed in sitting position, with hip, knee and ankle joints adjusted to 90 degrees. Separate recordings were carried out for both lower limbs as well as with and without visual feedback of the produced force (bar-scale showing a percentage of MVC).

In Paradigm B, the subjects were asked to carry out intermittent contractions of the ankle dorsiflexor for 6 s followed by 4 s relaxation periods. The initial contraction was 20 % MVC followed by 40 %, 60 %, 80 % and 100 % MVC which represented one cycle. This procedure was executed bilaterally in supine, standing and sitting position. Visual feedback was provided all the time.

In Paradigm C transcutaneous spinal cord stimulation was applied to elicit posterior-root muscle (PRM) reflexes. All recordings started with the elicitation of five unconditioned PRM reflexes during relaxation, followed by five responses elicited during unilateral dorsiflexion at a certain force level. The initial contraction level was 20 % MVC followed by 40 %, 60 %, 80 % and 100% MVC.

Results

Performing a volitional, unilateral, sustained dorsiflexion of the ankle usually led to the co-activation of several lower limb muscle groups in addition to the exercised ankle flexor TA. Co-activation was observed first in muscle groups ipsilateral to the motor task, and later in muscles on the contralateral side.

Among the ipsilateral muscle groups, Q was generally co-activated first. Interestingly, some co-activation was also found in the antagonistic TS.

Co-activation of lower limb muscle groups on the contralateral side was usually observed more seldom and occurred with a certain delay, compared to the ipsilateral side. Among the co-activated muscle groups, CQ was the first one to respond, followed by CHam. Further co-activation was observed in the homologous TA of the contralateral lower limb.

Visual feedback of the produced force generally shortened the times until muscle groups on the contralateral side became co-active, while these times were slightly increased for the ipsilateral muscle groups. While the observed co-activation patterns remained relatively unchanged, the probability of a particular muscle group to become co-activated was increased by providing visual feedback of the produced force.

Performing volitional, unilateral, intermittent contractions of the ankle dorsiflexor led to co-activation of several lower limb muscle groups bilaterally. The extent of co-activation - with respect to the number of co-activated muscle groups and the amount of muscular activity within a particular muscle group - was increased with increasing contraction levels of the exercised TA. As in the trials with sustained contraction, co-activation was first observed in muscle groups of the lower limb ipsilateral to the movement.

Irrespective of the tested body positions (standing, sitting, and supine), the synergistic IQ was co-activated first. Generally, the largest extent of co-activation occurred in the standing position, while the lowest level of co-activity was observed in the sitting position. Muscle groups on the contralateral side were mainly co-activated in the standing position.

Transcutaneous spinal cord stimulation applied over the lumbosacral spinal cord was used to elicit PRM reflexes in multiple lower limb muscles bilaterally, in supine and standing position.

Responses which were not unequivocally identified as reflexes were withdrawn from further analysis. Such responses, most likely M waves, were most frequently found in Q.

Modifications in the reflex gain during the execution of the motor task could be observed in all studied muscle groups. The effects were much weaker on the contralateral side. Any kind of reflex modification, i.e. either facilitation or suppression, was generally more expressed in standing position or by increasing the levels of the produced force. Trials in sitting position generally led to lower expressions of reflex modification.

PRM reflexes in the exercised TA and the synergistic IQ were distinctly facilitated, while the responses in the antagonistic ITS were suppressed at the same time.

Conclusion

The results of the present study proved the measurement equipment to be working properly in order to measure the force produced during a unilateral dorsiflexion of the ankle. Functional suitability was also verified by repeating the measurements conducted by Dimitrijevic et al. (1992). The device allowed for the standardization of the chosen motor task with respect to the degree of force being generated and thus, for the inter-individual comparison of the results obtained.

The present thesis described co-activation patterns of various lower limb muscles accompanying the execution of unilateral, volitional sustained or intermittent contractions of the ankle flexor TA. The observed recruitment orders were similar in all six subjects studied, hinting on a motor pattern generator as the source of activation.

The gain of PRM reflexes during the execution of a dorsiflexion of the ankle at different contraction levels reflected the functional roles of the (flexor and extensor) muscle groups assessed. Facilitated responses were generally found in the exercised TA and the synergistic IQ, whereas reflex suppression was found in the antagonistic ITS.

The presented approach provides a valuable basis for further larger-scale studies, to elucidate the mechanisms underlying the neural control of movement, in individuals with intact and altered CNS function.

Acknowledgements

I would like to express my gratitude to all those who gave me the possibility to complete this master thesis. I want to thank the whole team from the Center for Medical Physics and Biomedical Engineering, located at the general hospital in Vienna, Austria for their excellent assistance.

In first instance, I wish to acknowledge the outstanding supervision of Ursula Hofstötter, PhD, Center for Medical Physics and Biomedical Engineering, Medical University of Vienna, Austria, who motivated and supported me in so many different ways, right from the very beginning. Thanks to her great ideas, experience and commitment; I had the possibility to learn various new and interesting things. I will definitely benefit from her extraordinary encouragement, in my further works. Thank you very much!

Furthermore I have to thank Professor DDDr. Frank Rattay, Institute of Analysis and Scientific Computing, Vienna University of Technology, Vienna, Austria, for instructing and supporting this master thesis.

My sincere gratitude is extended to my former fellow student Christian Schwanzer, who assisted me in building and testing the measurement equipment as well as in performing the actual measurements. Thank you for your help, interest and all valuable hints – thank you for being a friend!

I also wish to acknowledge the support of Elisabeth and Friedrich Schmoll, who always stand behind me, during my whole life.

Table of Content

Declaration.....	1
Kurzfassung der Masterarbeit.....	2
Summary.....	7
Acknowledgements.....	12
Table of Content.....	13
Abbreviations	15
Introduction	16
Materials and methods	19
Subjects	19
Data acquisition and recording set-up.....	19
Force measurement.....	19
Electromyographic recordings	25
Transcutaneous spinal cord stimulation	26
Recording protocols.....	27
Paradigm A.....	27
Paradigm B.....	28
Paradigm C	30
Measurement schedule.....	32
Data analysis	33
Paradigm A.....	33
Paradigm B.....	37
Paradigm C	40

Results	42
Paradigm A.....	42
Paradigm B.....	47
Paradigm C.....	53
Supine position.....	54
Standing position.....	56
Discussion	58
Paradigm A.....	58
Paradigm B.....	59
Paradigm C.....	60
Conclusions.....	61
References.....	62
Appendix A.....	65
Data-capturing software	65
Paradigm A&B.....	65
Paradigm C	66
APPENDIX B	68
Matlab Source Codes.....	68
analysis_paradigm_A.m.....	68
emg2rms.m	78
emg2rmsmean.m.....	79
analysis_paradigm_B.m.....	80
analysis_paradigm_C.m	92
analysis_Mmax.m.....	99

Abbreviations

CHam	contralateral hamstrings
CNS	central nervous system
CNS	central nervous system
CQ	contralateral quadriceps
CTA	contralateral tibialis anterior
CTS	contralateral triceps surae
EMG recording	electro-myographic recording
ExTA	ipsilateral tibialis anterior
H reflex	Hoffman reflex
Ham	hamstrings
IHam	ipsilateral hamstrings
IQ	ipsilateral quadriceps
ISI	interstimulus interval
ITS	ipsilateral triceps surae
LHam	left hamstrings
LQ	left quadriceps
LTA	left tibialis anterior
LTS	left triceps surae
M wave	muscle wave
MVC	maximum volitional contraction
M-Welle	Muskel-Welle
MWK	maximale willentliche Kontraktion
PRM reflex	posterior root muscle reflex
PTP	peak-to-peak
Q	quadriceps
RHam	right hamstrings
RMS	root mean square
RQ	right quadriceps
RTA	right tibialis anterior
RTS	right triceps surae
SCS	spinal cord stimulation
SEM	standard error from mean
STD	standard deviation
T11/T12	11th and 12th thoracic vertebrae process
TA	tibialis anterior
TS	triceps surae
tSCS	transcutaneous spinal cord stimulation
ZNS	zentrales Nervensystem

Introduction

Neural control of movement and posture in man

Neural control of movement and posture is a complex process, organized in various interconnected control levels of the central nervous system (CNS) that are continuously regulating each other's activity (Brooks, 1986; Ghez & Krakauer, 2000). The process involves, in the first instance, the elaboration of perception and motor strategies, accomplished by the association areas of the brain. On the basis of these strategies, motor programs are being developed by the sensory-motor cortex, the cerebellum and the brain stem. At this level, the particular features underlying the execution of a specific motor task, such as the movement direction and velocity, as well as biomechanical requirements necessary e.g. to maintain equilibrium of the body during the task, are determined and adjusted correspondingly. Eventually, at the level of the spinal cord, the supraspinal drive is converted into commands that are subsequently mediated to the various muscles involved in the motor performance. Thereby, the capacity of the CNS to selectively activate or inhibit defined motoneuron pools pertinent or extraneous to the intended task, respectively, plays an integral role in achieving the movement goal (Dimitrijevic et al., 1992; Hwang & Abraham, 2001).

Yet, there are circumstances when muscle groups not involved in a certain motor task or even contralateral to the exercised limb become co-activated. Such motor overflow or motor irradiation (e.g. Cernacek, 1961; Armatas et al., 2001) can be extensively observed during effort-related tasks, i.e. during the effort to maintain force in a particular muscle group (Davis, 1942). Associated movements of proximal synergistic muscles were also described during the voluntary sustained and intermittent activation of isolated, distant muscle groups of the upper (Fog & Fog, 1963; Gellhorn, 1947) and lower limbs (Dimitrijevic et al., 1992).

With respect to unilateral isometric dorsiflexion of the ankle specifically, Dimitrijevic and colleagues (1992) showed that co-activation of various lower limb muscle groups bilaterally was a commonly observed phenomenon in individuals with intact CNS function. Usually, co-activity in addition to the primarily active ankle flexor tibialis anterior (TA) was first developed in muscle groups ipsilateral to the exercised limb, and subsequently spread to the contralateral side. Among the contralateral muscle groups assessed, the homologous TA was preferentially co-activated. Furthermore, visual feedback of the produced force generally led to a higher degree of co-activation occurring at shorter latencies than in the trials without visual feedback. Regarding the underlying mechanisms, Dimitrijevic and colleagues speculated about a potential general increase in the central state of excitability affecting also extraneous motoneuron pools. Also, the

sustained effort to maintain contraction of a particular muscle could potentially impede the selectivity of activation. Yet, taking into account the relatively consistent co-activation patterns observed inter-individually, the group rather suggested the involvement of a motor pattern generator that centrally processed and controlled the produced activities.

State-dependent regulation of spinal reflexes to assess spinal sensory-motor transmission

During the last decades, the concept of using spinal reflexes as an investigative tool to assess how the CNS controls sensory-motor transmission has emerged (Burke, 1999). Reflexes are stereotyped motor events that are automatically and reproducibly generated by the CNS following a particular stimulus. Yet, there are numerous studies providing evidence that spinal reflexes are regulated in a task-dependent manner and according to the phase of an ongoing movement (e.g. Misiaszek et al., 1996). In humans, the spinal reflex commonly studied in this context is the so-called Hoffmann reflex (H reflex; e.g. Capaday & Stein, 1986; 1987; Dyhre-Poulsen et al., 1991; Schneider et al., 2000; Knikou, 2008). The H reflex arises from the electrical stimulation of large-diameter group Ia afferents within a mixed peripheral nerve, the transmission of the evoked excitatory drive to the spinal cord, as well as the subsequent monosynaptic activation of homonymous alpha-motoneurons. The H reflex most extensively studied is the one elicited by stimulation of the rather superficially located tibial nerve in the popliteal fossa and recorded from the soleus muscle. Yet, the H reflex can be evoked in virtually all lower limb muscles, though its elicitation in some muscles requires facilitatory conditions or special techniques. Furthermore, the reflex elicitation from periphery, preserving constant stimulation conditions, is difficult to achieve, particularly during movement.

With the development of transcutaneous spinal cord stimulation (tSCS), a non-invasive method became available to excite large-diameter group Ia afferent fibers more centrally at their entry sites into the spinal cord (Minassian et al., 2007; Danner et al., 2011). This technique uses a pair of stimulation surface electrodes, placed on the back over the lumbosacral spinal cord (approx. between the 11th and 12th thoracal vertebrae process), as well as a pair of indifferent electrodes over the abdomen. It was shown that a single stimulus pulse, applied at this site, elicits short-latency responses in multiple lower limb muscle groups, bilaterally at the same time (Minassian et al. 2007; 2011; Hofstötter et al., 2008). According to their initiation and recording site, these responses are called posterior-root muscle (PRM) reflexes. They were shown to have similarities to the classical H reflex evoked peripherally (Minassian et al., 2011). Minassian and colleagues

(2007) also demonstrated the reflex nature of the elicited responses, by testing the refractory behavior by applying double pulses at different inter-stimulus intervals and by modifying the responses by vibration, as well as different active and passive manoeuvres.

Further, Hofstötter et al. (2008) used tSCS as investigative tool to assess modifications of sensory-motor transmission during the execution of different volitional and postural motor tasks, in subjects with intact CNS. They found, that the gain of the PRM reflexes elicited in the lower limb muscles was characteristically modulated, reflecting the functional requirements of a particular task. Leaning forward, for instance, was shown to be accompanied by an increase of the PRM reflex amplitudes recorded from hamstrings and triceps surae, i.e. from muscle groups that are normally activated during this particular task in order to preserve equilibrium. Furthermore, the group showed that during unilateral dorsiflexion of the ankle, PRM reflexes of hamstrings and triceps surae were generally depressed, while the responses in quadriceps and tibialis anterior were generally facilitated. Yet, the results obtained from the different subjects partially showed profound inter-individual variations. Taking into account the findings of Dimitrijevic et al. (1992), showing different co-activation patterns of the lower limb muscles (and thus, different central states of activity) during various levels of sustained and intermittent activation of TA, it is conceivable that the PRM reflexes elicited during dorsiflexion of the ankle will be modified differentially depending on the produced force (not monitored in the study of Hofstötter et al., 2008).

Taking these facts together, the aims of the present thesis were:

1. To build the equipment necessary to monitor the force produced during a unilateral dorsiflexion of the ankle, performed in supine, sitting, and standing position.
2. To verify the functional suitability of this equipment by repeating the measurements done by Dimitrijevic and colleagues (1992).
3. To assess the gain of sensory-motor transmission at several lumbosacral spinal cord levels simultaneously and bilaterally, in subjects with intact CNS function, during the execution of an unilateral ankle dorsiflexion at defined levels of produced force in supine and standing position.

Materials and methods

Subjects

Six volunteers (4 male and 2 female, mean age 25.0 years \pm 3.9 years) with intact nervous system participated to this study. The stimulation procedures employed were approved by the local ethics committee.

Data acquisition and recording set-up

Force measurement

The force produced during a unilateral dorsiflexion of the ankle was measured. Figure 1 shows the essential steps for the force measurement.

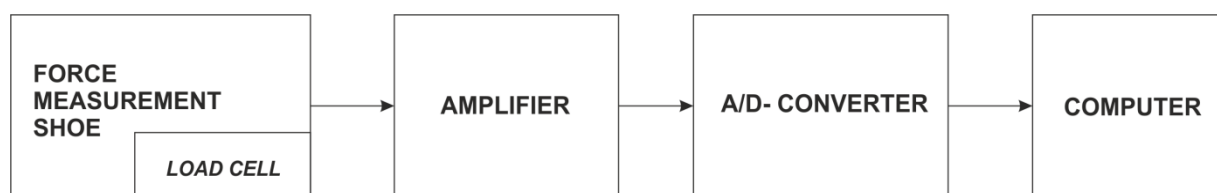


Figure 1. Flow chart for force measurement procedure.

To measure the produced force, the exercised foot was fixated via strap and buckle in a specially designed force measurement shoe (in the following, referred to as ‘shoe’, Fig. 2).

The shoe consisted of a rotatable plate, a custom built load cell and a rigid frame and was attached to a rigid platform. The pivot point of the rotatable plate matched the center of the ankle joint. When performing a dorsiflexion, the force was transmitted via the rotatable plate to the load cell.

There are different strategies how to generate this force. In order to make measurements inter-individually comparable, the subjects were instructed to pull their forefoot upwards while the heels should be pressed downwards against the platform.

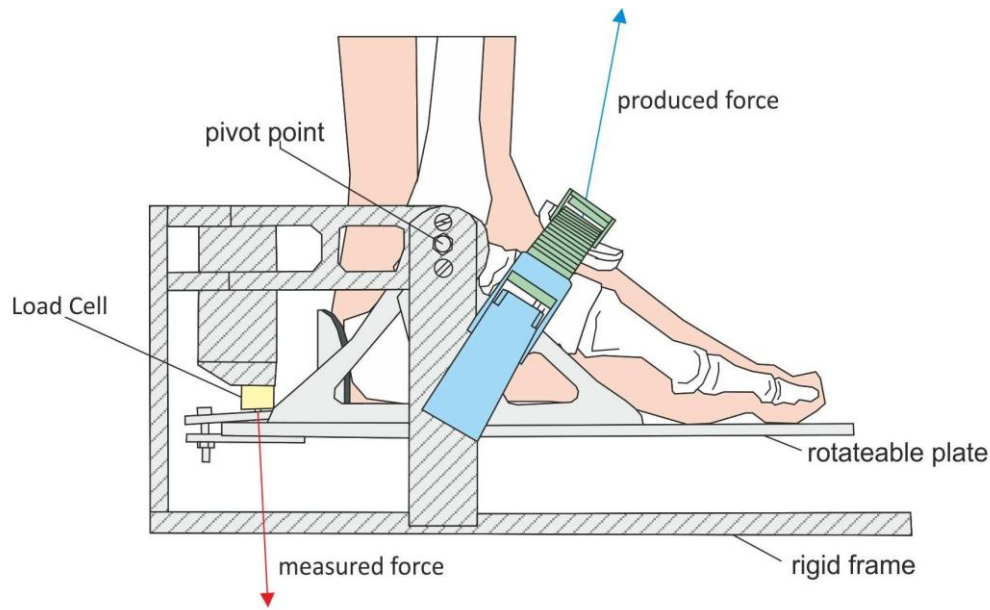


Figure 2. Sketch of the specially developed force-measurement shoe ('shoe') to measure the force produced by a unilateral dorsiflexion of the foot. Main parts are the rigid frame, the rotateable plate, as well as the load cell. Fixation of the exercised foot is achieved via strap and buckle.

The load cell measuring the produced force was manufactured at the Center for Medical Physics and Biomedical Engineering (Medical University of Vienna, Austria) and designed for the measurement of stretch- and compression-forces. Four 120- Ω strain gauges forming a half bridge were embedded into the device. The sensitivity of the load cell was 2 mV/V and the maximum strain was limited to 1000 N. Figure 3 shows a sketch of the load cell (Fig. 3A) along with the implemented circuit diagram (Fig. 3B). The load cell was connected to the amplifier using a 4-pole LEMO connector (Munich, Germany; cf. Fig. 4B).

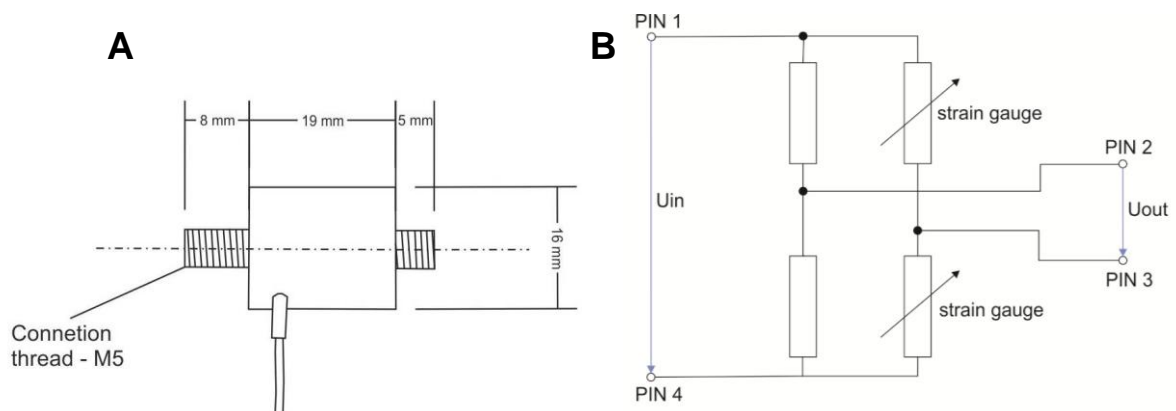


Figure 3. Illustration giving details on the load cell. **(A)** Sketch of the load cell and its dimensions. **(B)** Circuit diagram showing inner wiring and components along with according pin-out (cf. Fig. 4B)

The force signal (range: ± 10 mV) was amplified using a LAU 64.200 amplifier (Sensor Techniques Limited, Cowbridge, UK) set to a gain of 4 with a low-pass filter at 200 Hz. Figure 4 shows the circuit diagram (Fig. 4A), pin-out (Fig. 4B) and housing (Fig 4C) of the amplifier.

R_1 and R_2 were required to achieve an overall-resistance $>350 \Omega$, which was a limitation of the amplifier. The output current was within a range of 4 mA – 20 mA, the corresponding output voltage amounted to 1.08 V - 5.4 V (readout-resistor $R_3 = 270 \Omega$). Offset correction of 0.6 mV/V was used.

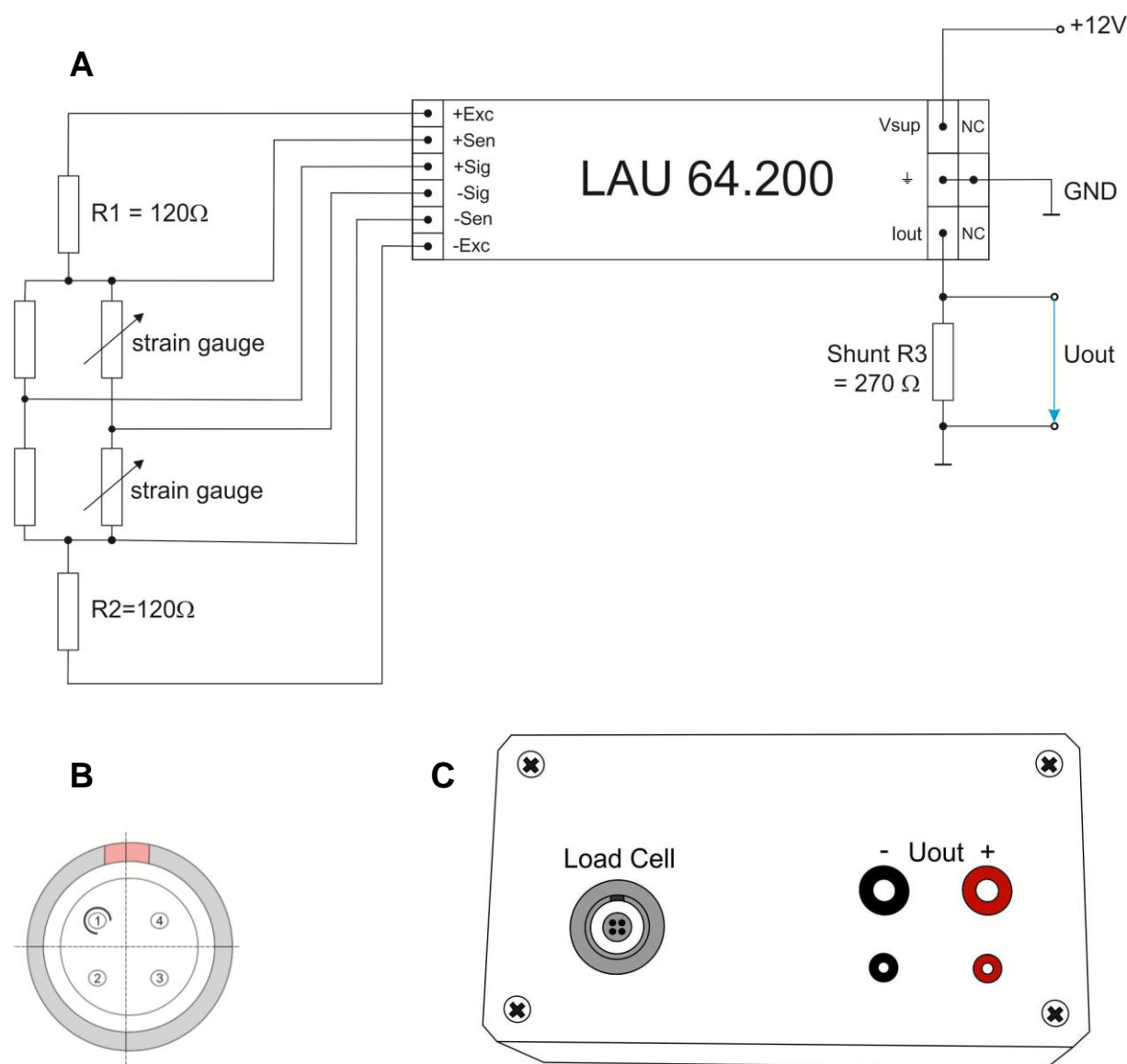


Figure 4. Illustration giving details of the amplifier. (A) Circuit diagram of the amplifier along with its components. (B) Pin assignment of the 4-pole LEMO connector used for the load cell. (C) Housing of the amplifier with connectors for the load cell, and output voltage; additional connector for 12 VDC voltage supply.

The NI PCI-6221 analog-digital converter (A/D converter, National Instruments Corporation, Austin, TX, USA) set at a sample rate of 2 kS/s was used. Data were recorded using DasyLab (Measurement Computing, Norton, MA, USA) and digitally low-pass filtered at 10 Hz with a second order Butterworth-filter. The recorded signal was converted into forces using following equations:

$$F = \frac{U_{out}-d}{k}; \text{ load} = \frac{F}{9.81 \text{ m/s}^2}.$$

Slope k and offset d were determined by linear regression during the calibration (for details see below).

Calibration of the system

Prior to the recordings with the subjects, the force measurement device was calibrated to allow for correlation between the measured voltage and the applied load. To this end, the shoe was turned upside-down and fixated on the rigid platform while defined loads were applied (Fig. 5). Table 1 describes the equipment employed for calibration, and Table 2 gives an overview over the weights used in different configurations.

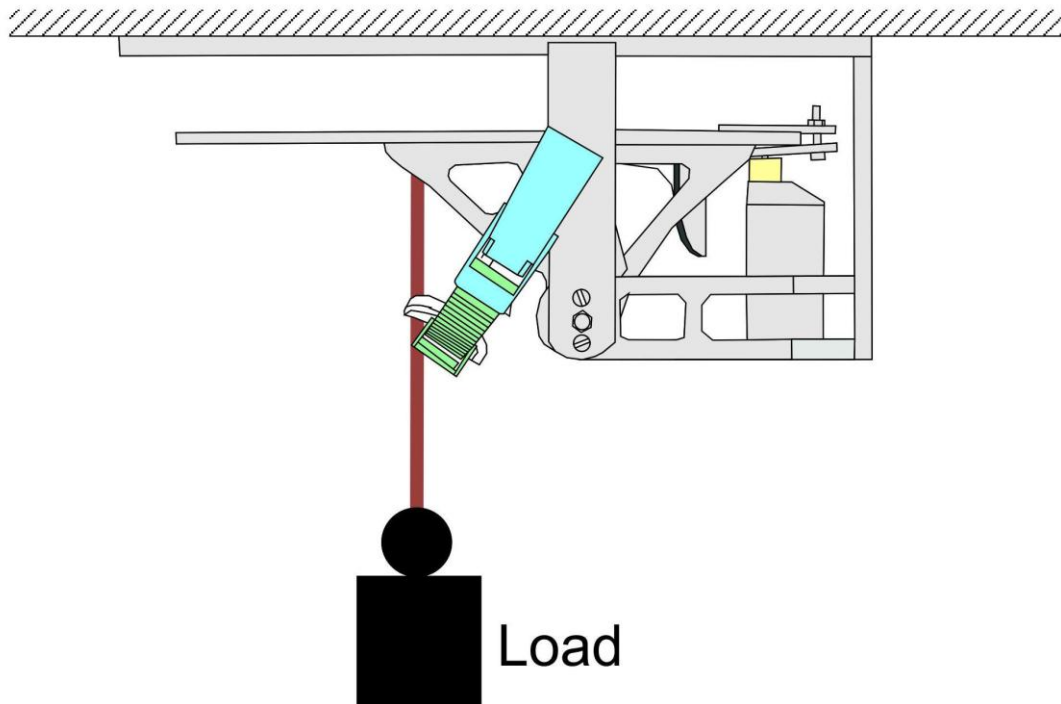


Figure 5. Test set-up for calibration of the force measurement device. The shoe was turned upside-down and fixated on the rigid platform while defined loads were applied.

Device	Description	Application
Fluke 183	Voltmeter 1	Measures U_{out}
Fluke 175	Voltmeter 2	Measures U_{out}
Measurement shoe	Forcemeter	Measures applied force
LAU 64.200	Amplifier	Amplifies the bridge signal of the load cell

Table 1. Equipment used for calibration of the force measurement device

No.	Weight [kg]	Force [N]	Description
0	0.015	0.14715	Connecting cord
1	2.445	23.986	2.5 kg weight disc
2	2.385	23.397	2.5 kg weight disc
3	4.855	47.628	5 kg weight disc
4	4.885	47.922	5 kg weight disc
5	9.815	96.285	10 kg weight disc
6	10.185	99.915	10 kg weight disc
7	9.925	97.364	10 kg weight disc

Table 2. Weights used for calibration of the force measurement device

Table 3 summarizes the calibration protocol. In order to minimize the measuring error, two separate voltmeters were used (cf. Table 1) and the mean value of the corresponding measurements was calculated. Linear regression was applied on the resulting mean values using the method of least squares. The residual error is depicted in a separate column of Table 3. The configuration of weights can be deduced from the column labeled as “comments”. Figure 6 shows the calibration curve along with measured points as well as positive and negative standard deviation.

Weight	Force	Voltmeter 1	Voltmeter 2	Mean	Regression	Residual error x_e	Comments
[kg]	[N]	[V]	[V]	[V]	[V]	[mV]	
0.000	0.000	0.781	0.783	0.782	0.793	11.4	Shoe without load
2.460	24.133	0.758	0.750	0.754	0.752	-1.9	0+1
4.900	48.069	0.696	0.708	0.702	0.711	9.7	0+4
7.345	72.054	0.654	0.659	0.656	0.670	14.2	0+1+4
9.940	97.511	0.635	0.629	0.632	0.627	-4.4	0+7
12.385	121.497	0.601	0.603	0.602	0.586	-15.1	0+1+7
14.825	145.433	0.562	0.558	0.560	0.546	-13.8	0+4+7
17.270	169.419	0.525	0.528	0.526	0.505	-21.1	0+1+4+7
20.125	197.426	0.470	0.480	0.475	0.457	-17.5	0+6+7
22.570	221.412	0.440	0.439	0.439	0.417	-22.7	0+1+6+7
25.010	245.348	0.406	0.378	0.392	0.376	-15.9	0+4+6+7
27.455	269.334	0.348	0.333	0.340	0.335	-5.2	0+1+4+6+7
29.940	293.711	0.287	0.280	0.283	0.294	10.6	0+5+6+7
32.385	317.697	0.240	0.240	0.240	0.253	12.8	0+1+5+6+7

Table 3. Calibration-protocol; linear regression was used ($k=-0.0017$; $d=0.7929$); column “comments” show weight configuration as introduced in Table 2.

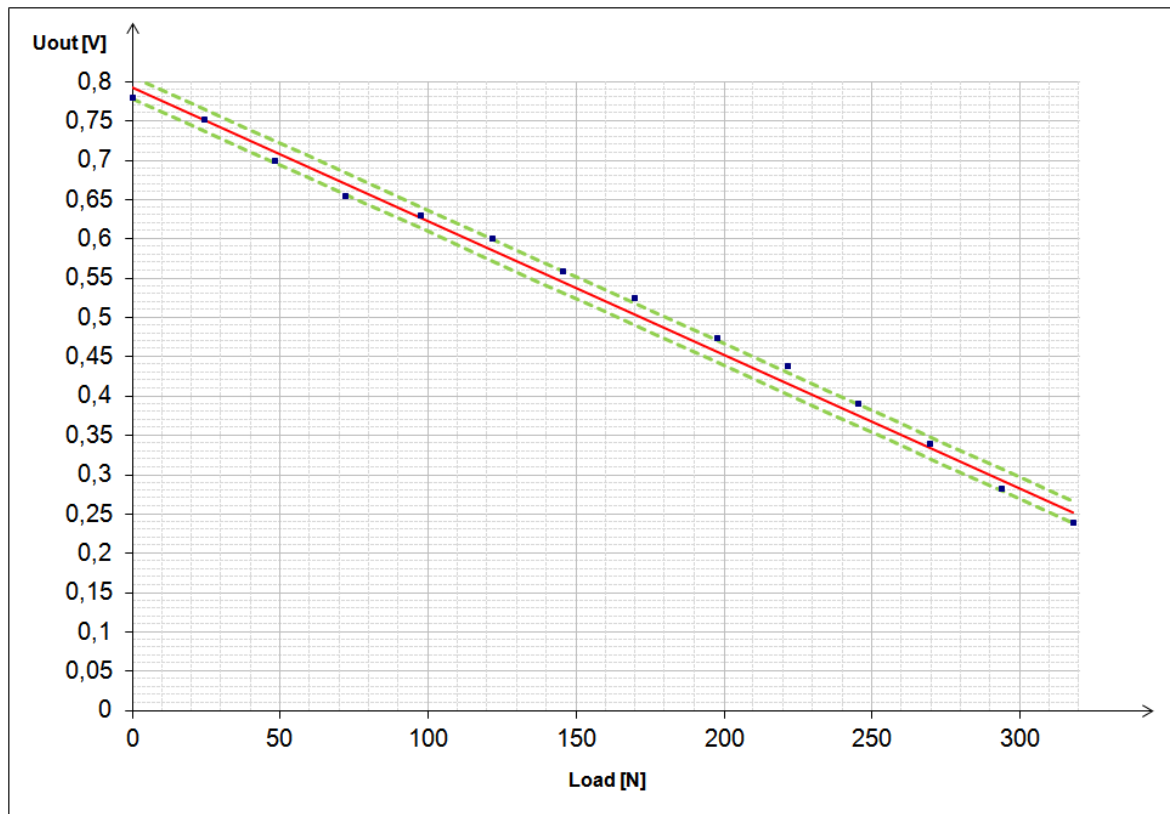


Figure 6. Calibration curve; The red curve shows the linear regression $U_{out} = k * load + d$, $k=-0.0017$, $d=0.792$. The blue dots depict the measured voltage for a certain load. The green curves are illustrating positive and negative standard deviation.

The measuring error of the force measurement was quantified by calculating the variance ($s^2 = \frac{1}{n} * \sum x_e^2$) as well as the standard deviation ($s = \sqrt{s^2}$) of the residual errors. The corresponding values amounted to:

$$\textbf{Variance: } s^2 = 192.42 \text{ mV}^2$$

$$\textbf{Standard deviation: } s = 13.87 \text{ mV}$$

This leads to a precision of $\pm 8.16 \text{ N } (\pm 0.83 \text{ kg})$.

Electromyographic recordings

The effect of unilateral sustained or intermittent (see below, *Paradigm A* and *Paradigm B*, respectively) exercise of the ankle flexor tibial anterior (TA) on the activity of several other lower limb muscles bilaterally was studied. To this end, electromyographic (EMG) activity was recorded from quadriceps (Q), hamstrings (Ham), TA and triceps surae (TS) bilaterally using pairs of Ag/AgCl-surface electrodes (Intec Medizintechnik GmbH, Klagenfurt, Austria) placed over the respective muscle bellies with an inter-electrode distance of 3 cm (Sherwood et al. 1996; Fig. 7). An additional pair of surface electrodes was placed on the right side below the ribs, oriented antero-posteriorly to detect stimulation artifacts, produced by transcutaneous spinal cord stimulation (details see below), in order to achieve triggered recordings.

A reference electrode was placed over the left fibular head. Skin impedance was improved by preparing the skin underneath the EMG electrodes using abrasive paste.

EMG signals were amplified using a custom-built EMG system (Center for Medical Physics and Biomedical Engineering, Medical University of Vienna, Austria) set to a gain of 600 with a bandwidth of 20 Hz – 600 Hz and digitized at 2000 samples per second and channel.

Data were processed and stored using DasyLab 11 (Measurement Computing, Norton, NA, USA) and analyzed offline (for details see below and Appendix A).

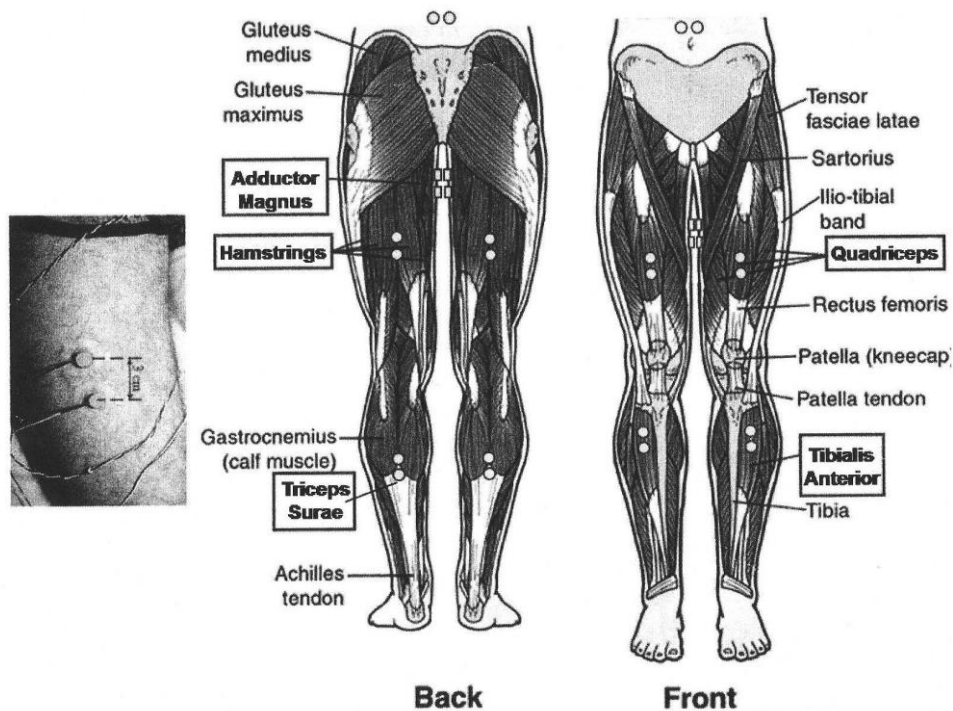


Figure 7. Placement of the EMG electrodes (Sherwood et al., 1996)

Transcutaneous spinal cord stimulation

Transcutaneous spinal cord stimulation (tSCS) was applied through self-adhesive surface electrodes (Schwa-medico GmbH, Ehringshausen, Germany). Two round stimulating electrodes (\varnothing 5 cm) were placed on the back between the T11/T12 vertebral processes, approximately 1 cm laterally to each side of the spine (Fig. 8, left). A pair of indifferent rectangular electrodes (8 x 13 cm each) was placed on the abdomen, left and right to the umbilicus. The two stimulating electrodes and the two indifferent electrodes were connected to serve as single electrodes. A voltage controlled stimulator delivered charge-balanced, symmetric, biphasic, rectangular pulses of 1 ms + 1 ms width. Double pulses with inter-stimulus intervals (ISI) of 50 ms were applied to verify the reflex nature of the elicited responses (cf. Minassian et al., 2007;2011; Hofstötter et al., 2008).

The final position of the stimulating electrodes on the back was individually adjusted (variations of up to one vertebra in rostro-caudal direction) to allow for the symmetric and simultaneous elicitation of posterior root-muscle reflexes (PRM reflexes; for details see Minassian et al., 2007; 2011; Hofstötter et al., 2008) in Q, Ham, TA, and TS bilaterally with peak-to-peak (PTP) amplitudes of ≥ 100 μ V.

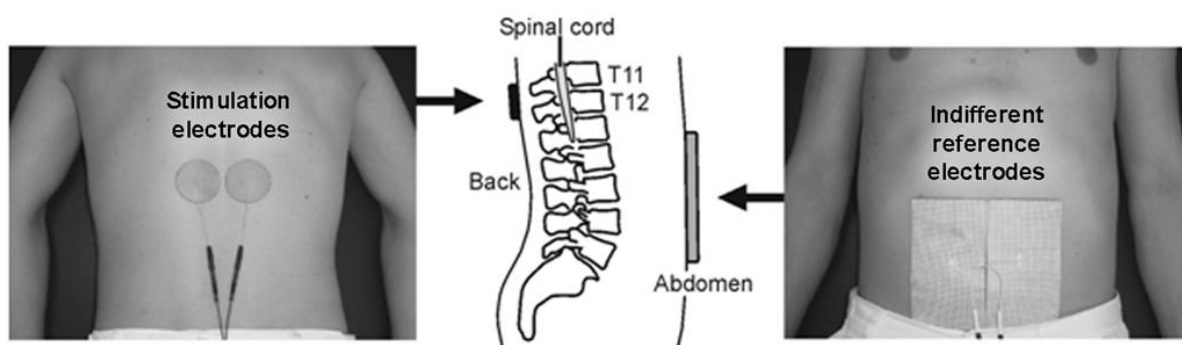


Figure 8. Position of stimulation and reference electrode placed on back and abdomen (cf. Minassian et al., 2007)

Recording protocols

Paradigm A

Paradigm A tested the changes of sustained exercise of unilateral TA on the motor outputs recorded from multiple lower limb muscles bilaterally. It was conducted with the subjects sitting on a chair that was adjusted to achieve 90° in the hip, knee and ankle joints, with one foot being fixated in the shoe that was mounted on a wooden platform allowing to place the contralateral foot on an equal level (Fig. 9).

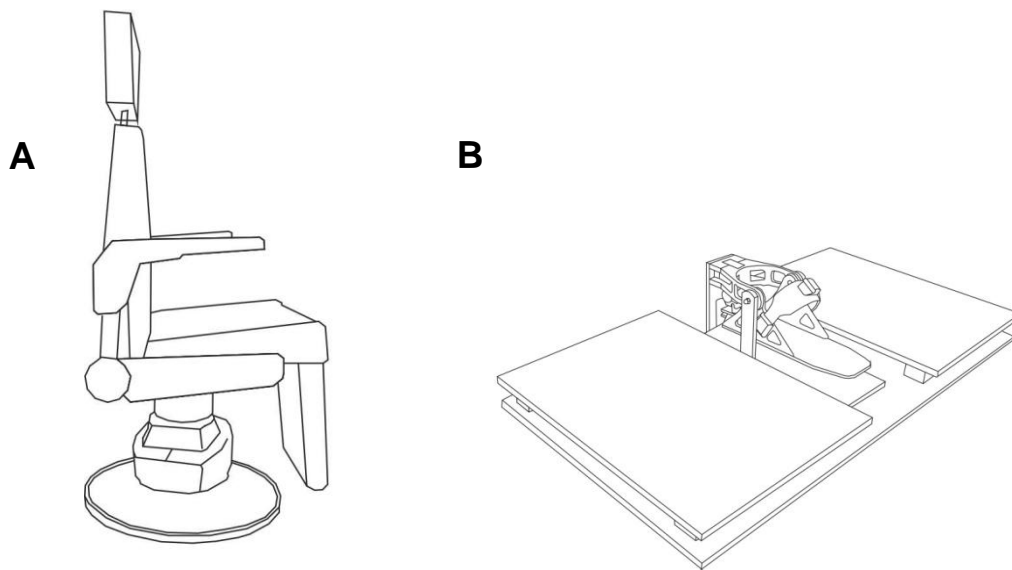


Figure 9. Illustration of equipment for Paradigm A. **(A)** An adjustable chair was used in order to achieve 90° in the hip, knee and angle joints. **(B)** The shoe was mounted on a wooden platform to place the contralateral foot on an equal level.

Prior to each measurement, the maximum force (maximum volitional contraction, MVC) that could be developed by the dorsiflexor TA of the fixated leg, was determined. For this purpose, the subjects were asked to perform a short dorsiflexion with maximum effort, while the respective force was recorded.

Paradigm A consisted of four individual recordings, intermitted by periods of relaxation, lasting for at least 3 minutes each. The flowchart of the recording procedure is shown in Figure 10.

In recording 1, subjects were asked to develop and maintain MVC of left TA without visual feedback to monitor the produced force. Once the produced force decreased to 50 % of its initial value, the recording was stopped. In recording 2, the same procedure was repeated for the right TA. In recordings 3 and 4, additional visual feedback was supplied, allowing the subjects to monitor the level of the produced force as percentage of MVC.

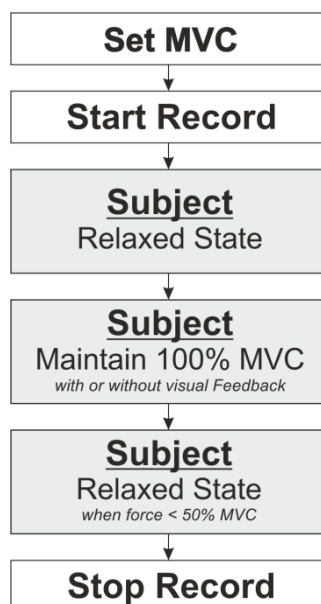


Figure 10. Flowchart of recording procedure of paradigm A. Highlighted boxes represent the different steps of the task performed by the subject. The procedure was repeated with both legs, with and without visual feedback (total of 4 recordings)

Paradigm B

Paradigm B was designed to test the effect of intermittent exercise of unilateral TA on the motor outputs recorded from multiple lower limb muscles bilaterally. It was conducted in separate recordings for left and right sides with the subjects in the supine, sitting, and standing position (total of 6 recordings).

In the standing position, the exercised foot was strapped into the shoe (Fig. 9B) while the other foot was standing directly on the wooden platform. The subjects were asked to stand upright distributing the body weight equally on both legs with the arms hanging loosely beside the body.

For the recordings in the supine position, the wooden platform (to which the shoe was mounted) was rigidly fixated on a specially designed frame on an examination bed (Fig. 11). The subjects were asked to lie relaxed on the bed with one foot strapped into to the shoe. The shoe was mounted on the same level as the lying surface. The unexercised foot rested load-free aside.

Recordings in sitting position were performed as described in Paradigm A.

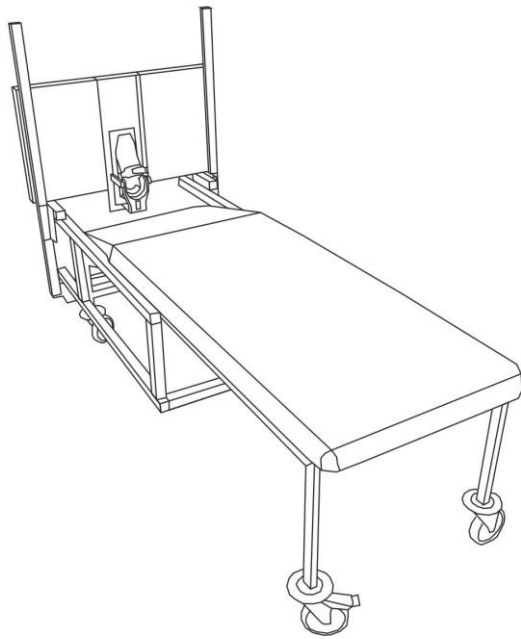


Figure 11. Sketch of examination bed with special designed frame on which the wooden platform and shoe were mounted, in order to perform measurements in supine position.

For each recording, MVC was first determined as described above (cf. Paradigm A). The recordings started with a short period of relaxation followed by periods of TA activation intermitted by periods of relaxation. The duration of the active phases was 6 s while periods of relaxation lasted for 4 s. The subjects were asked to increase the level of produced MVC during each active period in 20 %-MVC increments, starting from 20 % MVC during the first contraction period, until 100 % MVC were reached in the last contraction period. Visual feedback was provided throughout the whole measurement. After a final relaxation period (approx. 4 s), the recording was stopped (cf. flowchart given in Figure 12).

Paradigms A and B were designed in close accordance with the measurements described by Dimitrijevic and colleagues (1992).

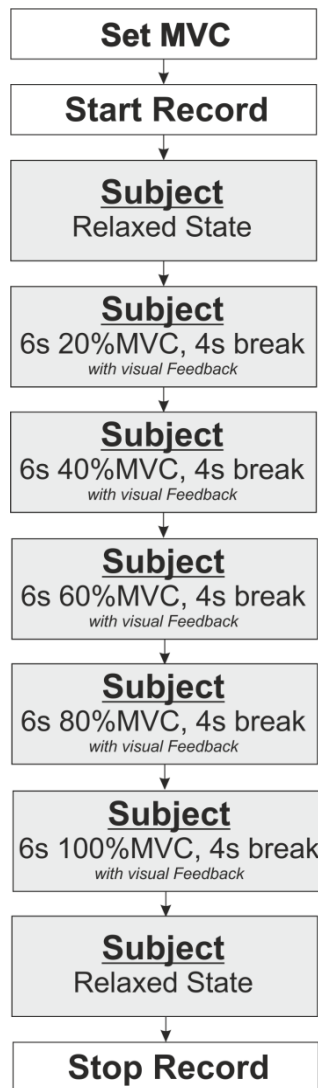


Figure 12. Flowchart of recording procedure of paradigm B; Highlighted boxes represent the different steps of the task performed by the subject. The procedure was repeated on both sides in supine, standing and sitting positions (6 recordings in total). Visual feedback was provided all the time.

Paradigm C

Paradigm C was designed to test the effect of intermittent contraction of unilateral TA on PRM reflexes. Prior to the reflex-measurements, the maximum obtainable M waves (M_{max}) of bilaterally TS were determined in prone and standing position (total of 4 recordings). To this end, single charge-balanced, symmetric, biphasic, rectangular pulses of 1 ms + 1 ms width were applied through a self-adhesive round surface electrode (\emptyset 3.2 cm), with an indifferent rectangular electrode (8 x 13 cm) placed over the patella. EMG was recorded from the stimulated TS and the ipsilateral Ham (Trigger). Stimulation intensities were stepwise increased from below motor threshold, until no further increase of the M wave was observed.

The PRM reflex studies were conducted in supine and standing position as described in Paradigm B. The applied stimulation intensities were adjusted such that the PTP amplitudes of the PRM reflexes elicited in TS amounted to approximately 30 % of the respective magnitudes of M_{\max} to allow for inter-individual comparison.

For each recording block, MVC was first determined as described above (cf. Paradigm A). All recordings started with the elicitation of five unconditioned PRM reflexes (relaxed state), followed by five responses elicited every 10 s under constant stimulation conditions but modified by the contraction level (certain percentage of MVC) of the exercised TA, using visual feedback. During each recording, the contraction level was increased stepwise by 20 % MVC, starting with 20 % until 100 % MVC were reached (cf. Fig. 13). The procedure was performed separately for both legs (total of 20 recordings).

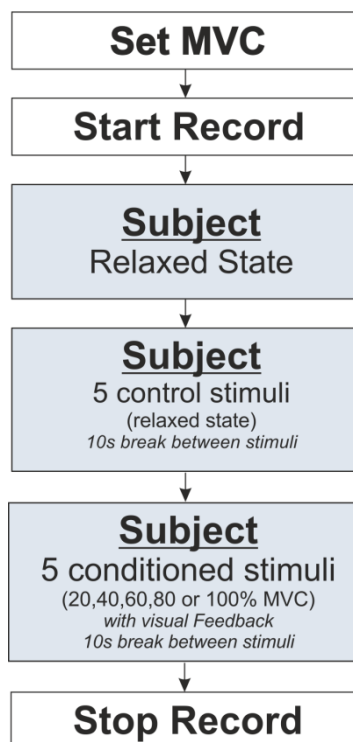


Figure 13. Flowchart of recording procedure of paradigm C; Highlighted boxes represent the different steps of the task performed by the subject. The procedure was repeated with both legs in supine and standing (total of 20 recordings)

Measurement schedule

Table 4 shows the measurement schedule and the corresponding names of the recording files.

Nr.	Description	Filename
1	TSmax – left – prone	11_LTSmax_prone
2	TSmax – left – standing	12_LTSmax_standing
3	TSmax – right – prone	11_RTSmax_prone
4	TSmax – right – standing	12_RTSmax_standing
5	Paradigm B – left – supine	21_dee_B_left_supine
6	PRM studies – left – supine – 20% MVC	31_PRM_20_left_supine
7	PRM studies – left – supine – 40% MVC	31_PRM_40_left_supine
8	PRM studies – left – supine – 60% MVC	31_PRM_60_left_supine
9	PRM studies – left – supine – 80% MVC	31_PRM_80_left_supine
10	PRM studies – left – supine – 100% MVC	31_PRM_100_left_supine
11	Paradigm B – right – supine	21_dee_B_right_supine
12	PRM studies – right – supine – 20% MVC	32_PRM_20_right_supine
13	PRM studies – right – supine – 40% MVC	32_PRM_40_right_supine
14	PRM studies – right – supine – 60% MVC	32_PRM_60_right_supine
15	PRM studies – right – supine – 80% MVC	32_PRM_80_right_supine
16	PRM studies – right – supine – 100% MVC	32_PRM_100_left_supine
17	Paradigm B – left – standing	22_dee_B_left_standing
18	PRM studies – left – standing – 20% MVC	33_PRM_20_left_standing
19	PRM studies – left – standing – 40% MVC	33_PRM_40_left_standing
20	PRM studies – left – standing – 60% MVC	33_PRM_60_left_standing
21	PRM studies – left – standing – 80% MVC	33_PRM_80_left_standing
22	PRM studies – left – standing – 100% MVC	33_PRM_100_left_standing
23	Paradigm B – right – standing	22_dee_B_right_standing
24	PRM studies – right – standing – 20% MVC	34_PRM_20_right_standing
25	PRM studies – right – standing – 40% MVC	34_PRM_40_right_standing
26	PRM studies – right – standing – 60% MVC	34_PRM_60_right_standing
27	PRM studies – right – standing – 80% MVC	34_PRM_80_right_standing
28	PRM studies – right – standing – 100% MVC	34_PRM_100_right_standing
29	Paradigm B – left – sitting	23_dee_B_left_sitting
30	Paradigm A – left – sitting – without Feedback	41_dee_A_left_-FB_1
31	Paradigm B – right – sitting	23_dee_B_right_sitting
32	Paradigm A – right – sitting – without Feedback	43_dee_A_right_-FB_1
33	Paradigm A – left – sitting – with Feedback	42_dee_A_left_+FB_1
34	Paradigm A – right – sitting – with Feedback	44_dee_A_right_+FB_1

Table 4. Measurement schedule and corresponding filenames

Data analysis

Data analysis was structured into two parts. The primary data analysis was performed on the saved raw data (ASCII-files) using Matlab R2010a (The MathWorks Inc., Natick, MA, USA). Data were exported using Microsoft Excel (Microsoft, Redmond, Washington, USA), with one worksheet being generated for each subject.

Secondary data analysis, combining the results obtained from the different subjects, was performed using Excel.

Paradigm A

Following parameters were determined:

- Duration:** Time between start and end of exercise.
- Onset-time:** Time between start of exercise and co-activation of a certain muscle group other than ExTA.
- Onset-force:** Force at the time when a certain muscle group other than ExTA became co-activated.
- Recruitment order:** Sequence in which particular muscle groups were co-activated.

Primary data analysis

For data analysis of paradigm A the routine “*analysis_paradigm_A.m*” was used. To quantify the amount of muscular activity (using the root mean square, RMS), the subroutine “*emg2rms.m*” was implemented. Another subroutine “*emg2rmsmean.m*” calculated the RMS of a given EMG sequence. For further information see ‘Appendix B/Matlab Source Codes/analysis_paradigm_A.m’, ‘Appendix B/Matlab Source Codes/emg2rms.m’ and ‘Appendix B/Matlab Source Codes/emg2rmsmean.m’.

EMG data was filtered using a second order Butterworth-filter ($f_g = 10 \text{ Hz} - 700 \text{ Hz}$). The analysis was performed semi-automatically. First, the operator identified the interval within the recording for which the analysis was performed in order to obtain the following values:

- **RMS Mean 0:** Calculated mean of muscular activity (using RMS) during rest.
- **RMS min:** Minimum of muscular activity during exercise.
- **RMS max:** Minimum of muscular activity during exercise.
- **RMS mean:** Mean of muscular activity during exercise.
- **RMS Std:** Standard deviation of muscular activity during exercise.
- **Onset:** Time elapsed from start of exercise to particular muscle activation ($\text{RMS} > 20\mu\text{V}$).
- **Duration:** Duration of exercise.
- **MVC:** Maximum measured Force during exercise.
- **F@ Onset:** Force at the beginning of the exercise.
- **F@ End:** Force at the end of the exercise.
- **Baseline:** Baseline of force during rest.

Figure 14 shows an overview of the whole data given by the data set. The first eight traces show EMG data of all studied muscle groups, the last one shows the produced force.

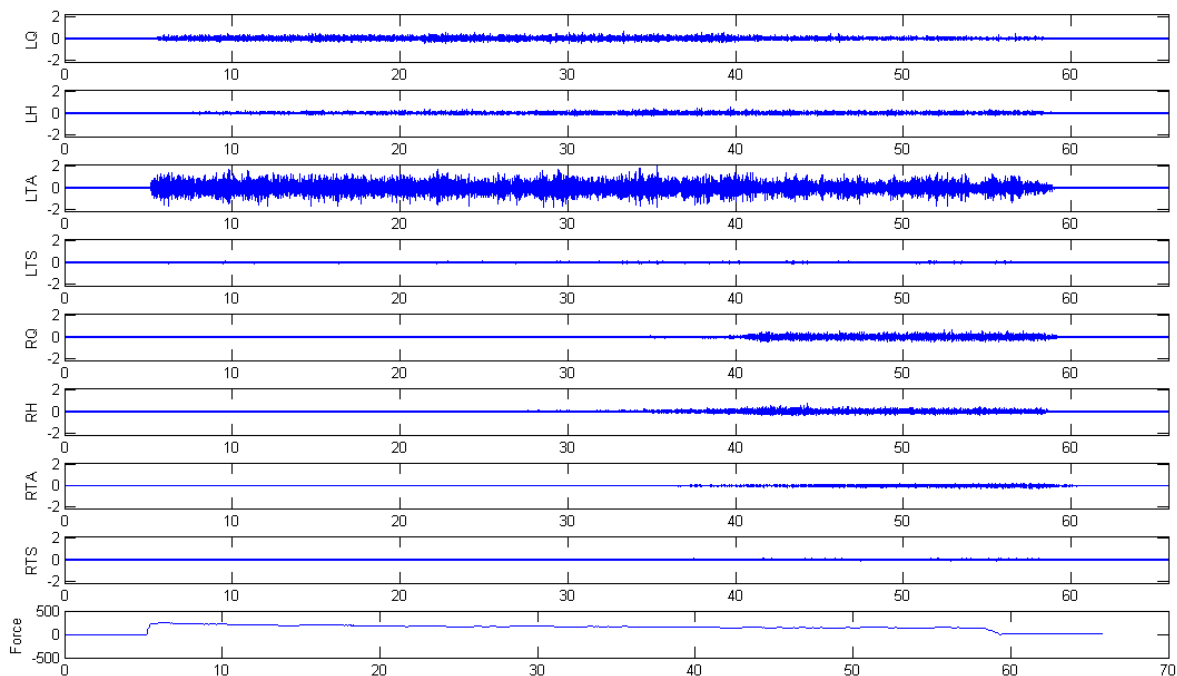


Figure 14. Example of data-overview showing EMG of LQ, LHam, LTA, LTS, RQ, RHam, RTA, RTS along with produced force. Data derived from subject 3 exercising LTA.

Certain limits were determined within every record (cf. Figure 15). Line (1) is the baseline of the force in resting state. Lines (2) and (3) are the boundaries for the resting state which are used to determine the ground tone. Lines (4) and (5) determine the beginning and the end of the exercise.

Some data was excluded from further analysis because the task was not executed properly. The exclusions were performed manually by evaluating the force diagram.

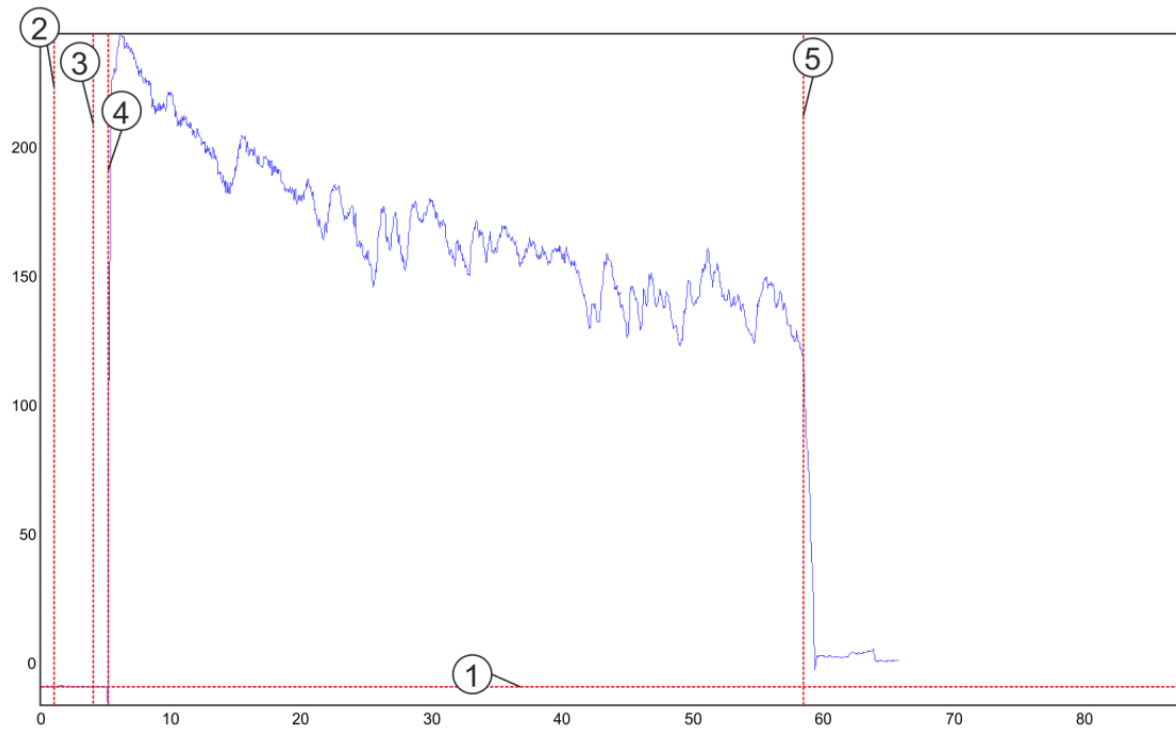


Figure 15. Example for annotated force diagram; Line (1) is the baseline of the force in resting state. Lines (2) and (3) are the boundaries for the resting state. Lines (4) and (5) determine the beginning and the end of the exercise. Data derived from subject 3 exercising LTA.

Each muscle group was analyzed for its activation. The threshold for a muscle to be considered as active was set to a value of 20 μV (cf. Dimitrijevic et al., 1992). A diagram, as shown in Figure 16, was used to determine the onset time of activation. The figure shows the rectified EMG data (blue curve) along with the calculated RMS signal (green curve). The horizontal line (1) shows the threshold of 20 μV . Line (2) was set to the first position where the RMS signal was clearly greater than the threshold. Lines (3) and (4) show the beginning and the end of the exercise.

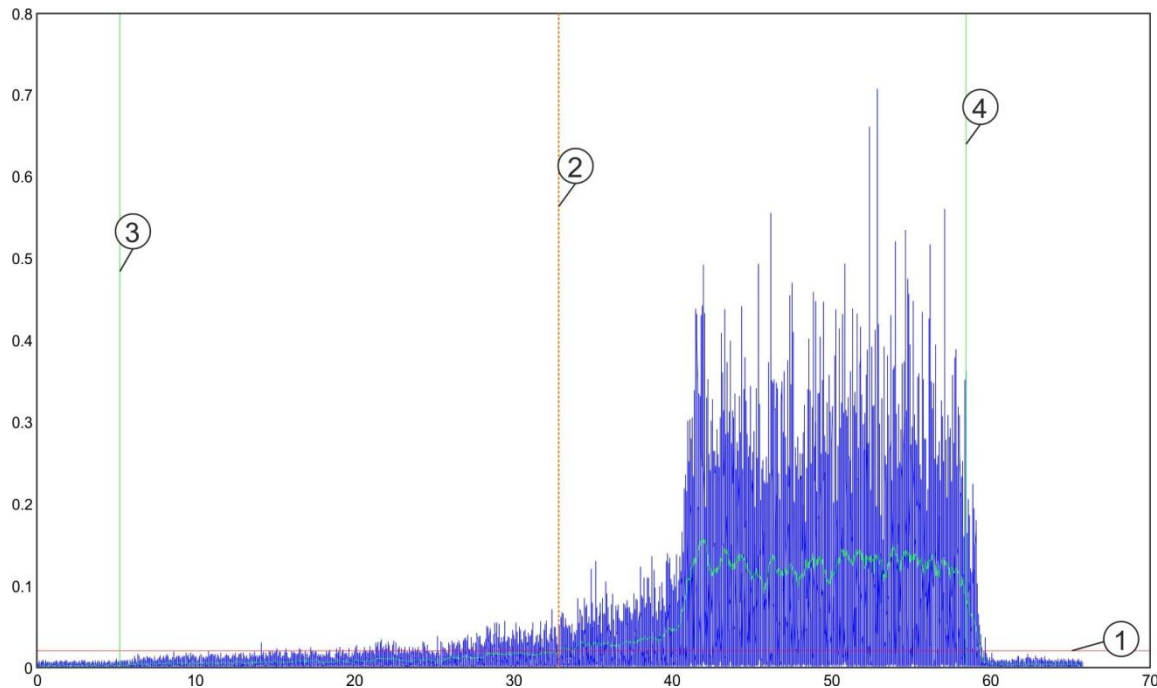


Figure 16. Example for selection of muscle activation; Diagram showing rectified EMG data recorded from RQ (blue curve) along with the calculated RMS signal (green curve). The horizontal line (1) marks the 20 μV threshold used to determine muscle activation. Line (2) was set to the first time position where the RMS signal was clearly greater than the threshold (onset time of activation). Lines (3) and (4) show beginning and end of the exercise. Data derived from subject 3.

Secondary data analysis

Duration

The values obtained for both lower limbs were intra-individually averaged for the trials with and without visual feedback. Mean group values were calculated on the basis of the resultant 6 values collected in the 6 subjects.

Onset times of activation

Onset times were analyzed separately for each muscle group (ipsi- and contralaterally) as well as for recordings with and without visual feedback. Mean group values were obtained as specified above.

Onset-force

Onset-forces were determined for recordings with and without visual feedback. Absolute values were normalized with respect to the MVC to allow for inter-individual comparison, mean values were computed like stated above.

Recruitment order

The recruitment order of the studied lower limb muscles was analyzed separately for each recording. The sequence of activation was determined on the basis of the onset-times for the different muscles.

It was counted how often a particular muscle group was co-activated as first, second, third, fourth or not at all. Data where the task was not executed properly were excluded.

The number of cases in which a particular muscle group was co-activated as first, second, third, fourth or not at all was then converted into percentages of the total number of valid samples.

Paradigm B

Primary data analysis

For data analysis of Paradigm B the routine “*analysis_paradigm_B.m*” was used. The amount of EMG activity during the execution of a unilateral dorsiflexion at a particular force level was calculated as RMS for each muscle group using “*emg2rmsmean.m*”. For further information see ‘Appendix B/Matlab Source Codes/*analysis_paradigm_B.m*’ and ‘Appendix B/Matlab Source Codes/*emg2rmsmean.m*’.

EMG data was filtered using a second order Butterworth-filter ($f_g = 10 \text{ Hz} - 700 \text{ Hz}$). The analysis was performed semi-automatically. First, the operator identified the interval within the recording for which the analysis was performed in order to obtain the following values:

- **RMS XX:** XX stands for LQ, LHam, LTA, LTS, RQ, RHam, RTA or RTS. RMS XX represents the RMS calculated for the respective muscle group during dorsiflexion at a certain force level (in % MVC).
- **Force:** Actually produced force in N during the phases of exercise at a certain percentage of MVC (target-value)
- **Std_Force:** Standard deviation of force.

Figure 17 shows an exemplary data set obtained when performing Paradigm B. EMG activities recorded from the thigh and lower leg muscle groups ipsilateral to the exercise are shown along with the channel capturing the produced force.

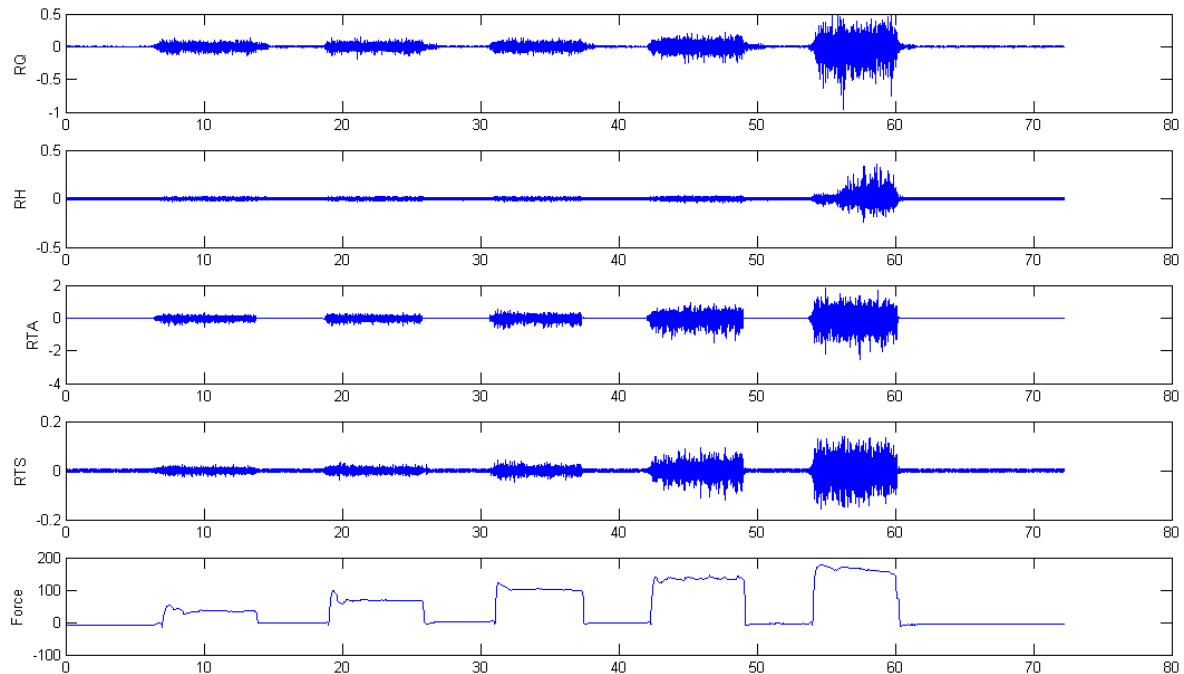


Figure 17. Example for data overview (exercised side); The top four traces show the recorded EMG activities. The last one shows the corresponding produced force. Data derived from subject 2.

The selection of certain limits was performed manually as follows (cf. Fig. 18):

- (1) Baseline
- (2)-(3) Resting state (0 % MVC)
- (4)-(5) dorsiflexion at 20 % MVC
- (6)-(7) dorsiflexion at 40 % MVC
- (7)-(8) dorsiflexion at 60 % MVC
- (9)-(10) dorsiflexion at 80 % MVC
- (11)-(12) dorsiflexion at 100 % MVC

Areas were selected such that initial periods of force development, generally exceeding the targeted value, were excluded from further analysis. Whole data sets were excluded from further analysis if the task was not executed properly. RMS and mean forces were calculated within the selected areas and exported in an Excel-file for secondary analysis.

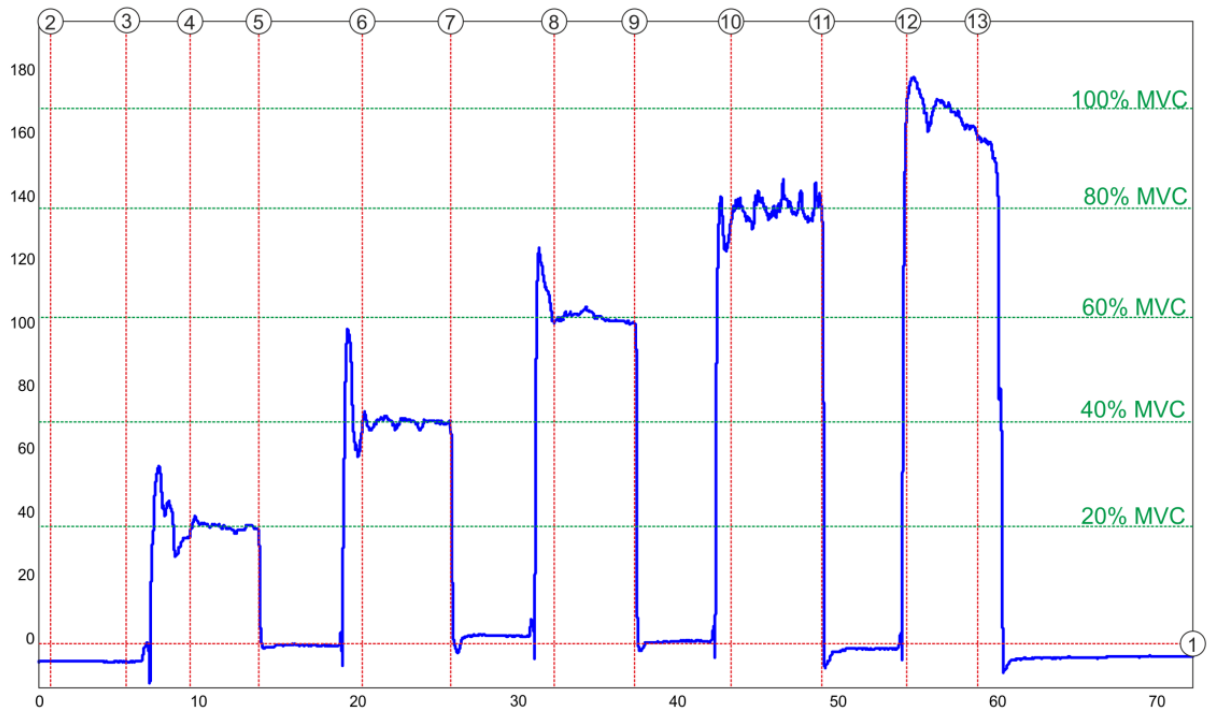


Figure 18. Example of area selection in force diagram(blue curve); Lines: (1) baseline,(2)-(3) resting state, (4)-(5) contraction with 20 % MVC, (6)-(7) contraction with 40 % MVC, (8)-(9) contraction with 60 % MVC, (10)-(11) contraction with 80 % MVC), (12)-(13) contraction with 100 % MVC

Secondary data analysis

Recruitment order

The recruitment order of the studied lower limb muscles to become co-activated was analyzed separately for supine, standing and sitting position

Paradigm C

Data were analyzed in order to compare peak-to-peak amplitudes of PRM reflexes. The ratio between control and conditioned response was calculated.

Primary data analysis

For data analysis the routine "*analysis_paradigm_C.m*" was implemented. For further details see '*Appendix B/Matlab Source Codes/analysis_paradigm_C.m*'.

Data were filtered using a second order Butterworth-filter ($f_g = 10 \text{ Hz} - 700 \text{ Hz}$). The analysis was performed automatically by adjusting the boundaries of the evaluation window.

PTP values of unconditioned and conditioned PRM reflexes were determined for all muscle groups. Results were exported into an Excel-file for further analysis.

Secondary data analysis

PTP amplitudes of the conditioned PRM reflexes were normalized with respect to the corresponding values of the unconditioned controls. Mean values were obtained for all contraction levels and subjects.

M_{max} measurement

Data were analyzed to evaluate the maximum obtainable M wave separately for both lower limbs using “*analysis_Mmax.m*” (for further details see ‘Appendix B/Matlab Source Codes/*analysis_Mmax.m*’). PTP amplitudes of the M wave were determined automatically and exported into an Excel-file. Maximum values were documented.

Figure 19 shows the user interface of the analysis program used to determine M_{max} . EMG responses of TS elicited by five consecutively stimuli applied to the tibial nerve in the popliteal fossa are shown superimposed. Data were filtered using a second order Butterworth-filter ($f_g = 10 \text{ Hz} - 700 \text{ Hz}$).

The dotted vertical bars represent the evaluation window for the automatic PTP calculation. If automatic evaluation was not possible, values were determined manually using crosshairs (copyright Darren Weber, <http://www.mathworks.com/matlabcentral/fileexchange/1038-plot-crosshairs>, December 2002).

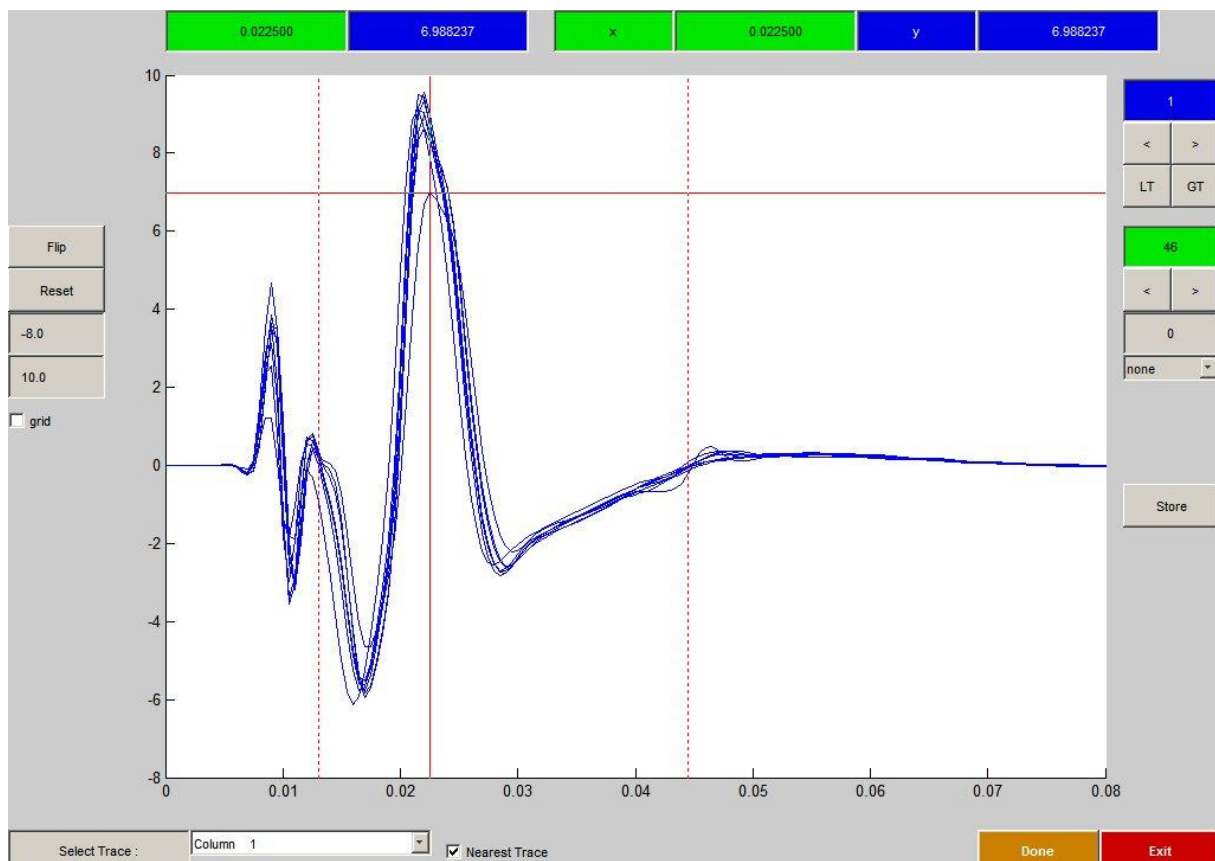


Figure 19. User-interface of analysis program “*analysis_Mmax.m*”; The EMG responses of TS were superimposed. The dotted vertical bars represent the evaluation window for the automatic PTP calculation. If automatic evaluation was not possible, values could be determined manually using crosshairs.

Results

Paradigm A

When performing a sustained volitional unilateral contraction of the ankle dorsiflexor, co-activation was observed in most muscle groups of both lower limbs. Muscles on the ipsilateral side were generally co-activated earlier than those on the contralateral side. In the trials with visual feedback shorter onset-times were usually observed. Figure 20 shows representative examples of typical recording sessions without (Fig. 20A) and with (Fig. 20B) visual feedback being provided. Displayed are EMG activities recorded from muscle groups ipsilateral and contralateral to the exercised TA (ExTA), along with a trace illustrating the produced force.

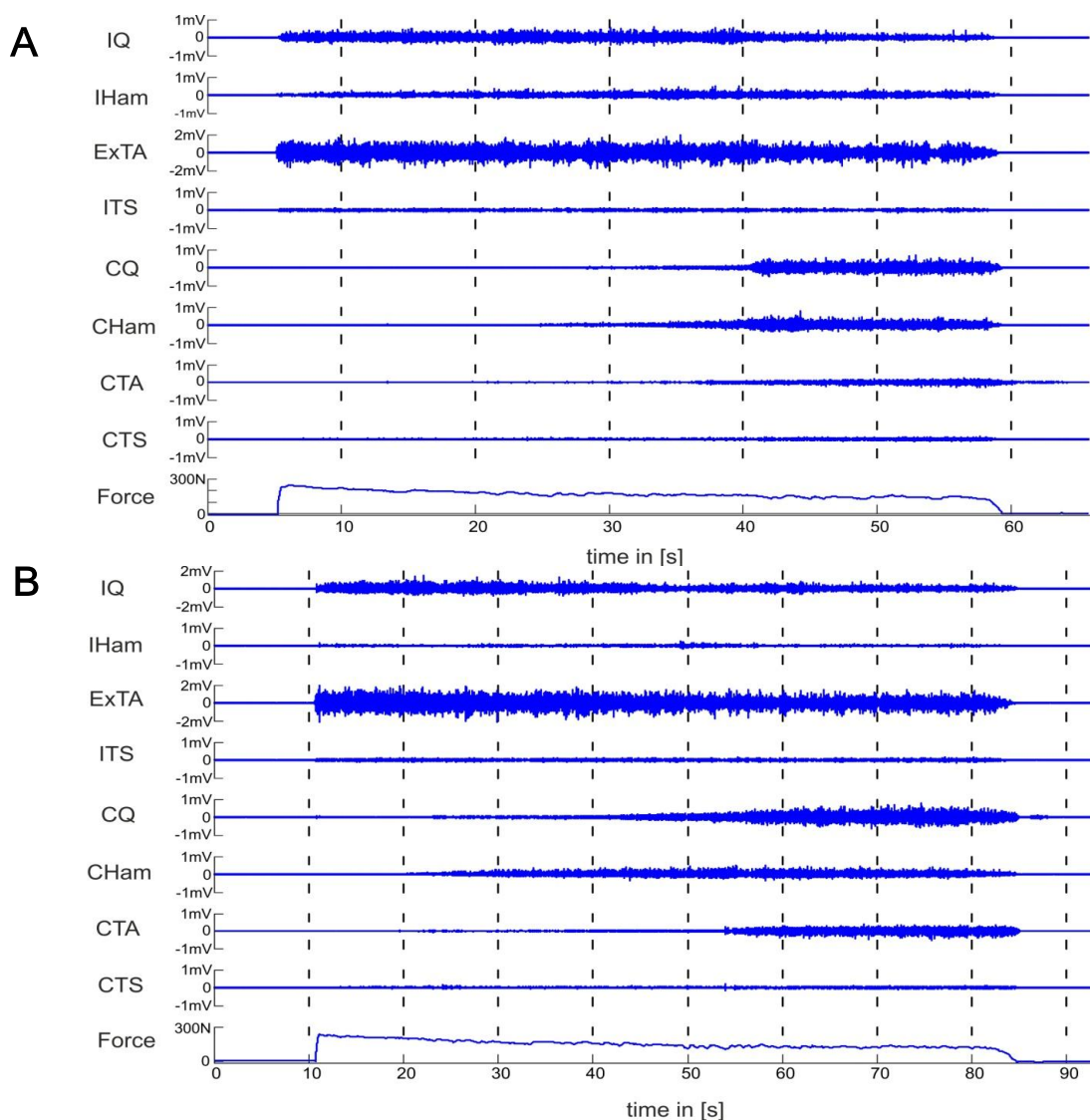


Figure 20. EMG activities recorded from ipsilateral quadriceps (IQ), ipsilateral hamstrings (IHam), exercised tibialis anterior (ExTA), ipsilateral triceps surae (ITS), contralateral quadriceps (CQ), contralateral hamstrings (CHam), contralateral tibialis anterior (CTA) and triceps surae (CTS) during sustained unilateral dorsiflexion of the ankle, along with a trace giving information on the produced force. Trials were recorded without (A) and with (B) provided visual feedback, of the produced force. Data was derived from subject 3 exercising LTA. Note the different scaling.

A separate force diagram was used to display the produced force in % of MVC (Fig. 21). The task was ended when the produced force dropped distinctly under the 50 % MVC threshold. Short peaks below the threshold were tolerated.

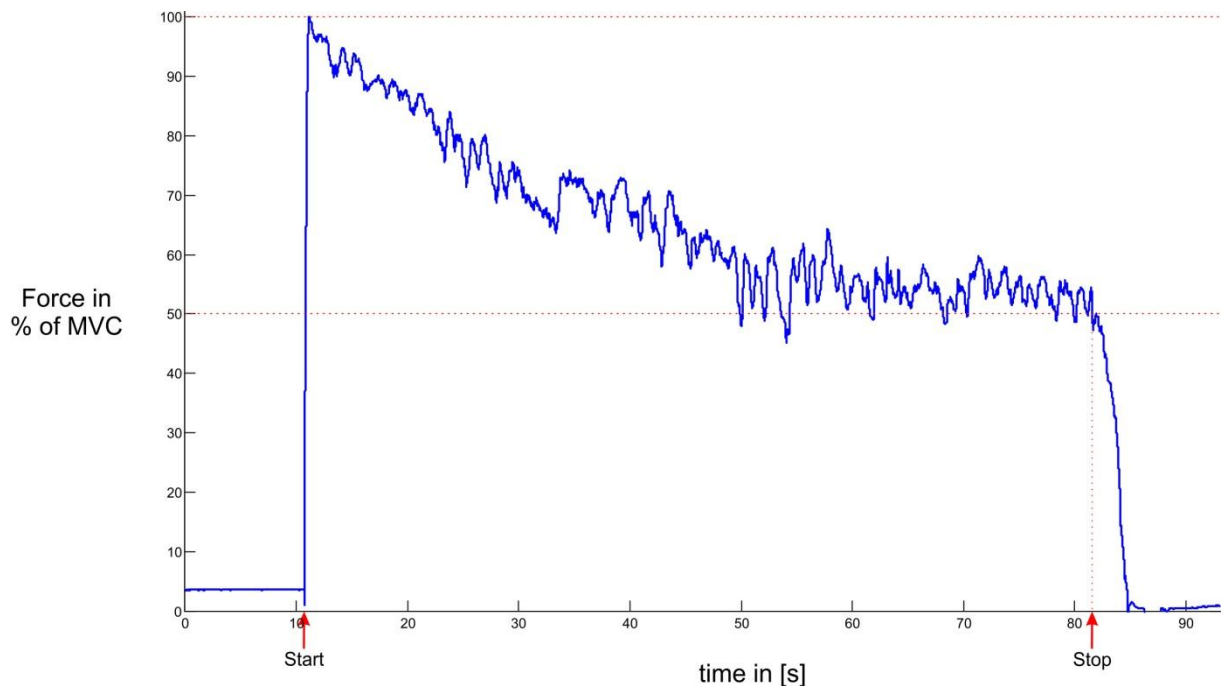


Figure 21. Illustration of produced force given as percentage of MVC (blue curve) during dorsiflexion of the left ankle. Red arrows are marking the beginning and the end of the task. The task was ended when the force dropped distinctly below 50 % MVC. Data derived from subject 3.

Durations

Mean durations from the beginning of the task, until the force dropped below 50 % MVC, amounted to $65.8 \text{ s} \pm 13.7 \text{ s}$ in the trials without visual feedback, and to $59.8 \text{ s} \pm 11.1 \text{ s}$ in the recordings with visual feedback of the produced force being provided.

Onset-forces and Onset-times

Onset-forces and onset-times were evaluated separately for lower limb muscle groups ipsi- and contralateral with respect to the ExTA. The first co-activation always occurred on the ipsilateral side.

The produced force, when the first ipsilateral muscle groups became co-activated, was $97.6 \% \pm 3.9 \% \text{ MVC}$ on average (mean of 10 samples) without visual feedback. In the recordings with visual feedback being provided, a mean onset-force of $97.2 \% \pm 3.6 \% \text{ MVC}$ (mean of 9 samples) was observed.

Regarding to the co-activation of muscle groups contralateral to the exercised ankle flexor, the onset-force without visual feedback amounted to $79.3 \% \pm 9.3 \%$ on average (mean of 8 samples). The corresponding value with visual feedback was $80 \% \pm 13.2 \% \text{ MVC}$ (mean of 8 samples). Figure 22A summarizes the observed onset-forces.

Onset-times without visual feedback were $0.5 \text{ s} \pm 0.8 \text{ s}$ for the ipsilateral and $19.1 \text{ s} \pm 10.7 \text{ s}$ for the contralateral muscle groups of the lower limb.

Providing visual feedback led to onset-times of $1.3 \text{ s} \pm 1.8 \text{ s}$ (ipsilateral muscle groups) and $12.3 \text{ s} \pm 6.1 \text{ s}$ (contralateral muscle groups). A diagram summarizing these results is given in Figure 22B.

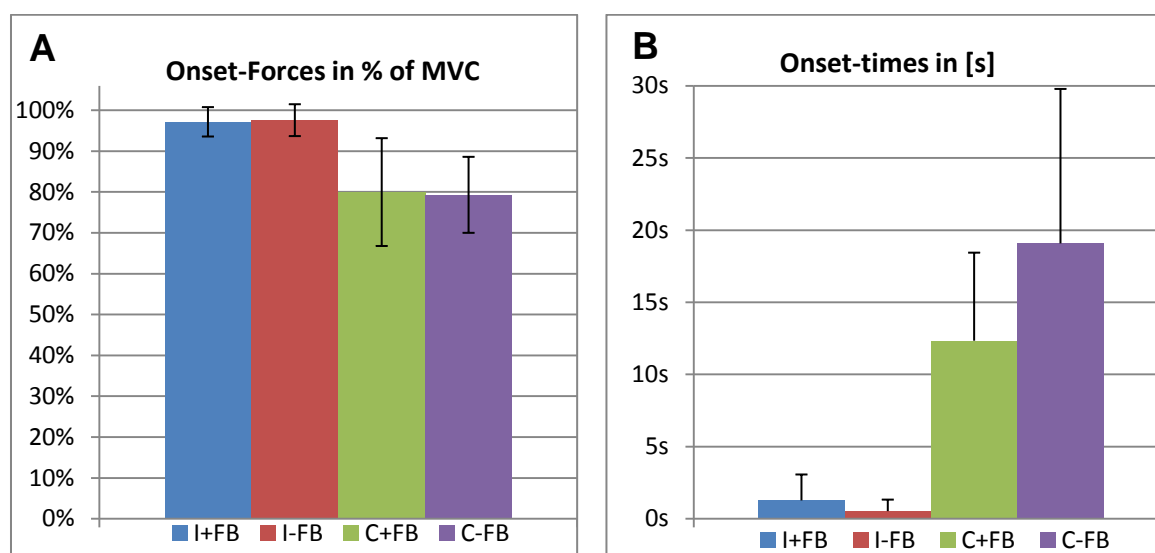


Figure 22. Diagram of onset-forces and onset-times. Results are summarized for ipsilateral muscles with visual feedback (I+FB; blue bar), ipsilateral muscles without visual feedback (I-FB; red bar), contralateral muscles with visual feedback (C+FB; green bar) and contralateral muscles without visual feedback (C-FB; violet bar). **A)** Onset-forces in % of MVC (\pm standard deviation) produced by ankle dorsiflexion, when the first lower limb muscles were co-activated. **B)** Onset-times in s (\pm standard deviation) of co-activation of the first lower limb muscles.

Recruitment order

The recruitment order of all studied muscle groups was evaluated separately for the ipsi- and contralateral lower limbs with respect to the exercised dorsiflexor. It was counted how often a particular muscle group was co-activated at first, second, third, fourth or not at all. The corresponding values of each studied muscle group, given as a percentage of the total number of valid recordings, are summarized in Table 5.

Without visual feedback IQ was co-activated in all subjects and recordings, usually as first one. Co-activation of IHam occurred in 60 % of all measurements and usually after the co-activation of IQ. ITS was co-activated in 40 % of all measurements.

On the contralateral side, CQ was co-activated in 78 % of all recordings and generally later than IQ. CHam was only co-activated in 40 %. In 70 % of all measurements, CTA was co-activated, mostly in third place. CTS showed co-activation in 60 % of all measurements. An illustration of the recruitment order without visual feedback is shown in Figure 23A.

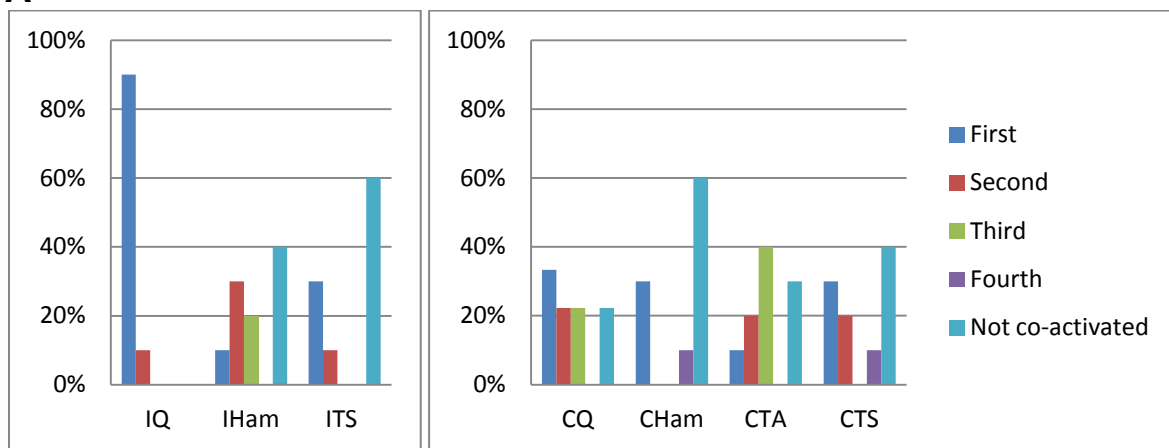
Providing visual feedback led to slightly different co-activation patterns. IQ still was co-activated in all measurements. IHam was co-activated in 70 % of all measurements, mostly as second. ITS was co-active in 50 % of all cases.

Looking at the contralateral side showed that CQ was co-active in all cases, preferably as first. CHam also showed slightly more co-activation when visual feedback was provided, but was still co-activated in only 50 % of all recordings. In CTA, co-activation was found in 60 % of the measurements, which were equally distributed over second and third rank. CTS was co-activated in 50 % of all cases. Figure 23B shows an illustration of the recruitment order with provided visual feedback.

Without visual feedback							With visual feedback						
Order	1.	2.	3.	4.	X	n	Order	1.	2.	3.	4.	X	n
IQ	90%	10%	0%	0%	0%	10	IQ	70%	10%	20%	0%	0%	10
IHam	10%	30%	20%	0%	40%	10	IHam	0%	60%	10%	0%	30%	10
ITS	30%	10%	0%	0%	60%	10	ITS	50%	0%	0%	0%	50%	10
CQ	33%	22%	22%	0%	22%	9	CQ	80%	20%	0%	0%	0%	10
CHam	30%	0%	0%	10%	60%	10	CHam	10%	20%	20%	0%	50%	10
CTA	10%	20%	40%	0%	30%	10	CTA	0%	30%	30%	0%	40%	10
CTS	30%	20%	0%	10%	40%	10	CTS	10%	10%	10%	20%	50%	10

Table 5. Recruitment-order as percentage of the total number (n) of recordings, giving information on when a particular muscle group was co-activated as first (1.), second (2.), third (3.), fourth (4.) or not at all (X). Separate evaluation for trials without (left) and with (right) visual feedback.

A



B

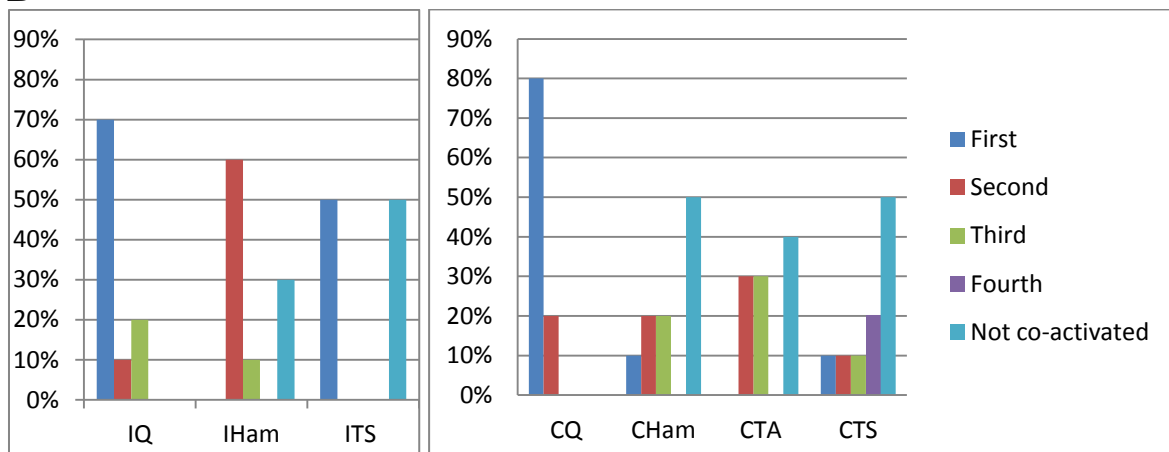


Figure 23. Recruitment-order of all recorded lower limb muscle groups. The percentage of co-activation as first (blue bars), second (red bars), third (green bars), fourth (violet bars) or not at all (light blue bars) was calculated for all studied muscle groups. **A)** Results without visual feedback. **B)** Results with visual feedback.

Paradigm B

When performing volitional unilateral intermittent contractions of the ankle dorsiflexor, the level of co-activation was increased with increasing contraction level, both with respect to the amount of activity observed in a particular muscle group as well as the number of muscle groups being co-activated. Visual feedback of the produced force was provided all the time. EMG was recorded from IQ, IHam, ExTA, ITS, CQ, CHam, CTA, CTS along with the produced force, in supine, standing and sitting position. Figures 24-26 show representative examples of recording sessions in supine, standing and sitting position, derived from a subject number 5.

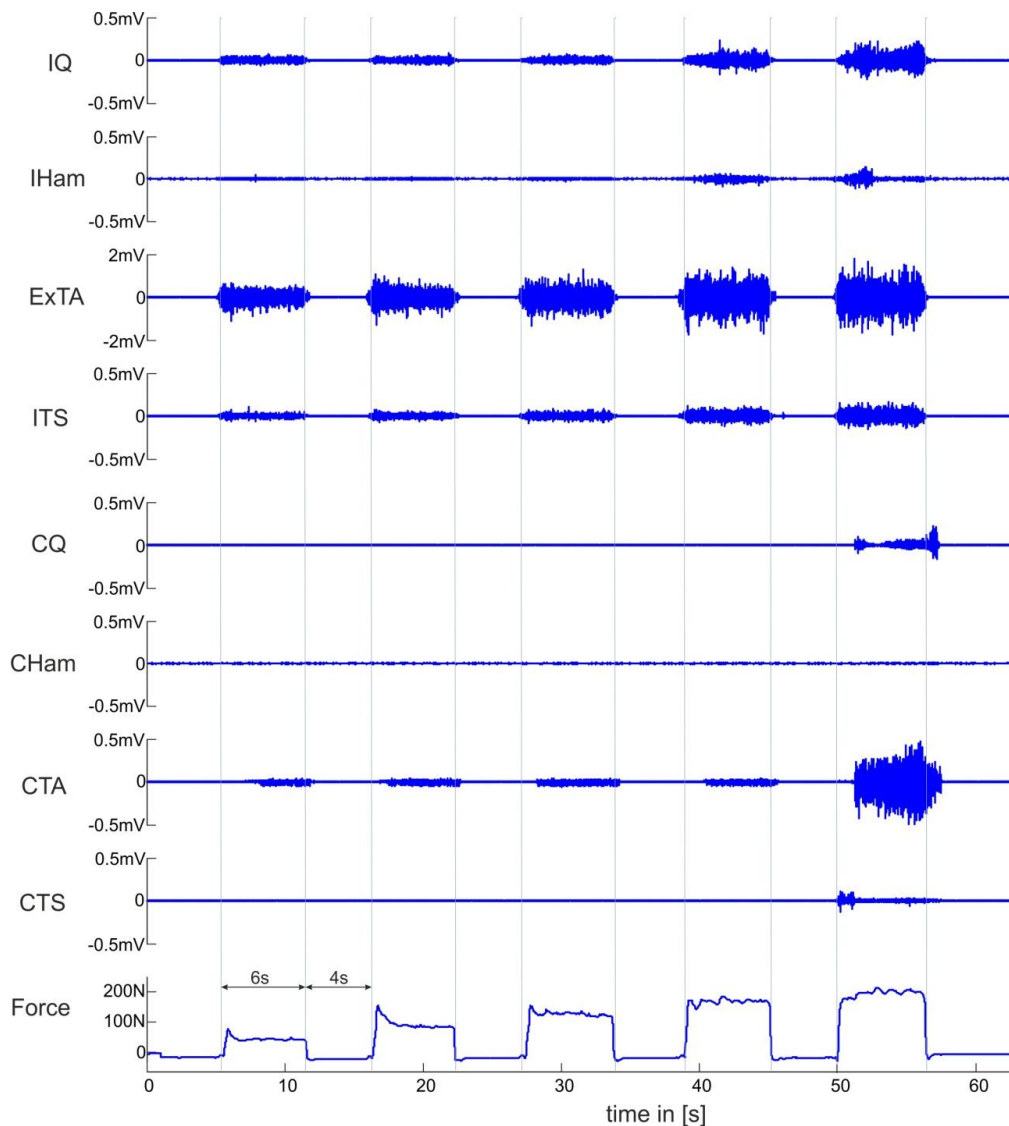


Figure 24. Supine position; The top eight traces giving information of EMG activities in ipsilateral quadriceps (IQ), ipsilateral hamstrings (IHam), exercised tibialis anterior (ExTA), ipsilateral triceps surae (ITS), contralateral quadriceps (CQ), contralateral hamstrings (CHam), contralateral tibialis anterior (CTA) and triceps surae (CTS) produced during intermittent contraction of the ankle flexor. The last trace shows the produced force. The subject was instructed to perform intervals of ankle dorsiflexion lasting for 6 s intermitted by 4 s resting phases. The level of the produced force was increased from 20 % to 100 % MVC in 20 % MVC steps. Data were derived from subject 5 while exercising RTA. Note the different scalings.

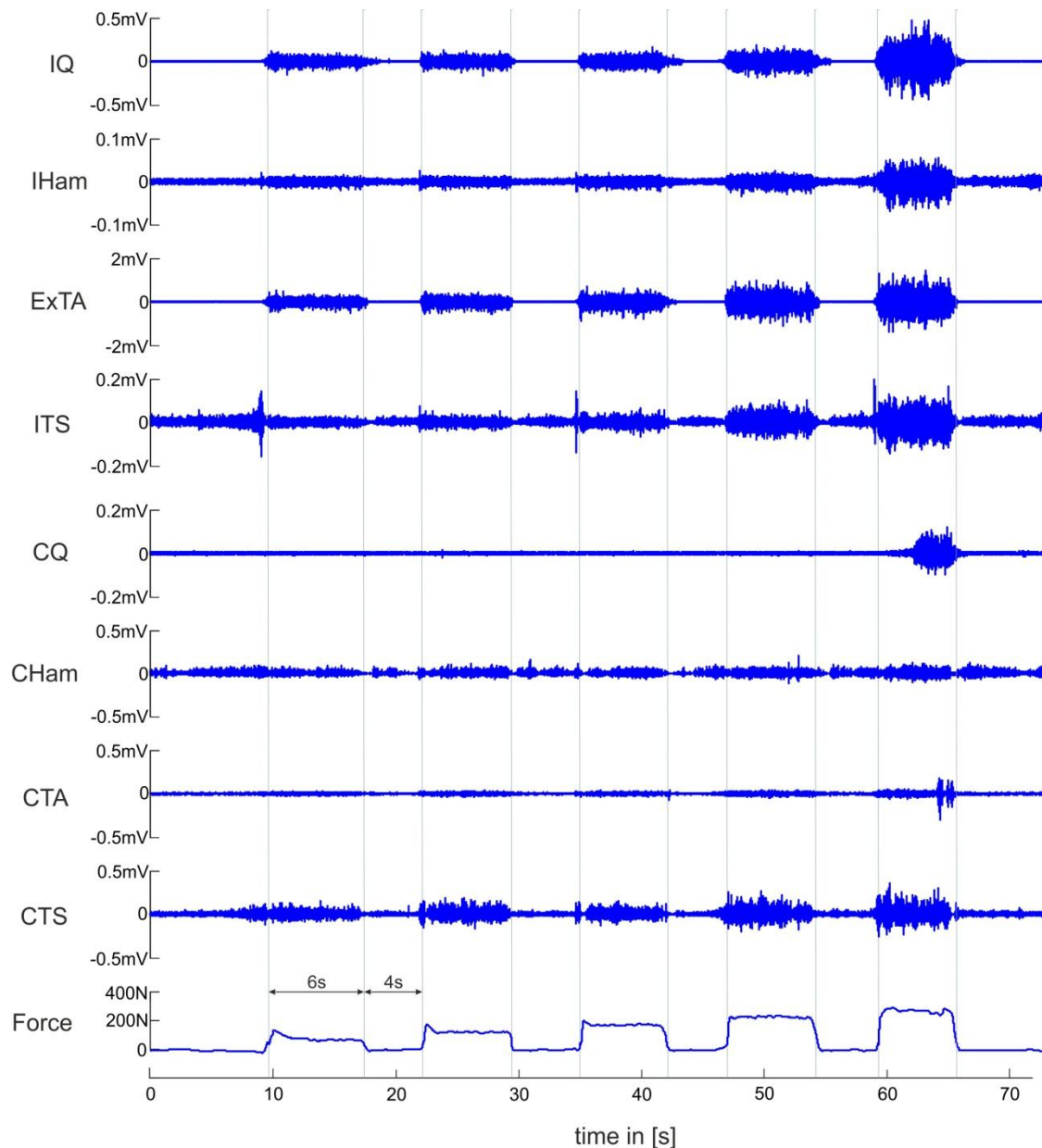


Figure 25. Standing position; The top eight traces giving information of EMG activities in ipsilateral quadriceps (IQ), ipsilateral hamstrings (IHam), exercised tibialis anterior (ExTA), ipsilateral triceps surae (ITS), contralateral quadriceps (CQ), contralateral hamstrings (CHam), contralateral tibialis anterior (CTA) and triceps surae (CTS) produced during intermittent contraction of the ankle flexor. The last trace shows the produced force. The subject was instructed to perform intervals of ankle dorsiflexion lasting for 6 s intermitted by 4 s resting phases. The level of the produced force was increased from 20 % to 100 % MVC in 20 % MVC steps. Data were derived from subject 5 while exercising LTA. Note the different scalings.

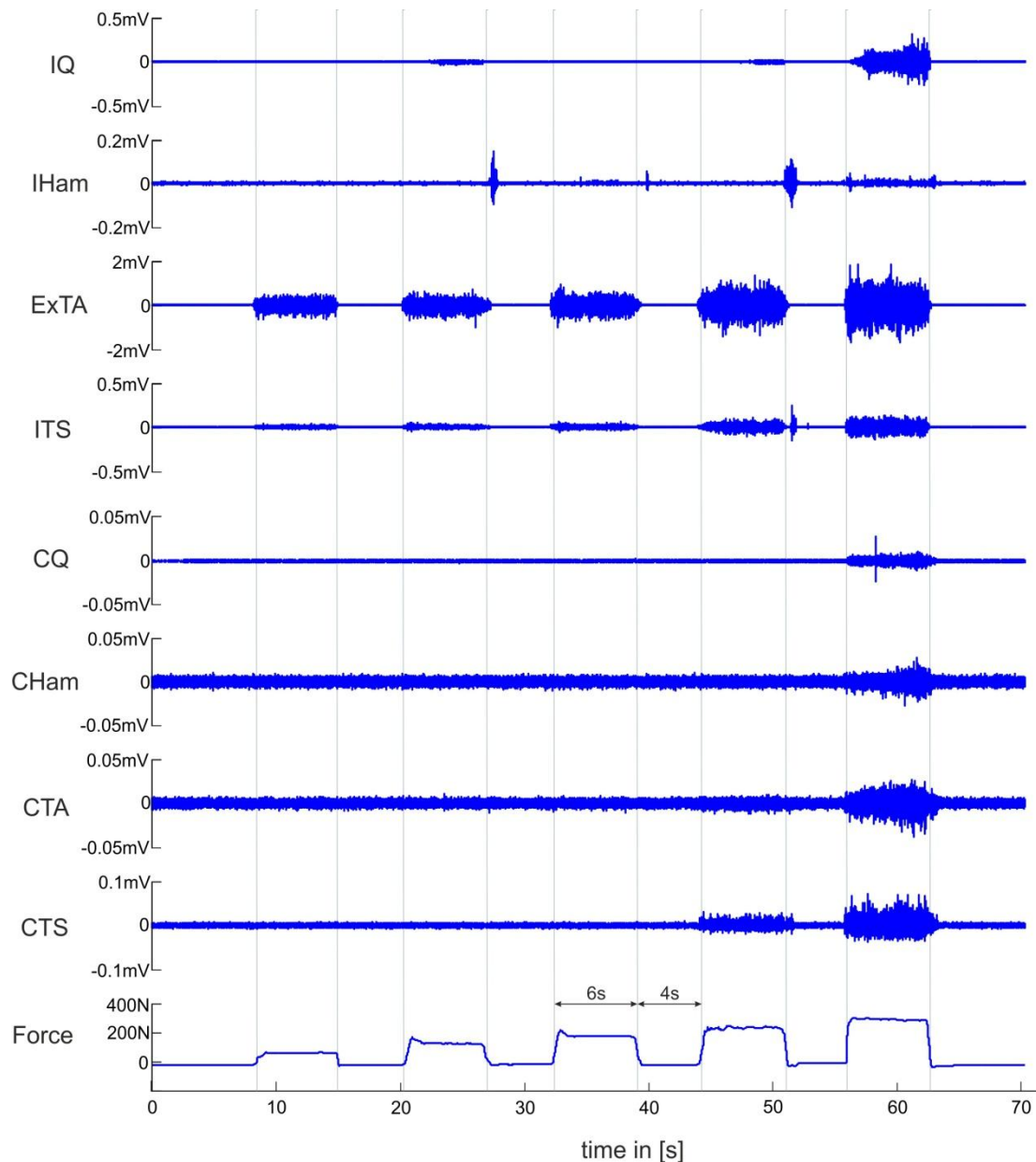


Figure 26. Sitting position; The top eight traces giving information of EMG activities in ipsilateral quadriceps (IQ), ipsilateral hamstrings (IHam), exercised tibialis anterior (ExTA), ipsilateral triceps surae (ITS), contralateral quadriceps (CQ), contralateral hamstrings (CHam), contralateral tibialis anterior (CTA) and triceps surae (CTS) produced during intermittent contraction of the ankle flexor. The last trace shows the produced force. The subject was instructed to perform intervals of ankle dorsiflexion lasting for 6 s intermitted by 4 s resting phases. The level of the produced force was increased from 20 % to 100 % MVC in 20 % MVC steps. Data were derived from subject 5 while exercising LTA. Note the different scalings.

A separate force diagram was used to verify that the target level of MVC was reached. Figure 27 gives an example of the produced force in detail. Data analysis was based on appropriately selected areas within the recording, thus avoiding the contamination of the results by the data not fulfilling the recording protocol (e.g. initial force overshooting).

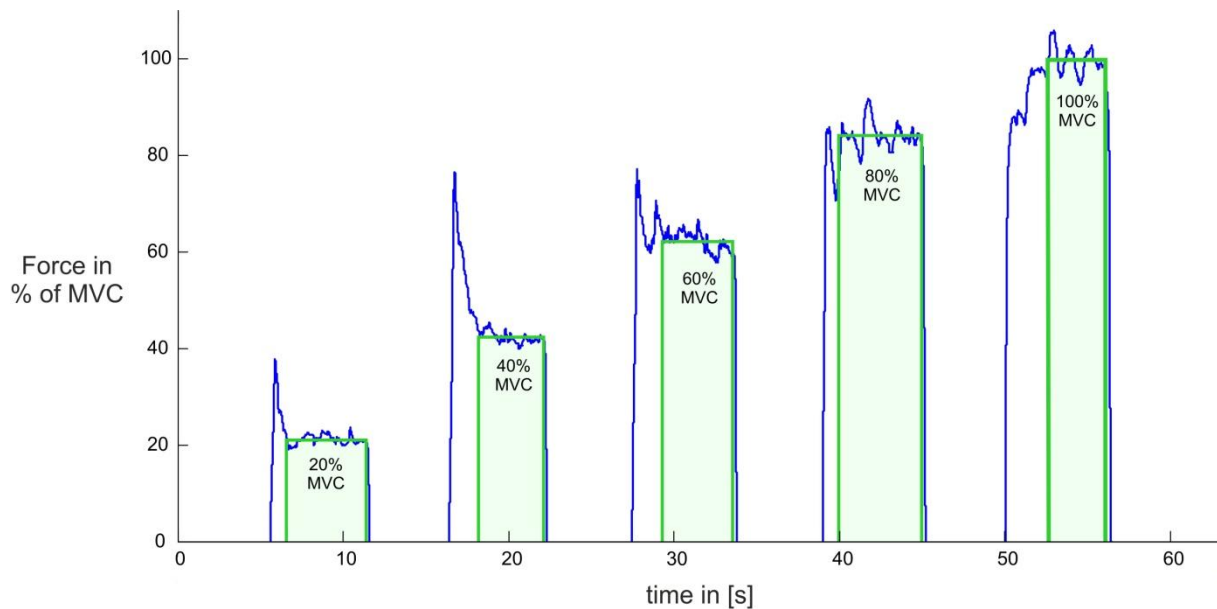


Figure 27: Example of produced force (blue curve) during the execution of an intermittent dorsiflexion of the ankle. Green areas represent the means of the produced force at a certain desired contraction level. Example derived from subject 5 in supine position, exercising RTA.

Recruitment order

The recruitment order was analyzed similar as described in Paradigm A. Instead of onset times, the contraction level was used to determine whether a muscle group was co-activated first, second, third or not at all. Again a relative distribution of co-activation was calculated for each muscle group as a percentage of the total number of recordings (Table 6).

In supine position IQ was co-activated in 92 % of all cases, always as first muscle. Co-activation in IHam occurred in 69 % of all recordings, mostly in first position, i.e. together with IQ. ITS showed co-activation in 92 % of all cases.

On the contralateral side CQ was only co-active in 17%, CHam in 33 %, CTA in 59 % and CTS in 16 % of all measurements. Figure 28A shows a diagram of the recruitment order in supine position.

The level of co-activation was highest in standing position. IQ was co-activated in all recordings, mostly in first position. IHam and ITS showed the same distribution and were co-activated in 66 % of all cases, mostly in second position.

Co-activation on the contralateral side was also increased. CQ was co-activated in 59 %, CHam in 50 %, CTA in 49 % and CTS in 75 % of all cases, respectively. A diagram of the recruitment order in standing position is shown in Figure 28B.

Sitting position led to the lowest level of co-activation of all tested body positions. IQ was co-activated in 80 % of the recordings, always as first. CHam showed co-activation in 40 % and CTS in 80 % of all measurements.

In sitting position, co-activation of the contralateral side was only seldom observed. CQ was co-active in 20 %, CHam in 10 %, CTA and CTS in 20 % of all recordings. Figure 28C shows a diagram of the recruitment order in supine position.

Supine position					
Order	1.	2.	3.	X	n
IQ	92%	0%	0%	8%	12
IHam	42%	0%	17%	41%	12
ITS	50%	42%	0%	8%	12
CQ	17%	0%	0%	83%	12
CHam	33%	0%	0%	67%	12
CTA	42%	17%	0%	41%	12
CTS	8%	8%	0%	84%	12

Standing position					
Order	1.	2.	3.	X	n
IQ	92%	8%	0%	0%	12
IHam	8%	58%	0%	34%	12
ITS	8%	58%	0%	34%	12
CQ	17%	25%	17%	41%	12
CHam	33%	17%	0%	50%	12
CTA	8%	33%	8%	51%	12
CTS	67%	8%	0%	25%	12

Sitting position					
Order	1.	2.	3.	X	n
IQ	80%	0%	0%	20%	10
IHam	20%	20%	0%	60%	10
ITS	60%	20%	0%	20%	10
CQ	20%	0%	0%	80%	10
CHam	10%	0%	0%	90%	10
CTA	20%	0%	0%	80%	10
CTS	20%	0%	0%	80%	10

Table 6. Recruitment-order as percentage of the total number (n) of recordings, giving information on when a particular muscle group was co-activated as first (1.), second (2.), third (3.) or not at all (X). Separate evaluation for supine (left), standing (middle) and sitting (right) position.

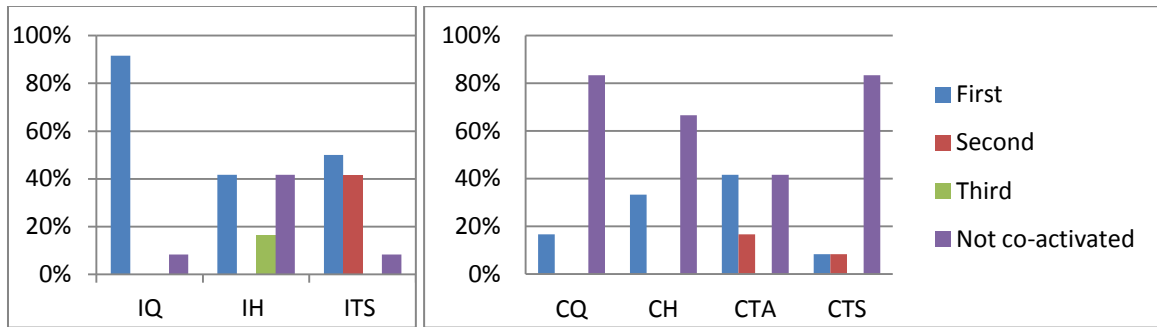
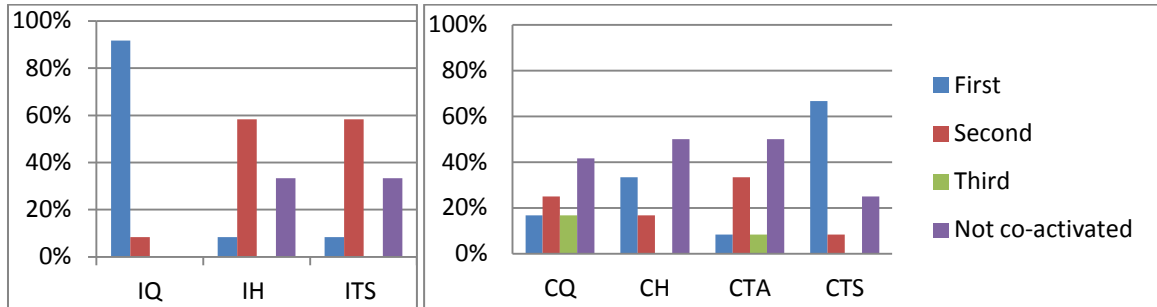
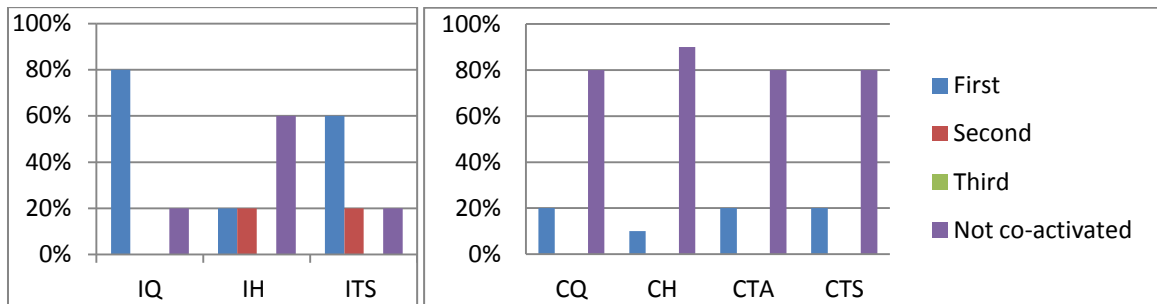
A**B****C**

Figure 28. Recruitment-order of all recorded muscle groups. The percentage of cases when a particular muscle group was co-activated as first (blue bars), second (red bars), third (green bars) or not at all (violet bars) was calculated for all studied muscle groups. **A)** Results in supine position **B)** Results in standing position **C)** Results in sitting position.

Paradigm C

PRM reflexes could be elicited in all studied muscle groups in supine and standing position. Characteristic examples of unconditioned PRM reflexes are shown in Figure 29A.

In order to verify the reflex nature of the responses, the stimulation was performed using double-pulses with an ISI of 50 ms. By applying a second stimulus within the relative refractory period of the reflex arc, leads to a depressed or completely suppressed second response, which is shown in Figure 29B. If the second response is equal or slightly facilitated, compared to the first one, the response is most probably a M wave and was excluded from further analysis.

Figure 29C shows a representative example of how a unilateral volitional contraction of the ankle dorsiflexor causes a reflex-depression of the antagonist ITS.

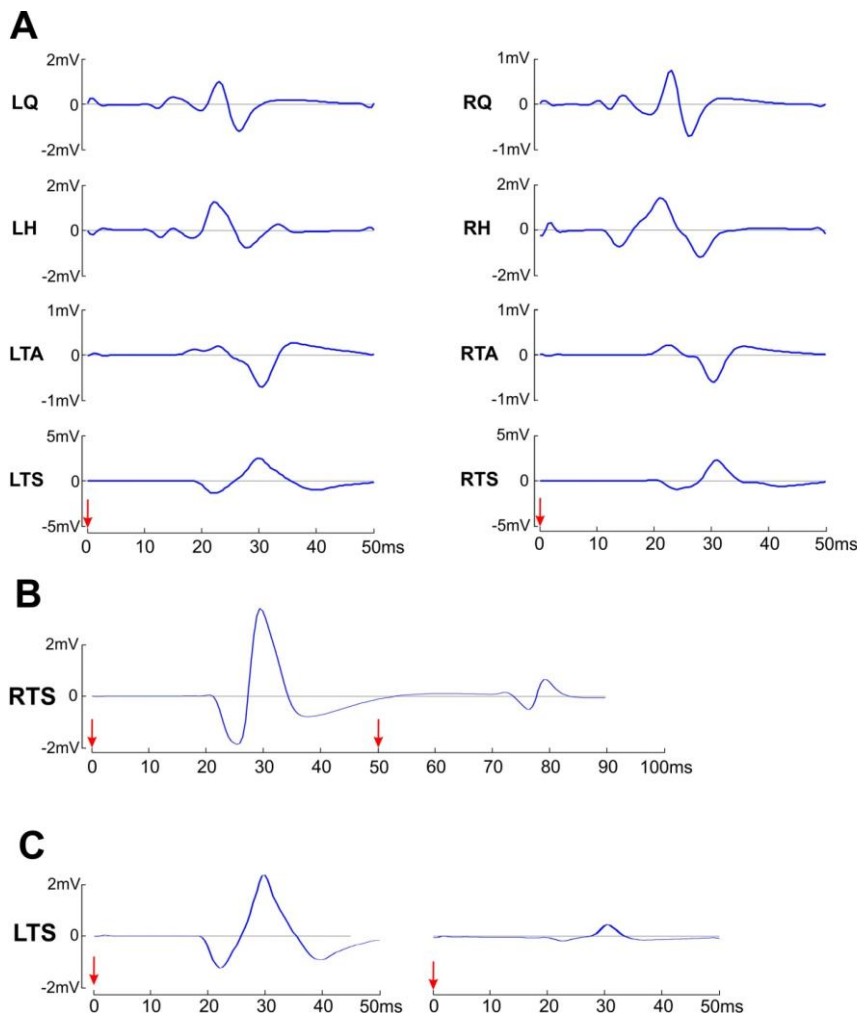


Figure 29. Illustration of EMG recordings and analysis of Paradigm C. The red arrows mark the stimulus application. **A)** Characteristic example of unconditioned PRM reflexes of bilateral quadriceps (Q), hamstrings (Ham), tibialis anterior (TA) and triceps surae (TS) elicited in subject 3. **B)** Responses of RTS to double-pulses applied with an inter-stimulus interval (ISI) of 50 ms; subject 2. The depression of the second response indicates the reflex nature of the recorded potential. **C)** Mean of five unconditioned (left) and five conditioned (right) PRM reflexes of LTS, elicited in subject 3. Conditioning was done by performing an ankle dorsiflexion with 60 % MVC on the left side.

Supine position

Performing a volitional unilateral ankle dorsiflexion in supine position, usually led to various modifications of PRM-reflexes in the different muscle groups. Figure 30 shows a characteristic example of the influence of contraction intensity on the modification of the PRM reflexes.

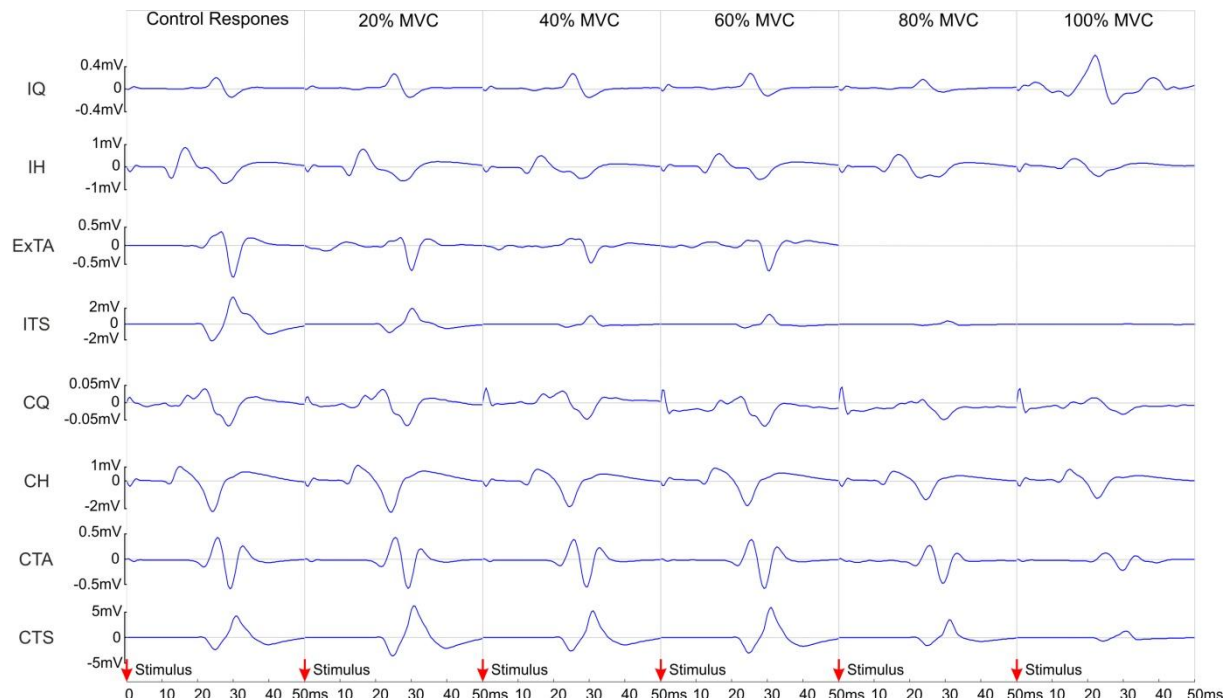


Figure 30: Characteristic example of reflex modifications while performing a volitional unilateral ankle dorsiflexion at different contraction levels. Data derived from subject 1 in supine position exercising the left ankle dorsiflexor. The means of five responses are shown from all studied muscle groups. Red arrows mark the times of stimulus application. Note the different scaling.

Generally responses in IQ and ExTA were facilitated. Increasing contraction levels led to increased responses in ExTA. PRM reflexes of IQ were generally increased but did not show a direct relation to the contraction level. IHam and ITS responses were generally suppressed. While suppression of PRM reflexes was increased in ITS at higher contraction levels, suppression in IHam remained constant throughout the different contraction levels.

Responses of CQ were slightly increased in general whereas the responses of the other contralateral muscles were slightly suppressed. Especially PRM reflexes of CTS showed a distinct depression at higher contraction levels.

Concrete values can be seen in Table 7 while the corresponding diagram is shown in Figure 31.

	20%	STD	n	40%	STD	n	60%	STD	n	80%	STD	n	100%	STD	n
IQ	2.38	±0.39	8	3.03	±1.57	8	2.17	±0.89	7	2.54	±0.90	8	2.29	±2.03	6
IHam	1.58	±0.22	12	1.51	±0.29	12	1.51	±0.16	12	1.38	±0.34	12	1.31	±0.59	11
ExTA	1.94	±0.36	11	1.70	±0.65	11	2.13	±0.82	11	1.72	±0.00	1			0
ITS	1.36	±0.23	12	1.28	±0.18	12	1.27	±0.11	12	0.53	±0.08	12	0.20	±0.10	11
CQ	2.41	±0.66	11	2.23	±0.66	12	2.09	±0.74	11	1.24	±0.70	9	1.55	±0.98	9
CHam	1.71	±0.51	12	1.64	±0.34	12	1.64	±0.27	12	1.69	±0.28	12	1.67	±0.53	12
CTA	1.71	±0.37	11	2.18	±0.75	12	1.30	±0.45	8	1.77	±0.23	12	1.47	±0.52	11
CTS	1.46	±0.06	12	1.38	±0.17	12	1.36	±0.07	12	1.61	±0.29	12	1.12	±0.40	12

Table 7. Modifications of PRM reflexes by ankle dorsiflexion in supine position, at different levels of produced force as indicated (20 %, 40 %, 60 %, 80 % and 100 % MVC). Values are ratios between mean PTP amplitudes of conditioned PRM reflexes and mean PTP amplitudes of unconditioned control responses (\pm standard deviation). Column “n” indicates the number of valid samples used for evaluation

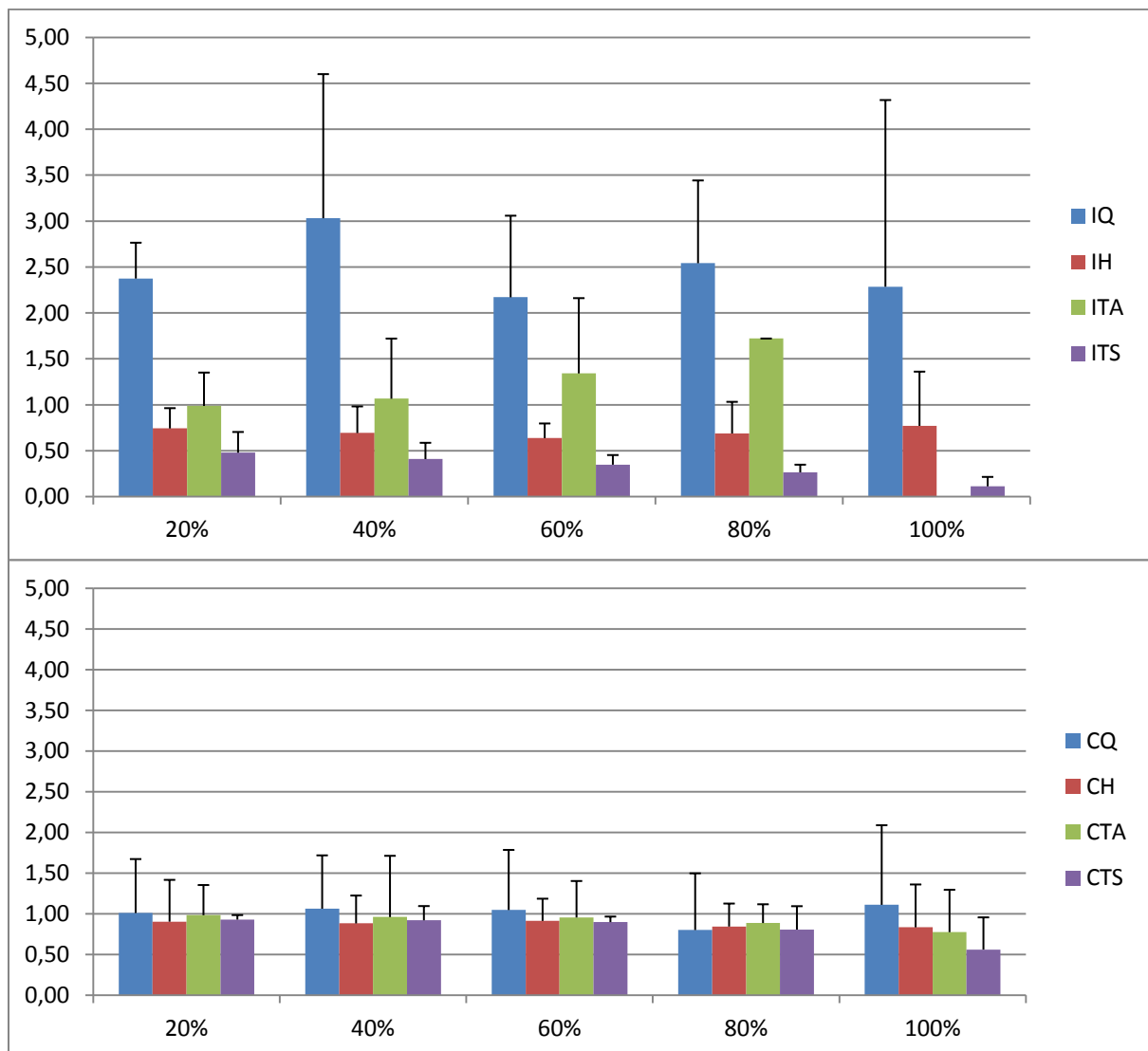


Figure 31. Diagram of summarized PRM reflex modifications by performing an ankle dorsiflexion in supine position, at different levels of produced force (20 %, 40 %, 60 %, 80 % and 100 % MVC). Bars represent ratios between mean PTP amplitudes of conditioned PRM reflexes and mean PTP amplitudes of unconditioned control responses (\pm standard deviation).

Standing position

Figure 32 shows a characteristic example of the influence of a volitional intermittent unilateral dorsiflexion at different force levels on the modification of the PRM reflexes, in standing position.

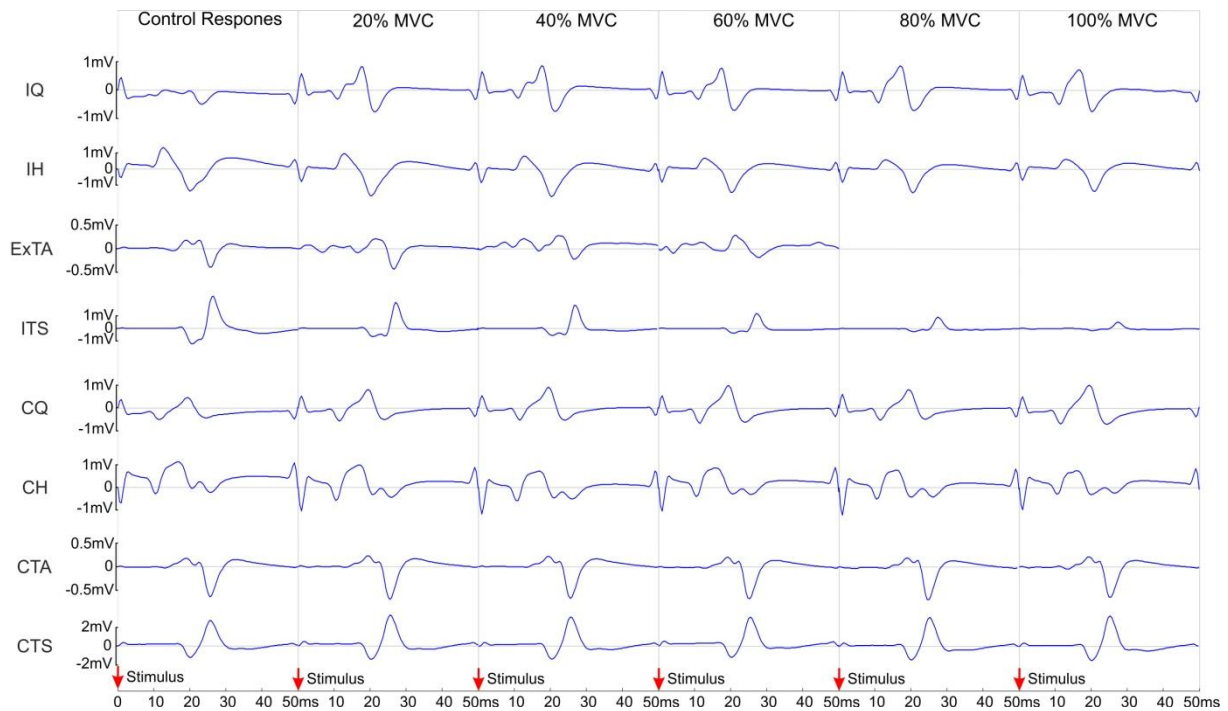


Figure 32: Characteristic example of reflex modifications while performing a volitional unilateral ankle dorsiflexion at different contraction levels. Data derived from subject 5 in standing position exercising the left ankle dorsiflexor. The means of five responses are shown from all studied muscle groups. Red arrows mark the times of stimulus application. Note the different scaling.

In standing position, responses in IQ and ExTA were also facilitated in general. PRM reflexes in IHam were suppressed at lower contraction levels but showed a slightly increase at 100 % MVC. Responses in ITS were highly depressed and decreased progressively at higher contraction levels.

As opposed to supine position, responses in almost all contralateral muscle groups were slightly increased. The strongest facilitation of PRM reflexes was observed in CQ, but without clear relation to the contraction intensity. Responses in the other contralateral muscle groups were slightly increased and remained constant throughout the different contraction levels. Concrete values can be seen in Table 8 while the corresponding diagram is shown in Figure 33.

	20%	STD	n	40%	STD	n	60%	STD	n	80%	STD	n	100%	STD	n
IQ	5.02	±1.54	6	3.80	±1.42	6	4.30	±3.37	7	3.55	±2.81	4	4.14	±3.23	4
IHam	0.76	±0.16	12	0.65	±0.11	12	0.69	±0.08	12	0.61	±0.19	12	1.08	±0.47	12
ExTA	0.92	±0.12	9	0.98	±0.33	7	1.62	±1.07	4	2.14	±0.00	1			0
ITS	0.60	±0.12	12	0.48	±0.10	12	0.40	±0.16	12	0.29	±0.15	12	0.16	±0.10	12
CQ	1.60	±0.29	5	0.87	±0.64	5	1.43	±0.74	6	1.31	±0.73	4	1.65	±0.74	5
CHam	1.14	±0.17	12	1.03	±0.19	12	1.15	±0.31	12	1.10	±0.25	12	1.49	±1.04	12
CTA	1.04	±0.07	8	0.99	±0.05	8	1.03	±0.14	9	1.04	±0.08	8	1.05	±0.24	8
CTS	1.08	±0.14	12	1.09	±0.16	12	1.19	±0.19	12	1.13	±0.07	12	1.37	±0.58	12

Table 8. Modifications of PRM reflexes by ankle dorsiflexion at different levels of produced force as indicated (20 %, 40 %, 60 %, 80 % and 100 % MVC). Values are ratios between mean PTP amplitudes of conditioned PRM reflexes and mean PTP amplitudes of unconditioned control responses (\pm standard deviation), in standing position. Column “n” indicates the number of valid samples used for evaluation.

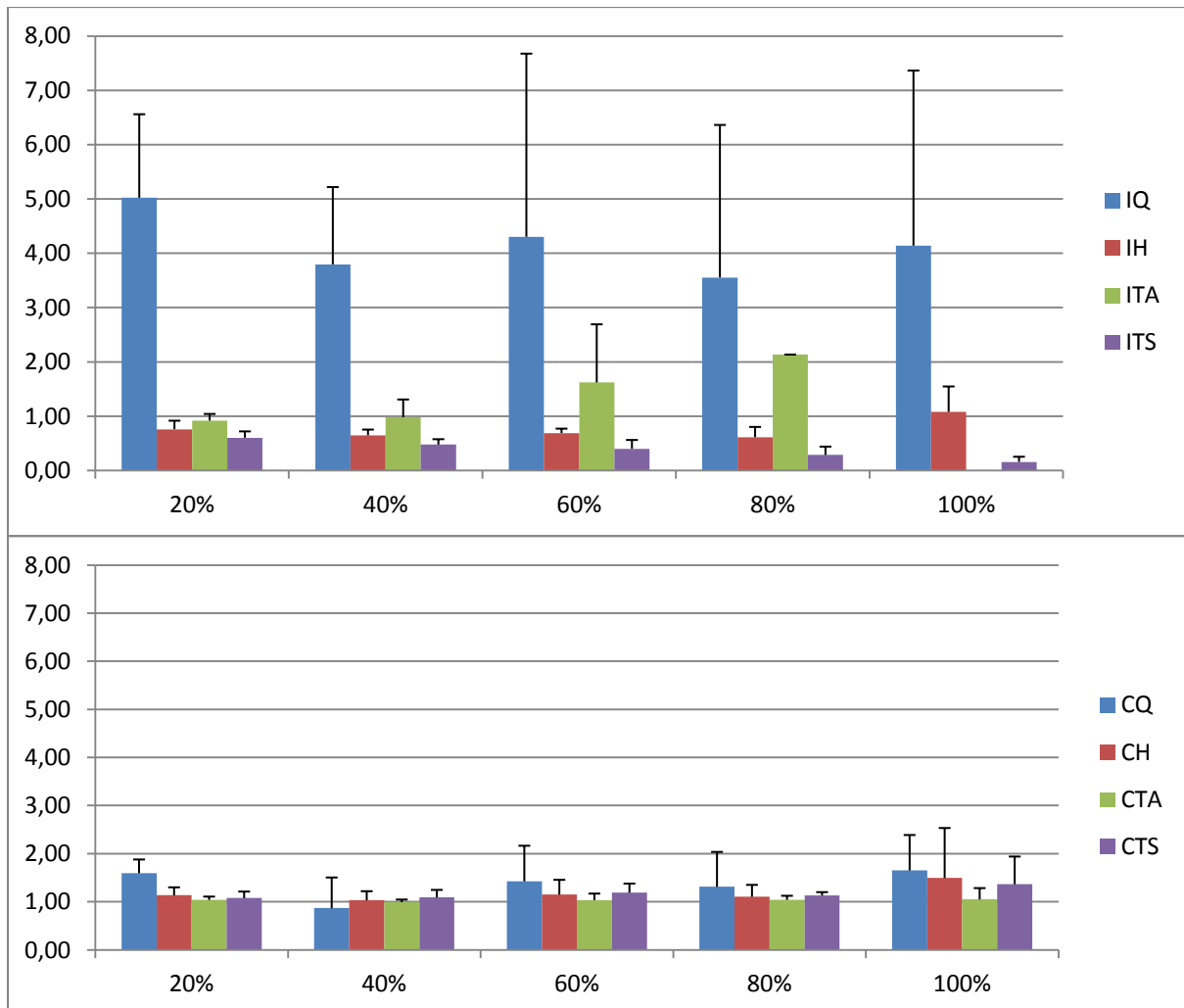


Figure 33. Diagram of summarized PRM reflex modifications by performing an ankle dorsiflexion in standing position, at different levels of produced force (20 %, 40 %, 60 %, 80 % and 100 % MVC). Bars represent ratios between mean PTP amplitudes of conditioned PRM reflexes and mean PTP amplitudes of unconditioned control responses (\pm standard deviation).

Discussion

The present thesis produced three main results:

1. The equipment to measure and online monitor the force produced during a unilateral sustained or intermittent dorsiflexion of the ankle in supine, standing, and sitting positions was designed and constructed. The functional suitability of the equipment was also verified by repeating the measurements conducted by Dimitrijevic et al. (1992). The device allowed for the standardization of the chosen motor task with respect to the degree of force being generated and thus, for the inter-individual comparison of the results obtained.
2. Electrophysiological recordings during the execution of a unilateral sustained or intermittent dorsiflexion of the ankle were conducted and revealed characteristic co-activation patterns of several lower limb muscle groups bilaterally.
3. The gain of sensory-motor transmission at several lumbosacral spinal cord levels was assessed during the execution of a sustained unilateral dorsiflexion of the ankle at different defined levels of force being produced. To this end, tSCS was used to elicit PRM reflexes in several lower limb muscles bilaterally and simultaneously. Modulations of the reflex gain were used as an indicator for changes in the synaptic transmission at spinal cord level.

Paradigm A

Performing a volitional, unilateral, sustained dorsiflexion of the ankle usually led to the co-activation of several lower limb muscle groups in addition to the exercised ankle flexor TA. Co-activation was observed first in muscle groups ipsilateral to the motor task, and later in muscles on the contralateral side.

Among the ipsilateral lower limb muscle groups, Q – acting as a synergist of the ExTA during the motor task of ankle dorsiflexion (cf. Tepperman et al., 1986) – was generally first co-activated. Interestingly, some co-activation was also found in the antagonistic TS, which may in part be attributed to a phenomenon called cross-talk, i.e., the spacial spread of the EMG signal from the exercised TA which is then captured by the EMG electrodes placed over the antagonistic TS. Other groups of researchers have estimated an average value of 5% – 6% of TA activity being detected by the TS electrodes (Merletti & De Luca, 1988; Dimitrijevic et al., 1992). Additionally, an involuntary attempt to stiffen the ankle joint as the sustained contraction persisted may have attributed to the co-activation of the antagonistic TS.

Co-activation of lower limb muscle groups on the contralateral side was usually observed more seldom and occurred with a certain delay, compared to the ipsilateral side. Among the co-activated muscle groups, Q was the first one to respond, followed by Ham, hence increasing the stability and maintaining equilibrium of the body during the sustained dorsiflexion. Co-activation was further also observed in the homologous TA of the contralateral lower limb. Such patterns of (homologous) co-activation on the contralateral side during the effort to maintain force are well described for the upper limbs (cf. Green, 1967).

Visual feedback of the produced force generally shortened the times until muscle groups on the contralateral side became co-active, while these times were slightly increased for muscle groups of the ipsilateral side. While the observed co-activation patterns remained relatively unchanged, the probability of a particular muscle group to become co-activated was increased by providing visual feedback of the produced force.

Paradigm B

Performing volitional, unilateral, intermittent contractions of the ankle dorsiflexor led to co-activation of several lower limb muscle groups bilaterally. The extent of co-activation - with respect to the number of co-activated muscle groups and the amount of muscular activity within a particular muscle group - was increased with increasing contraction levels of the exercised TA. As in the trials with sustained contraction, co-activation was first observed in muscle groups ipsilateral to ExTA.

Irrespective of the tested body position (standing, sitting, supine), the synergistic IQ was co-activated first. Muscle groups on the contralateral side were mainly co-activated in standing position. Generally, the largest extent of co-activation occurred in standing position, when additional muscular activity was needed to counteract perturbation of equilibrium, while the lowest level of co-activity was observed in sitting position.

While metabolic changes in the ExTA potentially leading to muscle fatigue could have occurred during the sustained effort to maintain force (cf. Paradigm A), such effects are unlikely to appear during the intermittent activation of the ankle flexor. Hence, peripheral muscle fatigue can be ruled out as the mechanism underlying the observed co-activation patterns. This was shown by Moussavi et al. (1989) using NMR spectroscopy while investigating metabolic changes, which are associated to muscle fatigue. Still, Dimitrijevic and colleagues (1992) claim that the perception of the imminent failure to produce or maintain a certain level of force could bring about changes in the CNS that eventually lead to observed co-activation of various lower limb

muscle groups. Furthermore, taking into account the inter-individually relatively consistent patterns of co-activation as well as the increased extent of co-activation at shorter delays, when providing visual feedback, the group concludes that the source of the increased excitatory drive associated with the spread of muscular activity is a motor pattern generator

Paradigm C

Transcutaneous SCS applied over the lumbosacral spinal cord was effective to elicit PRM reflexes in multiple lower limb muscles bilaterally in all six subjects tested, in supine and standing position. PRM reflexes are short-latency reflexes that are initiated within afferent fibers of the posterior roots, upon their entry into the spinal cord, (Minassian et al., 2007). A single pulse applied over the T11/T12 vertebral level on average stimulates posterior roots of the L2-S2 segments simultaneously, and hence leads to the elicitation of PRM reflexes in virtually all lower limb muscles bilaterally at the same time (Hofstötter et al., 2008).

Double stimuli with 50 ms ISI were applied to test the refractory behavior and thus the reflex nature of the elicited responses (cf. Minassian et al., 2007). Responses not unequivocally identified as reflexes were withdrawn from further analysis. Such responses, most likely M waves, were most frequently found in Q.

The test PRM reflexes were conditioned by a unilateral volitional dorsiflexion, performed at defined contraction levels, and modifications of the reflex magnitudes were expressed with respect to peak-to-peak amplitudes of the unconditioned control PRM reflexes.

Modifications in the reflex gain during the execution of unilateral dorsiflexion could be observed in all studied muscle groups, with the effects being weaker on the contralateral side. Any kind of reflex modification, i.e. either facilitation or suppression, was generally more expressed in standing position or by increasing the levels of the produced force. Trials in supine position generally led to lower expressions of reflex modification.

PRM reflexes in ExTA and the synergistic IQ were distinctly facilitated, reflecting the functional roles of these muscle groups during the execution of the motor task (cf. Hofstötter et al., 2008). At the same time, responses in the antagonistic ITS were suppressed, as could be expected. Similarly, the soleus H reflex evoked by peripheral nerve stimulation is attenuated during volitional dorsiflexion of the ankle (Crone & Nielsen, 1989).

Conclusions

In the present thesis, co-activation patterns of various lower limb muscles accompanying the execution of unilateral, volitional sustained or intermittent contractions of the ankle flexor TA were described. The observed co-activation patterns were similar in the six subjects studied and presented a relatively regular result, hinting on a motor pattern generator as the source of activation.

The gain of PRM reflexes during dorsiflexion of the ankle at different contraction levels reflected the functional roles of the (flexor and extensor) muscle groups assessed, with facilitated responses found in the ExTA and the synergistic IQ, as well as reflex suppression in the antagonistic ITS. The device measuring the produced force, which was designed and constructed for the present thesis, helped to inter-individually standardize the execution of the unilateral dorsiflexion, allowing for a better comparison of the results obtained from the different participants of the study.

The presented approach provides a valuable basis for further larger-scale studies on the mechanisms underlying the neural control of movement in individuals in people with intact and altered CNS function.

References

Armatas CA & Summers JJ (2001). The influence of task characteristics on the intermanual asymmetry of motor overflow. *J Clin Exp Neuropsychol.* 23, 557-567.

Brooks (1986). Motor Control – Implementation by the central nervous system. In: The Neural Basis of Motor Control. *Oxford University Press*, pp. 18-37.

Burke D & Gandevia SC (1999). Properties of human peripheral nerves: implications for studies of human motor control. *Prog Brain Res.* 123, 427-435.

Capaday C & Stein RB (1986). Amplitude modulation of the soleus H-reflex in the human during walking and standing. *J Neurosci.* 6, 1308-1313.

Capaday C & Stein RB (1987). Difference in the amplitude of the human soleus H reflex during walking and running. *J Physiol.* 392, 513-522.

Cernacek J (1961). Contralateral motor irradiation--cerebral dominance. Its changes in hemiparesis. *Arch Neurol.* 4, 165-172.

Crone C & Nielsen J (1989). Spinal mechanisms in man contributing to reciprocal inhibition during voluntary dorsiflexion of the foot. *J Physiol (Lond)* 416, 255-272.

Danner S, Hofstoetter U, Ladenbauer J, Rattay F, Minassian K (2011). Can the human lumbar posterior columns be stimulated by transcutaneous spinal cord stimulation? A modeling study. *Artif Organs.* 35, 257-262.

Davis R C (1942). The pattern of muscular action in simple voluntary movement. *J. Exp. Psych.* 31, 347-366.

Dimitrijevic M R, McKay W B, Sarjanovic I, Sherwood A M, Svrtlih L & Vrbova G (1992). Co-activation of ipsi- and contralateral muscle groups during contraction of ankle dorsiflexors. *Journal of the Neurological Sciences* 109, 49-55.

Dyhre-Poulsen P, Simonsen EB & Voigt M (1991). Dynamic control of muscle stiffness and H reflex modulation during hopping and jumping in man. *J Physiol.* 437, 287-304.

Fog E & Fog M (1963). Central inhibition examined by associated movements. In: Bax, M. and R.C. MacKeith (Eds.), *Minimal Cerebral Dysfunction, Clinics in Developmental Medicine*, No. 10, Spastic Society with Heinemann Medical, London , pp. 52-57.

Gellhorn E (1947). Patterns of muscular activity in man. *Arch. Phys. Med.* 28, 568-574.

Ghez & Krakauer (2000). The Organization of Movement. *Principles of Neuroscience. Eds. Kandel*, pp. 653-673.

Green J B (1967). An electromyographic study of mirror movements. *Neurology* 17, 91-94.

Hofstoetter U, Minassian K, Hofer C, Mayr W, Rattay F & Dimitrijevic M R (2008). Modification of Reflex Responses to Lumbar Posterior Root Stimulation by Motor Tasks in Healthy Subjects. *Artificial Organs* 32, 644–648.

Hwang I & Abraham L(2001). Quantitative EMG analysis to investigate synergistic coactivation of ankle and knee muscles during isokinetic ankle movement. Part 1: time amplitude analysis. *J Electromyogr Kinesiol.* 11, 319-325.

Knikou M (2008). The H-reflex as a probe: pathways and pitfalls. *J Neurosci. Methods.* 15, 1-12.

Merletti R & De Luca C J (1989). New techniques in surface electromyography. In: Desmedt, J. (Ed.), *Computer-Aided Electromyography and Expert Systems, Elsevier Science Publishers Amsterdam*, pp. 115-124.

Minassian K, Persy I, Rattay F, Dimitrijevic M R, Hofer C & Kern H (2007). Posterior root-muscle Reflexes elicited by transcutaneous stimulation of the human lumbosacral cord. *Muscle Nerve* 35, 327–336.

Minassian K, Hofstoetter U & Rattay F (2011). Transcutaneous lumbar posterior root stimulation for motor control studies and modification of motor activity after spinal cord injury. In: Restorative Neurology of Spinal Cord Injury. Editors: Milan R. Dimitrijevic, Byron A. Kakulas, Gerta Vrbova and W. Barry McKay. *Oxford University Press, NY*. Pp. 226-255.

Misiaszek JE, Barclay JK, Brooke JD(1996). Mechanisms within the spinal cord are involved in the movement-induced attenuation of an H reflex in the dog. *J Neurophysiol.* 76, 3589-3592.

Moussavi R S, Carson P J, Boska M D, Weiner M W & and Miller R G (1989). Nonmetabolic fatigue in exercising human muscle. *Neurology* 39, 1222-1226.

Schneider C, Lavoie BA & Capaday C (2000). On the origin of the soleus H-reflex modulation pattern during human walking and its task-dependent differences. *J Neurophysiol.* 83, 2881-2890.

Sherwood AM, McKay WB & Dimitrijevic M R (1996). Control after spinal cord injury: assessment using surface EMG. Muscle Nerve. *Muscle Nerve* 19, 966-979.

Tepperman PS, Mazliah J, Naumann S & Delmore T (1986). Effect of ankle position on isometric quadriceps strengthening. *J Phys Med.* 65, 69-74.

Appendix A

Data-capturing software

Data were captured using DasyLab 11. Different routines were implemented for the different measurements.

Paradigm A&B

The following routine was used for Paradigm A and B. EMG-data were recorded from all studied muscle groups (LQ, LH, LTA, LTS, RQ, RH, RTA and RTS), plotted and saved along with the produced force. EMG data were filtered using a second-order Butterworth-filter (bandwidth 20 Hz – 500 Hz). The force signal was filtered using a second-order Butterworth-filter (lowpass 10 Hz). MVC was either measured or defined manually. Visual feedback of the produced force (percentage of MVC) was provided by a bar-scale.

Figure 34 shows the user-interface to control the measurement. The left window shows the ongoing EMG of all muscle groups along with the produced force. This continuous data was saved on demand in an ASCII-file for further offline analysis. The right window shows the produced force in detail.

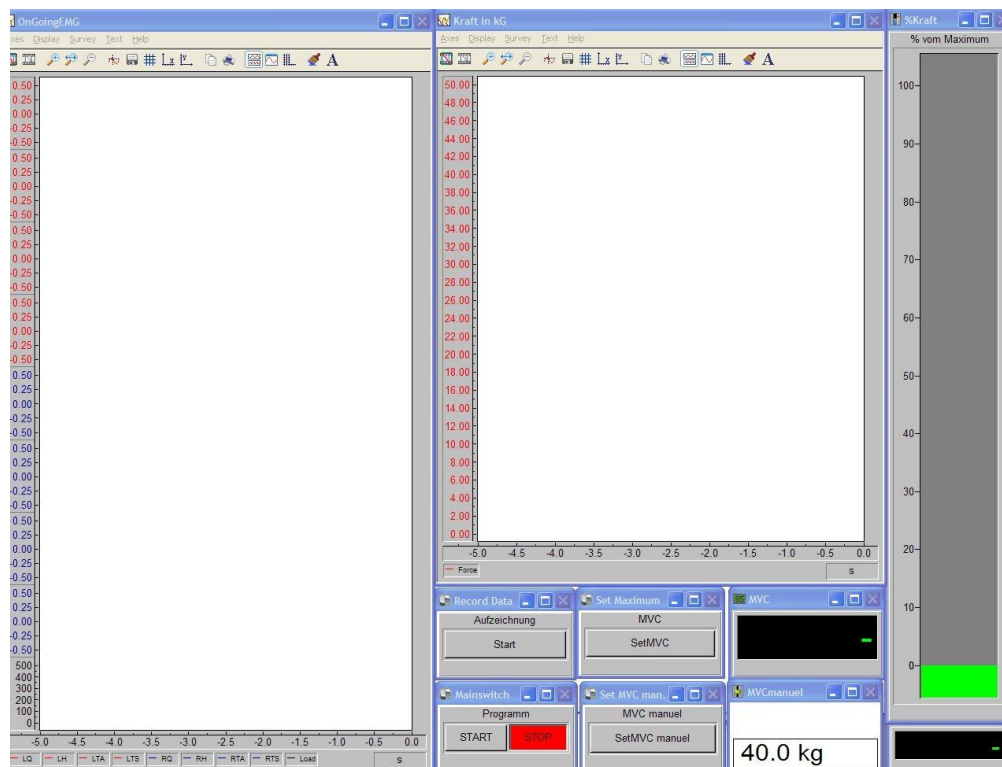


Figure 34. User-interface for Paradigm A&B; The left window shows the ongoing EMG of all eight muscle groups (red color for left muscle groups, blue color for right muscle groups) along with the produced force (in black color). The right window shows the produced force in detail. The bar-scale provides feedback of the force (% of MVC) produced during unilateral dorsiflexion of the ankle.

Paradigm C

The following routine was implemented for Paradigm C. PRM-reflexes recorded from all muscle groups (LQ, LH, LTA, LTS, RQ, RH, RTA and RTS) were recorded, plotted and saved along with the corresponding force. EMG data was filtered using a second-order butterworth-filter (bandwidth 20 Hz – 500 Hz). The force signal was filtered using a second-order butterworth-filter (lowpass 10 Hz). Visual feedback was provided as described above.

Figure 35 shows the user-interface to control the measurement. The left window shows the ongoing EMG of all muscle groups along with the produced force. The right window shows the stimulus triggered responses of all muscle groups along with the produced force. The routine captured data in a timeslot 10 ms before and 200 ms after the trigger was activated. The trigger was activated when the measured stimulus artifact exceeded a certain threshold. All generated data-blocks were saved in an ASCII-file for further analysis offline.

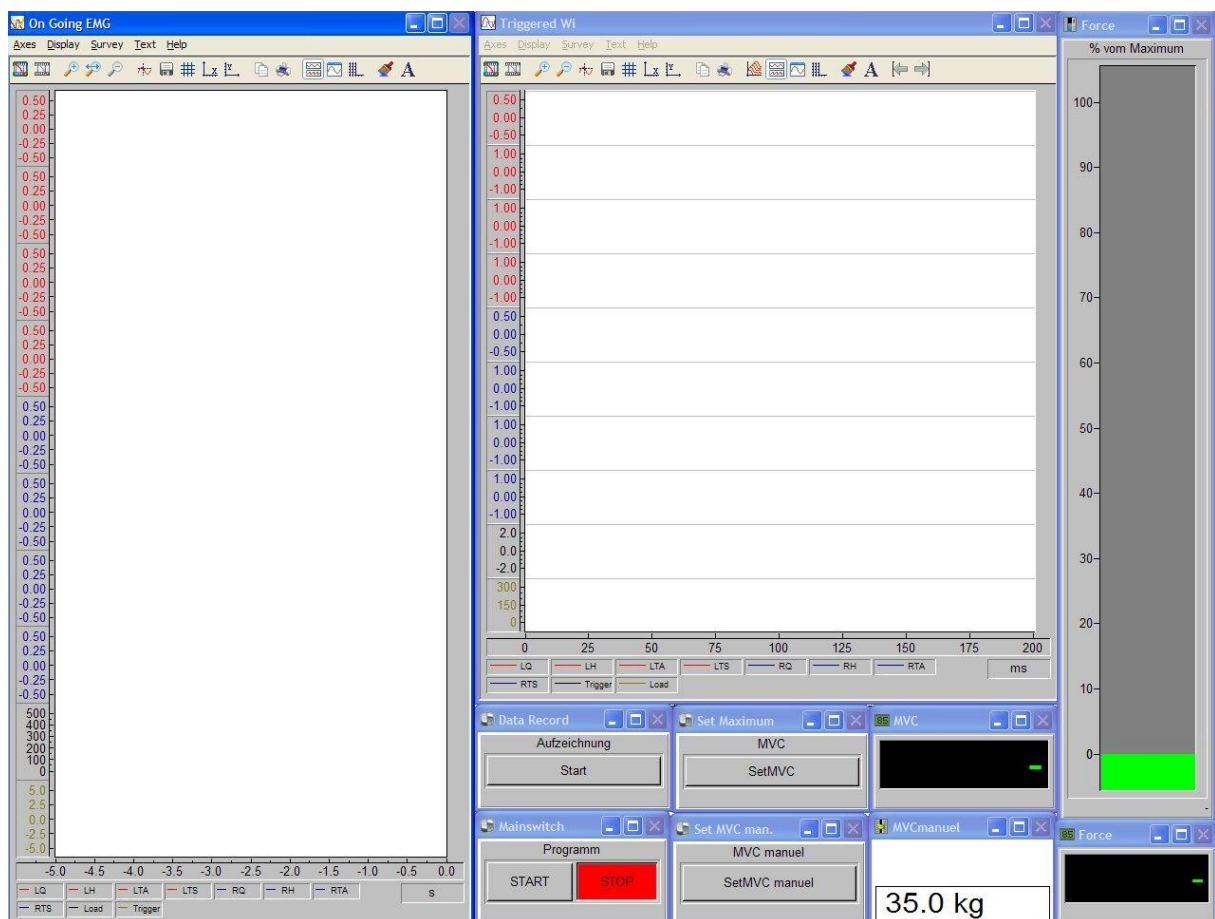


Figure 35. Userinterface of Paradigm C; The left window shows the ongoing EMG of all muscle groups along with the produced force. The right window shows the stimulus triggered responses of all muscle groups along with the produced force. The bar-scale gave the subject feedback about the strength of its contraction (percentage of MVC).

M_{max} measurement

This routine was implemented to determine the maximum M wave (M_{max}) of TS. Responses were plotted and saved.

Figure 36 shows the user-interface to control the measurement. The left window shows the ongoing EMG of all muscle groups (LQ, LH, LTA, LTS, RQ, RH, RTA and RTS) which was used to check if all channels are working properly. The right window shows stimulus-triggered responses of LTS (upper trace) and RTS (lower trace). The routine captured data in a timeslot 10 ms before and 200 ms after the trigger was activated. The trigger was activated when the measured stimulus artifact exceeded a certain threshold. All generated data-blocks where saved in an ASCII-file for further analysis offline.

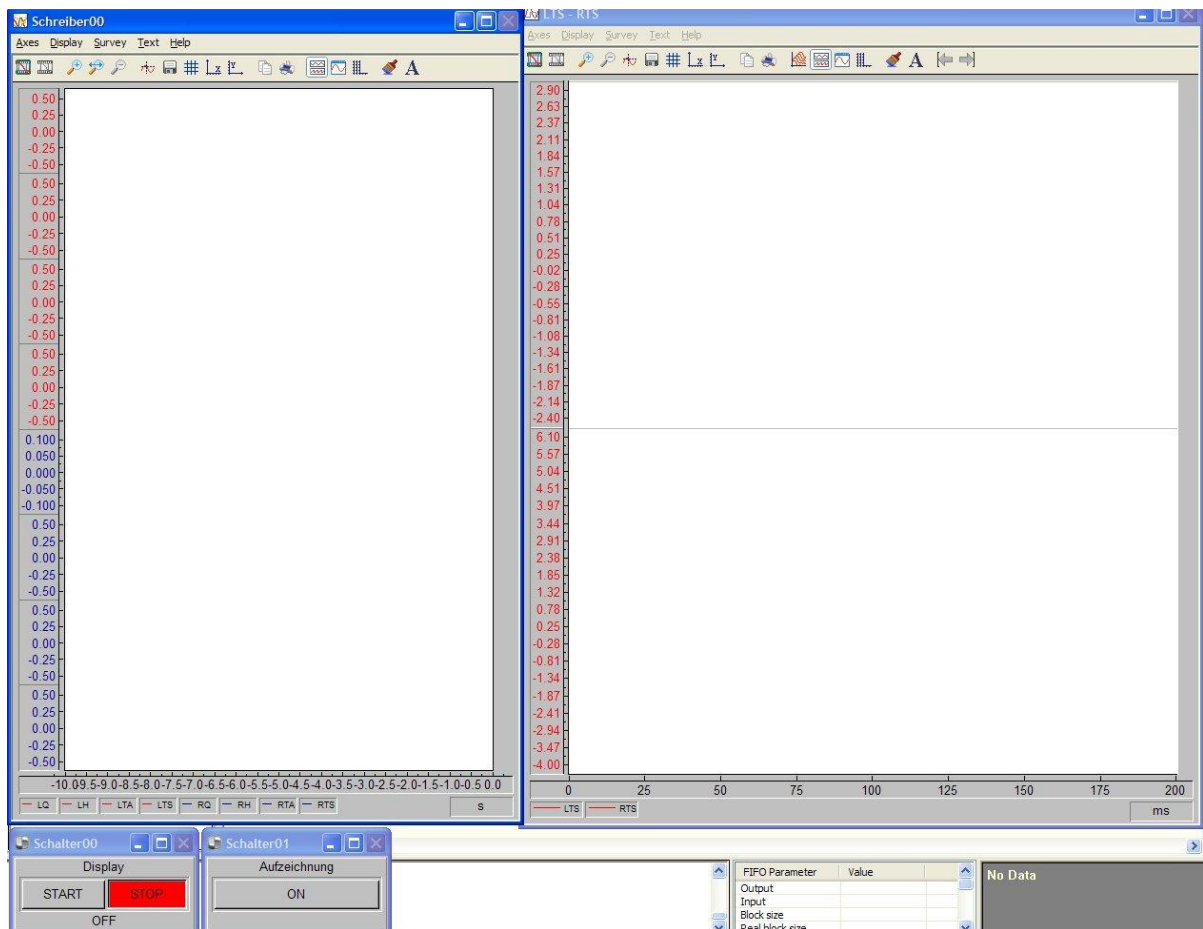


Figure 36. Userinterface of M_{max} routine; The left window shows the ongoing EMG of all muscle groups. The right window shows the stimulus triggered LTS (upper half) and RTS (lower half).

APPENDIX B

Matlab Source Codes

analysis_paradigm_A.m

```
%% -----
% Initialization
%-----

% Try's to close a previous opened Excel-Worksheet
if exist('w')
    try
        Excel.WorkBooks.Item('result4.xls').Close;
        Excel.Quit;
    catch
    end
end

% clear workspace
close all;
clear all;

% Set parameter
th = 0.020; % Threshold: 20μV - DEE 1992;

%% -----
% Load Data from ASCII-file
%-----

% Load all data
disp('file')
[s1, s2] = uigetfile ('*.asc', 'Open File');
disp(s1);
cd (s2);
A=dlmread (s1, ';', 11, 0);
length_A=length(A);

time=A(:,1);
LQ=A(:,2); LH=A(:,3); LTA=A(:,4); LTS=A(:,5);
RQ=A(:,6); RH=A(:,7); RTA=A(:,8); RTS=A(:,9);
Force=A(:,10);

LQ1=LQ; LH1=LH; LTA1=LTA; LTS1=LTS;
RQ1=RQ; RH1=RH; RTA1=RTA; RTS1=RTS;
Forcel=Force;

% normalize timescale
time1=0:0.0005:0.0005*(length(A)-1);
```

```

% Filtering data with Butterworth, 2.Order, fg = 10-700Hz
EMG1=[LQ1 LH1 LTA1 LTS1 RQ1 RH1 RTA1 RTS1];
cuthigh=10;
cutlow=700;
[b,a]=butter(2,cuthigh/2048,'high');
for i=1:8
    testfilter(:,i)=filtfilt(b,a,EMG1(:,i));
end
[b,a]=butter(2,cutlow/2048);
for i=1:8
    testfilter(:,i)=filtfilt(b,a,EMG1(:,i));
end

LQ1=testfilter(:,1); LH1=testfilter(:,2);
LTA1=testfilter(:,3); LTS1=testfilter(:,4);
RQ1=testfilter(:,5); RH1=testfilter(:,6);
RTA1=testfilter(:,7); RTS1=testfilter(:,8);

%% -----
% Overview of EMG - data
%-----

maxihaxi = max(max(abs(EMG1)));

% Left
figure
subplot(9,1,1)
plot(time1,LQ1)
ylabel('LQ')
axis([0 time1(end) -maxihaxi maxihaxi])
subplot(9,1,2)
plot(time1,LH1)
ylabel('LH')
axis([0 time1(end) -maxihaxi maxihaxi])
subplot(9,1,3)
plot(time1,LTA1)
ylabel('LTA')
axis([0 time1(end) -maxihaxi maxihaxi])
subplot(9,1,4)
plot(time1,LTS1)
ylabel('LTS')
axis([0 time1(end) -maxihaxi maxihaxi])

% Right
subplot(9,1,5)
plot(time1,RQ1)
ylabel('RQ')
axis([0 time1(end) -maxihaxi maxihaxi])
subplot(9,1,6)
plot(time1,RH1)
ylabel('RH')
axis([0 time1(end) -maxihaxi maxihaxi])
subplot(9,1,7)
plot(time1,RTA1)
ylabel('RTA')
axis([0 time1(end) -maxihaxi maxihaxi])
subplot(9,1,8)
plot(time1,RTS1)
ylabel('RTS')

```

```

axis([0 time1(end) -maxihaxi maxihaxi])
subplot(9,1,9)
plot(time1,Forcel)
ylabel('Force')

maxwindow;

%% -----
% Select positions
%-----

% Plot force
figure
plot(time1,Forcel)
axis([0 time(length_A) min(Forcel) max(Forcel)])
maxwindow;

% Baseline
read = ginput(1);
baseline = read(2);
hline(baseline);

% Start of relaxed state
read = ginput(1);
start0 = round(read(1)/0.0005); % calculates the postion in time-arrarray
vline(time1(start0));

% End of relaxed state
read = ginput(1);
stop0 = round(read(1)/0.0005); % calculates the postion in time-arrarray
vline(time1(stop0));

% Start of exercise
read = ginput(1);
start = round(read(1)/0.0005); % calculates the postion in time-arrarray
vline(time1(start));

% End of exercise
read = ginput(1);
stop = round(read(1)/0.0005); % ergibt die Zeitpunkte im Array
vline(time1(stop));

%% -----
% Determine onset-times of muscle-activation
%-----
% Threshold = 20µV choosen according to DEE 1992

% Rectification
rekLQ1=abs(LQ1);
rekLH1=abs(LH1);
rekLTA1=abs(LTA1);
rekLTS1=abs(LTS1);
rekRQ1=abs(RQ1);
rekRH1=abs(RH1);
rekRTA1=abs(RTA1);
rekRTS1=abs(RTS1);

```

```

% Calculate RMS-curves from EMG
RMS_LQ = emg2rms(LQ1);
RMS_LH = emg2rms(LH1);
RMS_LTA = emg2rms(LTA1);
RMS_LTS = emg2rms(LTS1);

RMS_RQ = emg2rms(RQ1);
RMS_RH = emg2rms(RH1);
RMS_RTA = emg2rms(RTA1);
RMS_RTS = emg2rms(RTS1);

% Left side
figure('Name','LQ - Select onset','NumberTitle','off')
hold on
plot(time1, rekLQ1)
plot(time1, RMS_LQ, '-g')
hold off
hline(th, 'r-');
vline(time1(start), 'g-');
vline(time1(stop), 'g-');
maxwindow;
read = ginput(1);
on_LQ = round(read(1)/0.0005);

figure('Name','LH - Select onset','NumberTitle','off')
hold on
plot(time1, rekLH1)
plot(time1, RMS_LH, '-g')
hold off
hline(th, 'r-');
vline(time1(start), 'g-');
vline(time1(stop), 'g-');
maxwindow;
read = ginput(1);
on_LH = round(read(1)/0.0005);

figure('Name','LTA - Select onset','NumberTitle','off')
hold on
plot(time1, rekLTA1)
plot(time1, RMS_LTA, '-g')
hold off
hline(th, 'r-');
vline(time1(start), 'g-');
vline(time1(stop), 'g-');
maxwindow;
read = ginput(1);
on_LTA = round(read(1)/0.0005);

figure('Name','LTS - Select onset','NumberTitle','off')
hold on
plot(time1, rekLTS1)
plot(time1, RMS_LTS, '-g')
hold off
hline(th, 'r-');
vline(time1(start), 'g-');
vline(time1(stop), 'g-');
maxwindow;
read = ginput(1);
on_LTS = round(read(1)/0.0005);

```



```

% Right side
figure('Name','RQ - Select onset','NumberTitle','off')
hold on
plot(time1,rekRQ1)
plot(time1,RMS_RQ,'-g')
hold off
hline(th,'r-');
vline(time1(start), 'g-');
vline(time1(stop), 'g-');
maxwindow;
read = ginput(1);
on_RQ = round(read(1)/0.0005);

figure('Name','RH - Select onset','NumberTitle','off')
hold on
plot(time1,rekRH1)
plot(time1,RMS_RH,'-g')
hold off
hline(th,'r-');
vline(time1(start), 'g-');
vline(time1(stop), 'g-');
maxwindow;
read = ginput(1);
on_RH = round(read(1)/0.0005);

figure('Name','RTA - Select onset','NumberTitle','off')
hold on
plot(time1,rekRTA1)
plot(time1,RMS_RTAS,'-g')
hold off
hline(th,'r-');
vline(time1(start), 'g-');
vline(time1(stop), 'g-');
maxwindow;
read = ginput(1);
on_RTAS = round(read(1)/0.0005);

figure('Name','RTS - Select onset','NumberTitle','off')
hold on
plot(time1,rekRTS1)
plot(time1,RMS_RTS,'-g')
hold off
hline(th,'r-');
vline(time1(start), 'g-');
vline(time1(stop), 'g-');
maxwindow;
read = ginput(1);
on_RTS = round(read(1)/0.0005);

```

```

%% -----
% Calculations
%-----

% check boundaries
if on_LQ < start
    on_LQ = start;
elseif on_LQ > stop
    on_LQ = stop;
end

if on_LH < start
    on_LH = start;
elseif on_LH > stop
    on_LH = stop;
end

if on_LTA < start
    on_LTA = start;
elseif on_LTA > stop
    on_LTA = stop;
end

if on_LTS < start
    on_LTS = start;
elseif on_LTS > stop
    on_LTS = stop;
end

if on_RQ < start
    on_RQ = start;
elseif on_RQ > stop
    on_RQ = stop;
end

if on_RH < start
    on_RH = start;
elseif on_RH > stop
    on_RH = stop;
end

if on_RTA < start
    on_RTA = start;
elseif on_RTA > stop
    on_RTA = stop;
end

if on_RTS < start
    on_RTS = start;
elseif on_RTS > stop
    on_RTS = stop;
end

```

```

% Calculate muscular activity in resting state
RMS_mean0_LQ = emg2rmsmean(LQ1(start0:stop0));
RMS_mean0_LH = emg2rmsmean(LH1(start0:stop0));
RMS_mean0_LTA = emg2rmsmean(LTA1(start0:stop0));
RMS_mean0_LTS = emg2rmsmean(LTS1(start0:stop0));
RMS_mean0_RQ = emg2rmsmean(RQ1(start0:stop0));
RMS_mean0_RH = emg2rmsmean(RH1(start0:stop0));
RMS_mean0_RTA = emg2rmsmean(RTA1(start0:stop0));
RMS_mean0_RTS = emg2rmsmean(RTS1(start0:stop0));

% calculate minimum of muscular activity during exercise
RMS_min_LQ = min(RMS_LQ(on_LQ:stop));
RMS_min_LH = min(RMS_LH(on_LH:stop));
RMS_min_LTA = min(RMS_LTA(on_LTA:stop));
RMS_min_LTS = min(RMS_LTS(on_LTS:stop));
RMS_min_RQ = min(RMS_RQ(on_RQ:stop));
RMS_min_RH = min(RMS_RH(on_RH:stop));
RMS_min_RTA = min(RMS_RTA(on_RTA:stop));
RMS_min_RTS = min(RMS_RTS(on_RTS:stop));

% calculate maximum of muscular activity during exercise
RMS_max_LQ = max(RMS_LQ(on_LQ:stop));
RMS_max_LH = max(RMS_LH(on_LH:stop));
RMS_max_LTA = max(RMS_LTA(on_LTA:stop));
RMS_max_LTS = max(RMS_LTS(on_LTS:stop));
RMS_max_RQ = max(RMS_RQ(on_RQ:stop));
RMS_max_RH = max(RMS_RH(on_RH:stop));
RMS_max_RTA = max(RMS_RTA(on_RTA:stop));
RMS_max_RTS = max(RMS_RTS(on_RTS:stop));

% calculate mean of muscular activity during exercise
RMS_mean_LQ = emg2rmsmean(LQ1(on_LQ:stop));
RMS_mean_LH = emg2rmsmean(LH1(on_LH:stop));
RMS_mean_LTA = emg2rmsmean(LTA1(on_LTA:stop));
RMS_mean_LTS = emg2rmsmean(LTS1(on_LTS:stop));
RMS_mean_RQ = emg2rmsmean(RQ1(on_RQ:stop));
RMS_mean_RH = emg2rmsmean(RH1(on_RH:stop));
RMS_mean_RTA = emg2rmsmean(RTA1(on_RTA:stop));
RMS_mean_RTS = emg2rmsmean(RTS1(on_RTS:stop));

% calculate standard deviation of muscular activity during exercise
RMS_std_LQ = std(RMS_LQ(on_LQ:stop));
RMS_std_LH = std(RMS_LH(on_LH:stop));
RMS_std_LTA = std(RMS_LTA(on_LTA:stop));
RMS_std_LTS = std(RMS_LTS(on_LTS:stop));
RMS_std_RQ = std(RMS_RQ(on_RQ:stop));
RMS_std_RH = std(RMS_RH(on_RH:stop));
RMS_std_RTA = std(RMS_RTA(on_RTA:stop));
RMS_std_RTS = std(RMS_RTS(on_RTS:stop));

% calculate onset-times of all muscle groups - refering to start-point
on_time_LQ = timel(on_LQ) - timel(start);
on_time_LH = timel(on_LH) - timel(start);
on_time_LTA = timel(on_LTA) - timel(start);
on_time_LTS = timel(on_LTS) - timel(start);
on_time_RQ = timel(on_RQ) - timel(start);
on_time_RH = timel(on_RH) - timel(start);
on_time_RTA = timel(on_RTA) - timel(start);
on_time_RTS = timel(on_RTS) - timel(start);

```

```

% F @ Onset
% mean of force in a time-slot +-1sec around selected start-point
F_on_LQ = mean(Forcel(on_LQ-1000:on_LQ+1000));
F_on_LH = mean(Forcel(on_LH-1000:on_LH+1000));
F_on_LTA = mean(Forcel(on_LTA-1000:on_LTA+1000));
F_on_LTS = mean(Forcel(on_LTS-1000:on_LTS+1000));
F_on_RQ = mean(Forcel(on_RQ-1000:on_RQ+1000));
F_on_RH = mean(Forcel(on_RH-1000:on_RH+1000));
F_on_RTA = mean(Forcel(on_RTA-1000:on_RTA+1000));
F_on_RTS = mean(Forcel(on_RTS-1000:on_RTS+1000));

% MVC
MVC = max(Forcel);

% Duration of the exercise
duration = timel(stop) - timel(start);

% F @ End
% mean of force in a time-slot +-1sec around selected end-point
F_off = mean(Forcel(stop-2000:stop));

%% -----
% Summary of results
% -----
% Shows: rectified EMG, RMS-curve, MIN/MAX/MEAN of RMS-curve,
%         exercise boundaries and onset-times

% Left side
figure
subplot(4,1,1)
hold on
plot(timel, rekLQ1)
plot(timel, RMS_LQ, '-g')
hold off
hline(RMS_mean_LQ, '-m')
hline(RMS_min_LQ, ':m')
hline(RMS_max_LQ, ':m')
vline(timel(on_LQ), 'g-');
vline(timel(stop), 'g-');

subplot(4,1,2)
hold on
plot(timel, rekLH1)
plot(timel, RMS_LH, '-g')
hold off
hline(RMS_mean_LH, '-m')
hline(RMS_min_LH, ':m')
hline(RMS_max_LH, ':m')
vline(timel(on_LH), 'g-');
vline(timel(stop), 'g-');

```

```

subplot(4,1,3)
hold on
plot(time1, rekLTA1)
plot(time1, RMS_LTA, '-g')
hold off
hline(RMS_mean_LTA, '-m')
hline(RMS_min_LTA, ':m')
hline(RMS_max_LTA, ':m')
vline(time1(on_LTA), 'g-');
vline(time1(stop), 'g-');

subplot(4,1,4)
hold on
plot(time1, rekLTS1)
plot(time1, RMS_LTS, '-g')
hold off
hline(RMS_mean_LTS, '-m')
hline(RMS_min_LTS, ':m')
hline(RMS_max_LTS, ':m')
vline(time1(on_LTS), 'g-');
vline(time1(stop), 'g-');
maxwindow;

% Right side
figure
subplot(4,1,1)
hold on
plot(time1, rekRQ1)
plot(time1, RMS_RQ, '-g')
hold off
hline(RMS_mean_RQ, '-m')
hline(RMS_min_RQ, ':m')
hline(RMS_max_RQ, ':m')
vline(time1(on_RQ), 'g-');
vline(time1(stop), 'g-');

subplot(4,1,2)
hold on
plot(time1, rekRH1)
plot(time1, RMS_RH, '-g')
hold off
hline(RMS_mean_RH, '-m')
hline(RMS_min_RH, ':m')
hline(RMS_max_RH, ':m')
vline(time1(on_RH), 'g-');
vline(time1(stop), 'g-');

subplot(4,1,3)
hold on
plot(time1, rekRTA1)
plot(time1, RMS_RTA, '-g')
hold off
hline(RMS_mean_RTA, '-m')
hline(RMS_min_RTA, ':m')
hline(RMS_max_RTA, ':m')
vline(time1(on_RTA), 'g-');
vline(time1(stop), 'g-');

```

```

subplot(4,1,4)
hold on
plot(time1, rekRTS1)
plot(time1, RMS_RTS, '-g')
hold off
hline(RMS_mean_RTS, '-m')
hline(RMS_min_RTS, ':m')
hline(RMS_max_RTS, ':m')
vline(time1(on_RTS), 'g-');
vline(time1(stop), 'g-');
maxwindow;

%% -----
% Export of results into EXCEL
%-----

output = [
    RMS_mean0_LQ*1000 RMS_min_LQ*1000 RMS_max_LQ*1000
    RMS_mean_LQ*1000 RMS_std_LQ*1000 on_time_LQ F_on_LQ MVC;
    RMS_mean0_LH*1000 RMS_min_LH*1000 RMS_max_LH*1000
    RMS_mean_LH*1000 RMS_std_LH*1000 on_time_LH F_on_LH F_off;
    RMS_mean0_LTA*1000 RMS_min_LTA*1000 RMS_max_LTA*1000
    RMS_mean_LTA*1000 RMS_std_LTA*1000 on_time_LTA F_on_LTA duration;
    RMS_mean0_LTS*1000 RMS_min_LTS*1000 RMS_max_LTS*1000
    RMS_mean_LTS*1000 RMS_std_LTS*1000 on_time_LTS F_on_LTS baseline;
    RMS_mean0_RQ*1000 RMS_min_RQ*1000 RMS_max_RQ*1000
    RMS_mean_RQ*1000 RMS_std_RQ*1000 on_time_RQ F_on_RQ 0;
    RMS_mean0_RH*1000 RMS_min_RH*1000 RMS_max_RH*1000
    RMS_mean_RH*1000 RMS_std_RH*1000 on_time_RH F_on_RH 0;
    RMS_mean0_RTA*1000 RMS_min_RTA*1000 RMS_max_RTA*1000
    RMS_mean_RTA*1000 RMS_std_RTA*1000 on_time_RTA F_on_RTA 0;
    RMS_mean0_RTS*1000 RMS_min_RTS*1000 RMS_max_RTS*1000
    RMS_mean_RTS*1000 RMS_std_RTS*1000 on_time_RTS F_on_RTS 0;
];

% Check data - set results in inactive muscle groups to '999'
if on_LQ == stop
    output(1,1:7)=999;
end
if on_LH == stop;
    output(2,1:7)=999;
end
if on_LTA == stop;
    output(3,1:7)=999;
end
if on_LTS == stop;
    output(4,1:7)=999;
end
if on_RQ == stop;
    output(5,1:7)=999;
end
if on_RH == stop;
    output(6,1:7)=999;
end
if on_RTA == stop;
    output(7,1:7)=999;
end
if on_RTS == stop;
    output(8,1:7)=999;
end

```

```
% Write into Excel-file
Excel = actxserver('Excel.Application');
Excel.Visible = 1;
w = Excel.Workbooks;
file = strcat(s2,'result4.xls');

xlswrite(file,output);
invoke(w, 'open', file);
```

Code 1. Matlab code of analysis_paradigm_A.m

emg2rms.m

This routine serves as simple converting function. Input is a sequence of EMG-data from which a continuous RMS-curve is generated. For every position x in the sequence, an evaluation-window ($x \pm 250\text{ms}$) was created. The RMS of this certain window serves as result in the output sequence on position x . This is done for all positions of the input. The source code can be seen below.

```
% This function generates a RMS-curve from given EMG-data
% input... EMG-sequence
% output... RMS-sequence

function rms = emg2rms(emg)

% Set Parameter
res = 500;           % defines the half window size; equal to 250ms
len = length(emg);   % length of the dataset

rms = emg;

% Set the first and the last 'res' positions to 0
rms(1:res) = 0;
rms(len-res:end) = 0;

% Calculate RMS for every position in data and shift evaluation window
for i = res+1:len-res
    rms(i) = calcRMS(emg(i-res:i+res));
end
return;

% Helper-function for calculation of RMS
function result = calcRMS(input)

d = length(input);
input = input.*input;

% Calculate RMS
result = sqrt(sum(input)/d);

return;
```

Code 2. Matlab code of emg2rms.m

emg2rmsmean.m

This routine calculates the RMS of a given EMG-data. Source code can be seen below.

```
%% Calculates the RMS-Value of a given EMG-signal
% input .... EMG data
% result ... RMS value

function result = emg2rmsmean(input)

d = length(input);
input = input.*input;

% Calculate RMS
result = sqrt(sum(input)/d);

return;
```

Code 3. Matlab code of `emg2rmsmean.m`

analysis_paradigm_B.m

```
%% -----
% Initialization
%-----

% Try's to close a previous opened Excel-Worksheet
if exist('w')
    try
        Excel.WorkBooks.Item('result3.xls').Close;
        Excel.Quit;
    catch
    end
end

close all;
clear all;

%% -----
% Load Data from ASCII-file
%-----

% Load all data
[s1, s2] = uigetfile ('*.asc', 'Open File');
cd (s2);
disp('file')
disp(s1)
A=dlmread (s1, ';', 11, 0);
length_A=length(A);

time=A(:,1);
LQ=A(:,2); LH=A(:,3); LTA=A(:,4); LTS=A(:,5);
RQ=A(:,6); RH=A(:,7); RTA=A(:,8); RTS=A(:,9);
Force=A(:,10);

LQ1=LQ; LH1=LH; LTA1=LTA; LTS1=LTS;
RQ1=RQ; RH1=RH; RTA1=RTA; RTS1=RTS;
Forcel=Force;

% Normalize timescale
time1=0:0.0005:0.0005*(length(A)-1);

% Filtering data with Butterworth, 2.Order, fg = 10-700Hz
EMG1=[LQ1 LH1 LTA1 LTS1 RQ1 RH1 RTA1 RTS1];
cuthigh=10;
cutlow=700;
[b,a]=butter(2,cuthigh/2048,'high');
for i=1:8
    testfilter(:,i)=filtfilt(b,a,EMG1(:,i));
end
[b,a]=butter(2,cutlow/2048);
for i=1:8
    testfilter(:,i)=filtfilt(b,a,EMG1(:,i));
end
```

```

LQ1=testfilter(:,1); LH1=testfilter(:,2);
LTA1=testfilter(:,3); LTS1=testfilter(:,4);
RQ1=testfilter(:,5); RH1=testfilter(:,6);
RTA1=testfilter(:,7); RTS1=testfilter(:,8);

percentage_MVC=(Forcel/MVC)*100;

%% -----
% Overview of EMG - data
%-----

% Left
figure
subplot(5,1,1)
plot(time1,LQ1)
ylabel('LQ')
subplot(5,1,2)
plot(time1,LH1)
ylabel('LH')
subplot(5,1,3)
plot(time1,LTA1)
ylabel('LTA')
subplot(5,1,4)
plot(time1,LTS1)
ylabel('LTS')
subplot(5,1,5)
plot(time1,Forcel)
ylabel('Force')

% Right
figure
subplot(5,1,1)
plot(time1,RQ1)
ylabel('RQ')
subplot(5,1,2)
plot(time1,RH1)
ylabel('RH')
subplot(5,1,3)
plot(time1,RTA1)
ylabel('RTA')
subplot(5,1,4)
plot(time1,RTS1)
ylabel('RTS')
subplot(5,1,5)
plot(time1,Forcel)
ylabel('Force')

%% -----
% Select positions
%-----

figure('Name','Select positions','NumberTitle','off')
plot(time1,Forcel)
grid on
axis([0 time1(length(Forcel)) min(Forcel)*1.1 max(Forcel)*1.1])

```

```

% Select baseline
read = ginput(1);
baseline = read(1,2);
hline(baseline);

% Select 0% MVC
% Start
read = ginput(1);
MVC0 = zeros(1,2);
MVC0(1)= read(1,1);
vline(MVC0(1));
% End
read = ginput(1);
MVC0(2)= read(1,1);
vline(MVC0(2));

% Select 20% MVC
% Start
read = ginput(1);
MVC20 = zeros(1,2);
MVC20(1)= read(1,1);
vline(MVC20(1));
% End
read = ginput(1);
MVC20(2)= read(1,1);
vline(MVC20(2));

% Select 40% MVC
% Start
read = ginput(1);
MVC40 = zeros(1,2);
MVC40(1)= read(1,1);
vline(MVC40(1));
% End
read = ginput(1);
MVC40(2)= read(1,1);
vline(MVC40(2));

% Select 60% MVC
% Start
read = ginput(1);
MVC60 = zeros(1,2);
MVC60(1)= read(1,1);
vline(MVC60(1));
% End
read = ginput(1);
MVC60(2)= read(1,1);
vline(MVC60(2));

% Select 80% MVC
% Start
read = ginput(1);
MVC80 = zeros(1,2);
MVC80(1)= read(1,1);
vline(MVC80(1));
% End
read = ginput(1);
MVC80(2)= read(1,1);
vline(MVC80(2));

```

```

% Select 100% MVC
% Start
read = ginput(1);
MVC100 = zeros(1,2);
MVC100(1)= read(1,1);
vline(MVC100(1));
% End
read = ginput(1);
MVC100(2)= read(1,1);
vline(MVC100(2));

%% -----
% Calculations
%-----

%% Calculate positions from time-selections
MVC0 = round(MVC0/0.0005);
MVC20 = round(MVC20/0.0005);
MVC40 = round(MVC40/0.0005);
MVC60 = round(MVC60/0.0005);
MVC80 = round(MVC80/0.0005);
MVC100 = round(MVC100/0.0005);

% Square EMG-Data
LQ2=LQ1.*LQ1;
LH2=LH1.*LH1;
LTA2=LTA1.*LTA1;
LTS2=LTS1.*LTS1;

RQ2=RQ1.*RQ1;
RH2=RH1.*RH1;
RTA2=RTA1.*RTA1;
RTS2=RTS1.*RTS1;

%% Calculate means of force
F0 = baseline;
F20 = mean(Forcel(MVC20(1):MVC20(2)));
hline(F20);
F40 = mean(Forcel(MVC40(1):MVC40(2)));
hline(F40);
F60 = mean(Forcel(MVC60(1):MVC60(2)));
hline(F60);
F80 = mean(Forcel(MVC80(1):MVC80(2)));
hline(F80);
F100 = mean(Forcel(MVC100(1):MVC100(2)));
hline(F100);

%% Calculate standard deviations of force
F0_std = 0;
F20_std = std(Forcel(MVC20(1):MVC20(2)));
F40_std = std(Forcel(MVC40(1):MVC40(2)));
F60_std = std(Forcel(MVC60(1):MVC60(2)));
F80_std = std(Forcel(MVC80(1):MVC80(2)));
F100_std = std(Forcel(MVC100(1):MVC100(2)));

%% Calculate RMS from EMG

```

```

% LTA
LQ0 = sqrt(sum(LQ2(MVC0(1):MVC0(2)))/(MVC0(2)-MVC0(1)));
LQ20 = sqrt(sum(LQ2(MVC20(1):MVC20(2)))/(MVC20(2)-MVC20(1)));
LQ40 = sqrt(sum(LQ2(MVC40(1):MVC40(2)))/(MVC40(2)-MVC40(1)));
LQ60 = sqrt(sum(LQ2(MVC60(1):MVC60(2)))/(MVC60(2)-MVC60(1)));
LQ80 = sqrt(sum(LQ2(MVC80(1):MVC80(2)))/(MVC80(2)-MVC80(1)));
LQ100 = sqrt(sum(LQ2(MVC100(1):MVC100(2)))/(MVC100(2)-MVC100(1)));

% LH
LH0 = sqrt(sum(LH2(MVC0(1):MVC0(2)))/(MVC0(2)-MVC0(1)));
LH20 = sqrt(sum(LH2(MVC20(1):MVC20(2)))/(MVC20(2)-MVC20(1)));
LH40 = sqrt(sum(LH2(MVC40(1):MVC40(2)))/(MVC40(2)-MVC40(1)));
LH60 = sqrt(sum(LH2(MVC60(1):MVC60(2)))/(MVC60(2)-MVC60(1)));
LH80 = sqrt(sum(LH2(MVC80(1):MVC80(2)))/(MVC80(2)-MVC80(1)));
LH100 = sqrt(sum(LH2(MVC100(1):MVC100(2)))/(MVC100(2)-MVC100(1)));

% LTA
LTA0 = sqrt(sum(LTA2(MVC0(1):MVC0(2)))/(MVC0(2)-MVC0(1)));
LTA20 = sqrt(sum(LTA2(MVC20(1):MVC20(2)))/(MVC20(2)-MVC20(1)));
LTA40 = sqrt(sum(LTA2(MVC40(1):MVC40(2)))/(MVC40(2)-MVC40(1)));
LTA60 = sqrt(sum(LTA2(MVC60(1):MVC60(2)))/(MVC60(2)-MVC60(1)));
LTA80 = sqrt(sum(LTA2(MVC80(1):MVC80(2)))/(MVC80(2)-MVC80(1)));
LTA100 = sqrt(sum(LTA2(MVC100(1):MVC100(2)))/(MVC100(2)-MVC100(1)));

% LTS
LTS0 = sqrt(sum(LTS2(MVC0(1):MVC0(2)))/(MVC0(2)-MVC0(1)));
LTS20 = sqrt(sum(LTS2(MVC20(1):MVC20(2)))/(MVC20(2)-MVC20(1)));
LTS40 = sqrt(sum(LTS2(MVC40(1):MVC40(2)))/(MVC40(2)-MVC40(1)));
LTS60 = sqrt(sum(LTS2(MVC60(1):MVC60(2)))/(MVC60(2)-MVC60(1)));
LTS80 = sqrt(sum(LTS2(MVC80(1):MVC80(2)))/(MVC80(2)-MVC80(1)));
LTS100 = sqrt(sum(LTS2(MVC100(1):MVC100(2)))/(MVC100(2)-MVC100(1)));

% RTA
RQ0 = sqrt(sum(RQ2(MVC0(1):MVC0(2)))/(MVC0(2)-MVC0(1)));
RQ20 = sqrt(sum(RQ2(MVC20(1):MVC20(2)))/(MVC20(2)-MVC20(1)));
RQ40 = sqrt(sum(RQ2(MVC40(1):MVC40(2)))/(MVC40(2)-MVC40(1)));
RQ60 = sqrt(sum(RQ2(MVC60(1):MVC60(2)))/(MVC60(2)-MVC60(1)));
RQ80 = sqrt(sum(RQ2(MVC80(1):MVC80(2)))/(MVC80(2)-MVC80(1)));
RQ100 = sqrt(sum(RQ2(MVC100(1):MVC100(2)))/(MVC100(2)-MVC100(1)));

% RH
RH0 = sqrt(sum(RH2(MVC0(1):MVC0(2)))/(MVC0(2)-MVC0(1)));
RH20 = sqrt(sum(RH2(MVC20(1):MVC20(2)))/(MVC20(2)-MVC20(1)));
RH40 = sqrt(sum(RH2(MVC40(1):MVC40(2)))/(MVC40(2)-MVC40(1)));
RH60 = sqrt(sum(RH2(MVC60(1):MVC60(2)))/(MVC60(2)-MVC60(1)));
RH80 = sqrt(sum(RH2(MVC80(1):MVC80(2)))/(MVC80(2)-MVC80(1)));
RH100 = sqrt(sum(RH2(MVC100(1):MVC100(2)))/(MVC100(2)-MVC100(1)));

% RTA
RTA0 = sqrt(sum(RTA2(MVC0(1):MVC0(2)))/(MVC0(2)-MVC0(1)));
RTA20 = sqrt(sum(RTA2(MVC20(1):MVC20(2)))/(MVC20(2)-MVC20(1)));
RTA40 = sqrt(sum(RTA2(MVC40(1):MVC40(2)))/(MVC40(2)-MVC40(1)));
RTA60 = sqrt(sum(RTA2(MVC60(1):MVC60(2)))/(MVC60(2)-MVC60(1)));
RTA80 = sqrt(sum(RTA2(MVC80(1):MVC80(2)))/(MVC80(2)-MVC80(1)));
RTA100 = sqrt(sum(RTA2(MVC100(1):MVC100(2)))/(MVC100(2)-MVC100(1)));

```

```

% RTS
RTS0 = sqrt(sum(RTS2(MVC0(1):MVC0(2)))/(MVC0(2)-MVC0(1)));
RTS20 = sqrt(sum(RTS2(MVC20(1):MVC20(2)))/(MVC20(2)-MVC20(1)));
RTS40 = sqrt(sum(RTS2(MVC40(1):MVC40(2)))/(MVC40(2)-MVC40(1)));
RTS60 = sqrt(sum(RTS2(MVC60(1):MVC60(2)))/(MVC60(2)-MVC60(1)));
RTS80 = sqrt(sum(RTS2(MVC80(1):MVC80(2)))/(MVC80(2)-MVC80(1)));
RTS100 = sqrt(sum(RTS2(MVC100(1):MVC100(2)))/(MVC100(2)-MVC100(1)));

%% -----
% Plots in detail
%-----

%LQ
figure('Name','LQ','NumberTitle','off')
subplot(6,1,1);
plot(time1(1:MVC0(2)-MVC0(1)+1),abs(LQ1(MVC0(1):MVC0(2))))
ylabel('0%')
hline(LQ0,'r','RMS');
axis([0 time1(MVC0(2)-MVC0(1)) 0 max(abs(LQ1(MVC100(1):MVC100(2))))])

subplot(6,1,2);
plot(time1(1:MVC20(2)-MVC20(1)+1),abs(LQ1(MVC20(1):MVC20(2))))
ylabel('20%')
hline(LQ20,'r','RMS');
axis([0 time1(MVC20(2)-MVC20(1)) 0 max(abs(LQ1(MVC100(1):MVC100(2))))])

subplot(6,1,3);
plot(time1(1:MVC40(2)-MVC40(1)+1),abs(LQ1(MVC40(1):MVC40(2))))
ylabel('40%')
hline(LQ40,'r','RMS');
axis([0 time1(MVC40(2)-MVC40(1)) 0 max(abs(LQ1(MVC100(1):MVC100(2))))])

subplot(6,1,4);
plot(time1(1:MVC60(2)-MVC60(1)+1),abs(LQ1(MVC60(1):MVC60(2))))
ylabel('60%')
hline(LQ60,'r','RMS');
axis([0 time1(MVC60(2)-MVC60(1)) 0 max(abs(LQ1(MVC100(1):MVC100(2))))])

subplot(6,1,5);
plot(time1(1:MVC80(2)-MVC80(1)+1),abs(LQ1(MVC80(1):MVC80(2))))
ylabel('80%')
hline(LQ80,'r','RMS');
axis([0 time1(MVC80(2)-MVC80(1)) 0 max(abs(LQ1(MVC100(1):MVC100(2))))])

subplot(6,1,6);
plot(time1(1:MVC100(2)-MVC100(1)+1),abs(LQ1(MVC100(1):MVC100(2))))
ylabel('100%')
hline(LQ100,'r','RMS');
axis([0 time1(MVC100(2)-MVC100(1)) 0 max(abs(LQ1(MVC100(1):MVC100(2))))])

```

```

% LH
figure('Name','LH','NumberTitle','off')
subplot(6,1,1);
plot(time1(1:MVC0(2)-MVC0(1)+1),abs(LH1(MVC0(1):MVC0(2))))
ylabel('0%')
hline(LH0,'r','RMS');
axis([0 time1(MVC0(2)-MVC0(1)) 0 max(abs(LH1(MVC100(1):MVC100(2))))])

subplot(6,1,2);
plot(time1(1:MVC20(2)-MVC20(1)+1),abs(LH1(MVC20(1):MVC20(2))))
ylabel('20%')
hline(LH20,'r','RMS');
axis([0 time1(MVC20(2)-MVC20(1)) 0 max(abs(LH1(MVC100(1):MVC100(2))))])

subplot(6,1,3);
plot(time1(1:MVC40(2)-MVC40(1)+1),abs(LH1(MVC40(1):MVC40(2))))
ylabel('40%')
hline(LH40,'r','RMS');
axis([0 time1(MVC40(2)-MVC40(1)) 0 max(abs(LH1(MVC100(1):MVC100(2))))])

subplot(6,1,4);
plot(time1(1:MVC60(2)-MVC60(1)+1),abs(LH1(MVC60(1):MVC60(2))))
ylabel('60%')
hline(LH60,'r','RMS');
axis([0 time1(MVC60(2)-MVC60(1)) 0 max(abs(LH1(MVC100(1):MVC100(2))))])

subplot(6,1,5);
plot(time1(1:MVC80(2)-MVC80(1)+1),abs(LH1(MVC80(1):MVC80(2))))
ylabel('80%')
hline(LH80,'r','RMS');
axis([0 time1(MVC80(2)-MVC80(1)) 0 max(abs(LH1(MVC100(1):MVC100(2))))])

subplot(6,1,6);
plot(time1(1:MVC100(2)-MVC100(1)+1),abs(LH1(MVC100(1):MVC100(2))))
ylabel('100%')
hline(LH100,'r','RMS');
axis([0 time1(MVC100(2)-MVC100(1)) 0 max(abs(LH1(MVC100(1):MVC100(2))))])

% LTA
figure('Name','LTA','NumberTitle','off')
subplot(6,1,1);
plot(time1(1:MVC0(2)-MVC0(1)+1),abs(LTA1(MVC0(1):MVC0(2))))
ylabel('0%')
hline(LTA0,'r','RMS');
axis([0 time1(MVC0(2)-MVC0(1)) 0 max(abs(LTA1(MVC100(1):MVC100(2))))])

subplot(6,1,2);
plot(time1(1:MVC20(2)-MVC20(1)+1),abs(LTA1(MVC20(1):MVC20(2))))
ylabel('20%')
hline(LTA20,'r','RMS');
axis([0 time1(MVC20(2)-MVC20(1)) 0 max(abs(LTA1(MVC100(1):MVC100(2))))])

subplot(6,1,3);
plot(time1(1:MVC40(2)-MVC40(1)+1),abs(LTA1(MVC40(1):MVC40(2))))
ylabel('40%')
hline(LTA40,'r','RMS');
axis([0 time1(MVC40(2)-MVC40(1)) 0 max(abs(LTA1(MVC100(1):MVC100(2))))])

```

```

subplot(6,1,4);
plot(time1(1:MVC60(2)-MVC60(1)+1),abs(LTA1(MVC60(1):MVC60(2))))
ylabel('60%')
hline(LTA60,'r','RMS');
axis([0 time1(MVC60(2)-MVC60(1)) 0 max(abs(LTA1(MVC100(1):MVC100(2))))])

subplot(6,1,5);
plot(time1(1:MVC80(2)-MVC80(1)+1),abs(LTA1(MVC80(1):MVC80(2))))
ylabel('80%')
hline(LTA80,'r','RMS');
axis([0 time1(MVC80(2)-MVC80(1)) 0 max(abs(LTA1(MVC100(1):MVC100(2))))])

subplot(6,1,6);
plot(time1(1:MVC100(2)-MVC100(1)+1),abs(LTA1(MVC100(1):MVC100(2))))
ylabel('100%')
hline(LTA100,'r','RMS');
axis([0 time1(MVC100(2)-MVC100(1)) 0 max(abs(LTA1(MVC100(1):MVC100(2))))])

% LTS
figure('Name','LTS','NumberTitle','off')
subplot(6,1,1);
plot(time1(1:MVC0(2)-MVC0(1)+1),abs(LTS1(MVC0(1):MVC0(2))))
ylabel('0%')
hline(LTS0,'r','RMS');
axis([0 time1(MVC0(2)-MVC0(1)) 0 max(abs(LTS1(MVC100(1):MVC100(2))))])

subplot(6,1,2);
plot(time1(1:MVC20(2)-MVC20(1)+1),abs(LTS1(MVC20(1):MVC20(2))))
ylabel('20%')
hline(LTS20,'r','RMS');
axis([0 time1(MVC20(2)-MVC20(1)) 0 max(abs(LTS1(MVC100(1):MVC100(2))))])

subplot(6,1,3);
plot(time1(1:MVC40(2)-MVC40(1)+1),abs(LTS1(MVC40(1):MVC40(2))))
ylabel('40%')
hline(LTS40,'r','RMS');
axis([0 time1(MVC40(2)-MVC40(1)) 0 max(abs(LTS1(MVC100(1):MVC100(2))))])

subplot(6,1,4);
plot(time1(1:MVC60(2)-MVC60(1)+1),abs(LTS1(MVC60(1):MVC60(2))))
ylabel('60%')
hline(LTS60,'r','RMS');
axis([0 time1(MVC60(2)-MVC60(1)) 0 max(abs(LTS1(MVC100(1):MVC100(2))))])

subplot(6,1,5);
plot(time1(1:MVC80(2)-MVC80(1)+1),abs(LTS1(MVC80(1):MVC80(2))))
ylabel('80%')
hline(LTS80,'r','RMS');
axis([0 time1(MVC80(2)-MVC80(1)) 0 max(abs(LTS1(MVC100(1):MVC100(2))))])

subplot(6,1,6);
plot(time1(1:MVC100(2)-MVC100(1)+1),abs(LTS1(MVC100(1):MVC100(2))))
ylabel('100%')
hline(LTS100,'r','RMS');
axis([0 time1(MVC100(2)-MVC100(1)) 0 max(abs(LTS1(MVC100(1):MVC100(2))))])

```



```

% RQ
figure('Name','RQ','NumberTitle','off')
subplot(6,1,1);
plot(time1(1:MVC0(2)-MVC0(1)+1),abs(RQ1(MVC0(1):MVC0(2))))
ylabel('0%')
hline(RQ0,'r','RMS');
axis([0 time1(MVC0(2)-MVC0(1)) 0 max(abs(RQ1(MVC100(1):MVC100(2))))])

subplot(6,1,2);
plot(time1(1:MVC20(2)-MVC20(1)+1),abs(RQ1(MVC20(1):MVC20(2))))
ylabel('20%')
hline(RQ20,'r','RMS');
axis([0 time1(MVC20(2)-MVC20(1)) 0 max(abs(RQ1(MVC100(1):MVC100(2))))])

subplot(6,1,3);
plot(time1(1:MVC40(2)-MVC40(1)+1),abs(RQ1(MVC40(1):MVC40(2))))
ylabel('40%')
hline(RQ40,'r','RMS');
axis([0 time1(MVC40(2)-MVC40(1)) 0 max(abs(RQ1(MVC100(1):MVC100(2))))])

subplot(6,1,4);
plot(time1(1:MVC60(2)-MVC60(1)+1),abs(RQ1(MVC60(1):MVC60(2))))
ylabel('60%')
hline(RQ60,'r','RMS');
axis([0 time1(MVC60(2)-MVC60(1)) 0 max(abs(RQ1(MVC100(1):MVC100(2))))])

subplot(6,1,5);
plot(time1(1:MVC80(2)-MVC80(1)+1),abs(RQ1(MVC80(1):MVC80(2))))
ylabel('80%')
hline(RQ80,'r','RMS');
axis([0 time1(MVC80(2)-MVC80(1)) 0 max(abs(RQ1(MVC100(1):MVC100(2))))])

subplot(6,1,6);
plot(time1(1:MVC100(2)-MVC100(1)+1),abs(RQ1(MVC100(1):MVC100(2))))
ylabel('100%')
hline(RQ100,'r','RMS');
axis([0 time1(MVC100(2)-MVC100(1)) 0 max(abs(RQ1(MVC100(1):MVC100(2))))])

% RH
figure('Name','RH','NumberTitle','off')
subplot(6,1,1);
plot(time1(1:MVC0(2)-MVC0(1)+1),abs(RH1(MVC0(1):MVC0(2))))
ylabel('0%')
hline(RH0,'r','RMS');
axis([0 time1(MVC0(2)-MVC0(1)) 0 max(abs(RH1(MVC100(1):MVC100(2))))])

subplot(6,1,2);
plot(time1(1:MVC20(2)-MVC20(1)+1),abs(RH1(MVC20(1):MVC20(2))))
ylabel('20%')
hline(RH20,'r','RMS');
axis([0 time1(MVC20(2)-MVC20(1)) 0 max(abs(RH1(MVC100(1):MVC100(2))))])

subplot(6,1,3);
plot(time1(1:MVC40(2)-MVC40(1)+1),abs(RH1(MVC40(1):MVC40(2))))
ylabel('40%')
hline(RH40,'r','RMS');
axis([0 time1(MVC40(2)-MVC40(1)) 0 max(abs(RH1(MVC100(1):MVC100(2))))])

```

```

subplot(6,1,4);
plot(time1(1:MVC60(2)-MVC60(1)+1),abs(RH1(MVC60(1):MVC60(2))))
ylabel('60%')
hline(RH60,'r','RMS');
axis([0 time1(MVC60(2)-MVC60(1)) 0 max(abs(RH1(MVC100(1):MVC100(2))))])

subplot(6,1,5);
plot(time1(1:MVC80(2)-MVC80(1)+1),abs(RH1(MVC80(1):MVC80(2))))
ylabel('80%')
hline(RH80,'r','RMS');
axis([0 time1(MVC80(2)-MVC80(1)) 0 max(abs(RH1(MVC100(1):MVC100(2))))])

subplot(6,1,6);
plot(time1(1:MVC100(2)-MVC100(1)+1),abs(RH1(MVC100(1):MVC100(2))))
ylabel('100%')
hline(RH100,'r','RMS');
axis([0 time1(MVC100(2)-MVC100(1)) 0 max(abs(RH1(MVC100(1):MVC100(2))))])

% RTA
figure('Name','RTA','NumberTitle','off')
subplot(6,1,1);
plot(time1(1:MVC0(2)-MVC0(1)+1),abs(RTA1(MVC0(1):MVC0(2))))
ylabel('0%')
hline(RTA0,'r','RMS');
axis([0 time1(MVC0(2)-MVC0(1)) 0 max(abs(RTA1(MVC100(1):MVC100(2))))])

subplot(6,1,2);
plot(time1(1:MVC20(2)-MVC20(1)+1),abs(RTA1(MVC20(1):MVC20(2))))
ylabel('20%')
hline(RTA20,'r','RMS');
axis([0 time1(MVC20(2)-MVC20(1)) 0 max(abs(RTA1(MVC100(1):MVC100(2))))])

subplot(6,1,3);
plot(time1(1:MVC40(2)-MVC40(1)+1),abs(RTA1(MVC40(1):MVC40(2))))
ylabel('40%')
hline(RTA40,'r','RMS');
axis([0 time1(MVC40(2)-MVC40(1)) 0 max(abs(RTA1(MVC100(1):MVC100(2))))])

subplot(6,1,4);
plot(time1(1:MVC60(2)-MVC60(1)+1),abs(RTA1(MVC60(1):MVC60(2))))
ylabel('60%')
hline(RTA60,'r','RMS');
axis([0 time1(MVC60(2)-MVC60(1)) 0 max(abs(RTA1(MVC100(1):MVC100(2))))])

subplot(6,1,5);
plot(time1(1:MVC80(2)-MVC80(1)+1),abs(RTA1(MVC80(1):MVC80(2))))
ylabel('80%')
hline(RTA80,'r','RMS');
axis([0 time1(MVC80(2)-MVC80(1)) 0 max(abs(RTA1(MVC100(1):MVC100(2))))])

subplot(6,1,6);
plot(time1(1:MVC100(2)-MVC100(1)+1),abs(RTA1(MVC100(1):MVC100(2))))
ylabel('100%')
hline(RTA100,'r','RMS');
axis([0 time1(MVC100(2)-MVC100(1)) 0 max(abs(RTA1(MVC100(1):MVC100(2))))])

```

```

% RTS
figure('Name','RTS','NumberTitle','off')
subplot(6,1,1);
plot(time1(1:MVC0(2)-MVC0(1)+1),abs(RTS1(MVC0(1):MVC0(2))))
ylabel('0%')
hline(RTS0,'r','RMS');
axis([0 time1(MVC0(2)-MVC0(1)) 0 max(abs(RTS1(MVC100(1):MVC100(2))))])

subplot(6,1,2);
plot(time1(1:MVC20(2)-MVC20(1)+1),abs(RTS1(MVC20(1):MVC20(2))))
ylabel('20%')
hline(RTS20,'r','RMS');
axis([0 time1(MVC20(2)-MVC20(1)) 0 max(abs(RTS1(MVC100(1):MVC100(2))))])

subplot(6,1,3);
plot(time1(1:MVC40(2)-MVC40(1)+1),abs(RTS1(MVC40(1):MVC40(2))))
ylabel('40%')
hline(RTS40,'r','RMS');
axis([0 time1(MVC40(2)-MVC40(1)) 0 max(abs(RTS1(MVC100(1):MVC100(2))))])

subplot(6,1,4);
plot(time1(1:MVC60(2)-MVC60(1)+1),abs(RTS1(MVC60(1):MVC60(2))))
ylabel('60%')
hline(RTS60,'r','RMS');
axis([0 time1(MVC60(2)-MVC60(1)) 0 max(abs(RTS1(MVC100(1):MVC100(2))))])

subplot(6,1,5);
plot(time1(1:MVC80(2)-MVC80(1)+1),abs(RTS1(MVC80(1):MVC80(2))))
ylabel('80%')
hline(RTS80,'r','RMS');
axis([0 time1(MVC80(2)-MVC80(1)) 0 max(abs(RTS1(MVC100(1):MVC100(2))))])

subplot(6,1,6);
plot(time1(1:MVC100(2)-MVC100(1)+1),abs(RTS1(MVC100(1):MVC100(2))))
ylabel('100%')
hline(RTS100,'r','RMS');
axis([0 time1(MVC100(2)-MVC100(1)) 0 max(abs(RTS1(MVC100(1):MVC100(2))))])

%% -----
% Export into Excel-file
%-----

output= [
    LQ0*1000 LQ20*1000 LQ40*1000 LQ60*1000 LQ80*1000 LQ100*1000;
    LH0*1000 LH20*1000 LH40*1000 LH60*1000 LH80*1000 LH100*1000;
    LTA0*1000 LTA20*1000 LTA40*1000 LTA60*1000 LTA80*1000 LTA100*1000;
    LTS0*1000 LTS20*1000 LTS40*1000 LTS60*1000 LTS80*1000 LTS100*1000;
    RQ0*1000 RQ20*1000 RQ40*1000 RQ60*1000 RQ80*1000 RQ100*1000;
    RH0*1000 RH20*1000 RH40*1000 RH60*1000 RH80*1000 RH100*1000;
    RTA0*1000 RTA20*1000 RTA40*1000 RTA60*1000 RTA80*1000 RTA100*1000;
    RTS0*1000 RTS20*1000 RTS40*1000 RTS60*1000 RTS80*1000 RTS100*1000;
    F0 F20 F40 F60 F80 F100;
    F0_std F20_std F40_std F60_std F80_std F100_std;
]

```

```
Excel = actxserver('Excel.Application');
Excel.Visible = 1;
w = Excel.Workbooks;
file = strcat(s2,'result3.xls');

% Write
xlswrite(file,output);

% Open file
invoke(w, 'open', file);
```

Code 4. Matlab Code of analysis_paradigm_B.m

analysis_paradigm_C.m

```
%% -----
% Initialization
%-----

% Try's to close a previous opened Excel-Worksheet
if exist('w')
    try
        Excel.WorkBooks.Item('result.xls').Close;
        Excel.Quit;
    catch
    end
end

% Clear workspace
close all;
clear all;

% Set parameter
% PTP-limits
low =41;          % left limit for upper muscles equals 20.5ms
low_down = 57     % left limit for lower muscles equals 27.5ms
high = 111;       % right limit for all muscles equals 55.5ms
t0 = 24;          % windowssize for force measurement equals 12ms

% Set number of controls and conditioned reflexes
number_contr=5;
number_conditioned=5;

%% -----
% Load Data from ASCII-file
%-----

% Load all data
[s1, s2] = uigetfile ('*.asc', 'Open File');
cd (s2);

% Anzeigen des Filenamens
disp('file: ')
disp(s1)

A=dlmread (s1,',' ,11,0);
length_A=length(A);

time=A(:,1);
LQ=A(:,2); LH=A(:,3); LTA=A(:,4); LTS=A(:,5);
RQ=A(:,6); RH=A(:,7); RTA=A(:,8); RTS=A(:,9);
Force=A(:,11);

LQ1=LQ; LH1=LH; LTA1=LTA; LTS1=LTS;
RQ1=RQ; RH1=RH; RTA1=RTA; RTS1=RTS;
Forcel=Force;
```

```

% Normalize timescale
    time1=time-time(1);

% Filtering data with Butterworth, 2.Order, fg = 10-700Hz
EMG1=[LQ1 LH1 LTA1 LTS1 RQ1 RH1 RTA1 RTS1];
cuthigh=10;
cutlow=700;
[b,a]=butter(2,cuthigh/2048,'high');

for i=1:8
    testfilter(:,i)=filtfilt(b,a,EMG1(:,i));
end
[b,a]=butter(2,cutlow/2048);
for i=1:8
    testfilter(:,i)=filtfilt(b,a,EMG1(:,i));
end

LQ1=testfilter(:,1); LH1=testfilter(:,2);
LTA1=testfilter(:,3); LTS1=testfilter(:,4);
RQ1=testfilter(:,5); RH1=testfilter(:,6);
RTA1=testfilter(:,7); RTS1=testfilter(:,8);

%% -----
% Detailplot - LQ
%-----
figure('Name','LQ','NumberTitle','off')
subplot(1,2,1)
title('controls')
hold on
for i=1:number_contr
    plot(time1(1:420),LQ1(420*(i-1)+1:420*i))
end
vline(time1(low))
vline(time1(high))
hold off
axis([0 0.1 -3 3])
ylabel('LQ')

subplot(1,2,2)
title('conditioned')
hold on
for i=1:number_conditioned
    plot(time1(1:420),LQ1(420*(number_contr+i-1)+1:420*(number_contr+i)))
end
vline(time1(low))
vline(time1(high))
hold off
axis([0 0.1 -3 3])
crosshair_subplots;

```

```

%% -----
% Detailplot - LH
% -----
figure('Name','LH','NumberTitle','off')
subplot(1,2,1)
title('controls')
hold on
for i=1:number_contr
    plot(time1(1:420),LH1(420*(i-1)+1:420*i))
end
vline(time1(low))
vline(time1(high))
hold off
axis([0 0.1 -3 3])
ylabel('LQ')

subplot(1,2,2)
title('conditioned')
hold on
for i=1:number_conditioned
    plot(time1(1:420),LH1(420*(number_contr+i-1)+1:420*(number_contr+i)))
end
vline(time1(low))
vline(time1(high))
hold off
axis([0 0.1 -3 3])
crosshair_subplots;

%% -----
% Detailplot - LTA
% -----
figure('Name','LTA','NumberTitle','off')
subplot(1,2,1)
title('controls')
hold on
for i=1:number_contr
    plot(time1(1:420),LTA1(420*(i-1)+1:420*i))
end
vline(time1(low_down))
vline(time1(high))
hold off
axis([0 0.1 -3 3])
ylabel('LQ')

subplot(1,2,2)
title('conditioned')
hold on
for i=1:number_conditioned
    plot(time1(1:420),LTA1(420*(number_contr+i-1)+1:420*(number_contr+i)))
end
vline(time1(low_down))
vline(time1(high))
hold off
axis([0 0.1 -3 3])
crosshair_subplots;

```

```

%% -----
% Detailplot - LTS
%-----
figure('Name','LTS','NumberTitle','off')
subplot(1,2,1)
title('controls')
hold on
for i=1:number_contr
    plot(time1(1:420),LTS1(420*(i-1)+1:420*i))
end
vline(time1(low_down))
vline(time1(high))
hold off
axis([0 0.1 -3 3])
ylabel('LQ')

subplot(1,2,2)
title('conditioned')
hold on
for i=1:number_conditioned
    plot(time1(1:420),LTS1(420*(number_contr+i-1)+1:420*(number_contr+i)))
end
vline(time1(low_down))
vline(time1(high))
hold off
axis([0 0.1 -3 3])
crosshair_subplots;

%% -----
% Detailplot - RQ
%-----
figure('Name','RQ','NumberTitle','off')
subplot(1,2,1)
title('controls')
hold on
for i=1:number_contr
    plot(time1(1:420),RQ1(420*(i-1)+1:420*i))
end
vline(time1(low))
vline(time1(high))
hold off
axis([0 0.1 -3 3])
ylabel('LQ')

subplot(1,2,2)
title('conditioned')
hold on
for i=1:number_conditioned
    plot(time1(1:420),RQ1(420*(number_contr+i-1)+1:420*(number_contr+i)))
end
vline(time1(low))
vline(time1(high))
hold off
axis([0 0.1 -3 3])
crosshair_subplots;

```



```

%% -----
% Detailplot - RH
% -----
figure('Name','RH','NumberTitle','off')
subplot(1,2,1)
title('controls')
hold on
for i=1:number_contr
    plot(time1(1:420),RH1(420*(i-1)+1:420*i))
end
vline(time1(low))
vline(time1(high))
hold off
axis([0 0.1 -3 3])
ylabel('LQ')

subplot(1,2,2)
title('conditioned')
hold on
for i=1:number_conditioned
    plot(time1(1:420),RH1(420*(number_contr+i-1)+1:420*(number_contr+i)))
end
vline(time1(low))
vline(time1(high))
hold off
axis([0 0.1 -3 3])
crosshair_subplots;

%% -----
% Detailplot - RTA
% -----
figure('Name','RTA','NumberTitle','off')
subplot(1,2,1)
title('controls')
hold on
for i=1:number_contr
    plot(time1(1:420),RTA1(420*(i-1)+1:420*i))
end
vline(time1(low_down))
vline(time1(high))
hold off
axis([0 0.1 -3 3])
ylabel('LQ')

subplot(1,2,2)
title('conditioned')
hold on
for i=1:number_conditioned
    plot(time1(1:420),RTA1(420*(number_contr+i-1)+1:420*(number_contr+i)))
end
vline(time1(low_down))
vline(time1(high))
hold off
axis([0 0.1 -3 3])
crosshair_subplots;

```

```

%% -----
% Detailplot - RTS
%-----
figure('Name','RTS','NumberTitle','off')
subplot(1,2,1)
title('controls')
hold on
for i=1:number_contr
    plot(time1(1:420),RTS1(420*(i-1)+1:420*i))
end
vline(time1(low_down))
vline(time1(high))
hold off
axis([0 0.1 -3 3])
ylabel('LQ')

subplot(1,2,2)
title('conditioned')
hold on
for i=1:number_conditioned
    plot(time1(1:420),RTS1(420*(number_contr+i-1)+1:420*(number_contr+i)))
end
vline(time1(low_down))
vline(time1(high))
hold off
axis([0 0.1 -3 3])
crosshair_subplots;

%% -----
% Calculations
%-----

% Calculate PTP-Amplitudes
for i=1:(number_contr+number_conditioned)
    min_LQ(i)=min(LQ1(420*(i-1)+low:420*(i-1)+high));
    min_LH(i)=min(LH1(420*(i-1)+low:420*(i-1)+high));
    min_LTA(i)=min(LTA1(420*(i-1)+low_down:420*(i-1)+high));
    min_LTS(i)=min(LTS1(420*(i-1)+low_down:420*(i-1)+high));
    max_LQ(i)=max(LQ1(420*(i-1)+low:420*(i-1)+high));
    max_LH(i)=max(LH1(420*(i-1)+low:420*(i-1)+high));
    max_LTA(i)=max(LTA1(420*(i-1)+low_down:420*(i-1)+high));
    max_LTS(i)=max(LTS1(420*(i-1)+low_down:420*(i-1)+high));
    min_RQ(i)=min(RQ1(420*(i-1)+low:420*(i-1)+high));
    min_RH(i)=min(RH1(420*(i-1)+low:420*(i-1)+high));
    min_RTA(i)=min(RTA1(420*(i-1)+low_down:420*(i-1)+high));
    min_RTS(i)=min(RTS1(420*(i-1)+low_down:420*(i-1)+high));
    max_RQ(i)=max(RQ1(420*(i-1)+low:420*(i-1)+high));
    max_RH(i)=max(RH1(420*(i-1)+low:420*(i-1)+high));
    max_RTA(i)=max(RTA1(420*(i-1)+low_down:420*(i-1)+high));
    max_RTS(i)=max(RTS1(420*(i-1)+low_down:420*(i-1)+high));
end

```

```

peak_to_peak_LQ=max_LQ+abs(min_LQ);
peak_to_peak_LH=max_LH+abs(min_LH);
peak_to_peak_LTA=max_LTA+abs(min_LTA);
peak_to_peak_LTS=max_LTS+abs(min_LTS);
peak_to_peak_RQ=max_RQ+abs(min_RQ);
peak_to_peak_RH=max_RH+abs(min_RH);
peak_to_peak_RTA=max_RTA+abs(min_RTA);
peak_to_peak_RTS=max_RTS+abs(min_RTS);

peak_to_peak_amplitudes=[peak_to_peak_LQ
peak_to_peak_LH
peak_to_peak_LTA
peak_to_peak_LTS
peak_to_peak_RQ
peak_to_peak_RH
peak_to_peak_RTA
peak_to_peak_RTS];

% Calculate force at stimulus
disp('Number of measurements: ')
anzahl = length_A/420;
disp(anzahl);

Mean_Force = zeros(1,anzahl);

for i=1:anzahl
    Mean_Force(i) = mean (Forcel(420*(i-1)+1:420*(i-1)+t0));
end

%% -----
% Export into Excel-file
% -----
output = [peak_to_peak_amplitudes; Mean_Force ];

Excel = actxserver('Excel.Application');
Excel.Visible = 1;
w = Excel.Workbooks;
file = strcat(s2,'result.xls');

% Write
xlswrite(file,output);

% Open Excelfile
invoke(w, 'open', file);

```

Code 5. Matlab Code of analysis_paradigm_C.m

analysis_Mmax.m

```
%-----  
%% Initialization  
%-----  
  
% Try's to close a previous opened Excel-Worksheet  
if exist('w')  
    try  
        Excel.WorkBooks.Item('result2.xls').Close;  
        Excel.Quit;  
    catch  
    end  
end  
  
% Clearing the workspace  
clear all;  
close all;  
  
% Parameter setting, sets the limits of the evaluation window  
low = 28;  
high = 90;  
  
%-----  
%% Load Data from ASCII-file  
%-----  
  
% Load all data  
disp('file')  
[s1, s2] = uigetfile ('*.asc', 'Open File');  
cd (s2);  
A=dlmread (s1, ';', 11, 0);  
length_A=length(A);  
  
% Selecting particular data  
time=A(:,1); LTS=A(:,2); RTS=A(:,3);  
  
% Normalize timescale  
time1=time-time(1);  
  
% Filtering data with Butterworth, 2.Order, fg = 10-700Hz  
EMG1=[LTS1 RTS1];  
cuthigh=10;  
cutlow=700;  
[b,a]=butter(2,cuthigh/2048,'high');  
for i=1:2  
    testfilter(:,i)=filtfilt(b,a,EMG1(:,i));  
end  
[b,a]=butter(2,cutlow/2048);  
for i=1:2  
    testfilter(:,i)=filtfilt(b,a,EMG1(:,i));  
end
```

```

LTS1=testfilter(:,1);
RTS1=testfilter(:,2);

% Calculate number of measurements
number_controls=round(length_A/420);

%-----
%% Plot responses and crosshairs
%-----
figure
hold on
for i=1:number_controls
    plot(time1(1:400),LTS1(420*(i-1)+1:420*(i-1)+400))
end
vline(time1(low));
vline(time1(high));
hold off
axis ([0 0.08 -8 10])
crosshair

%-----
%% Calculate peak-to-peak amplitudes for a certain window
%-----
for i=1:number_controls
    min_LTS(i)=min(LTS1(420*(i-1)+low:420*(i-1)+high));
    max_LTS(i)=max(LTS1(420*(i-1)+low:420*(i-1)+high));
    min_RTS(i)=min(RTS1(420*(i-1)+low:420*(i-1)+high));
    max_RTS(i)=max(RTS1(420*(i-1)+low:420*(i-1)+high));
end

peak_to_peak_LTS=max_LTS+abs(min_LTS);
peak_to_peak_RTS=max_RTS+abs(min_RTS);

peak_to_peak_LTS'
peak_to_peak_RTS'

output = [peak_to_peak_LTS' peak_to_peak_RTS' ];

%-----
%% Export into Excelfile
%-----
Excel = actxserver('Excel.Application');
Excel.Visible = 1;
w = Excel.Workbooks;
file = strcat(s2,'result2.xls');

xlswrite(file,output);

invoke(w, 'open', file);

```

Code 6. Matlab Code of analysis_Mmax.m